UNIVERSIDADE DE LISBOA

FACULDADE DE CIÊNCIAS DE LISBOA

DEPARTAMENTO DE BIOLOGIA ANIMAL

ROLE OF THE NODAL SIGNALING PATHWAY IN LEFT-RIGHT MORPHOGENESIS OF THE ZEBRAFISH (*Danio rerio*) HEART

Maria Inês Medeiros de Campos Baptista

DOUTORAMENTO EM BIOLOGIA

(Biologia do Desenvolvimento)

2009

UNIVERSIDADE DE LISBOA

FACULDADE DE CIÊNCIAS DE LISBOA

DEPARTAMENTO DE BIOLOGIA ANIMAL

ROLE OF THE NODAL SIGNALING PATHWAY IN LEFT-RIGHT MORPHOGENESIS OF THE ZEBRAFISH (*Danio rerio*) HEART

Maria Inês Medeiros de Campos Baptista

Tese Orientada por:

Professora Doutora Sólveig Thorsteinsdóttir e

Professor Doutor Alexander Schier

DOUTORAMENTO EM BIOLOGIA

(Biologia do Desenvolvimento)

2009

Os trabalhos apresentados nesta tese foram realizados com o apoio financeiro da Fundação para a Ciência e a Tecnologia (bolsa de referência **SFRH/BD/11801/2003**) e **NIH grant R01 GM56211**.

1) Para a elaboração da presente tese de doutoramento foi usado integralmente, como capítulo, um artigo científico publicado numa revista científica internacional indexada. Uma vez que este trabalho foi realizado em colaboração com outros investigadores, e de acordo com o disposto no nº 1 do Artigo 41º do Regulamento de Estudos Pós-Graduados da Universidade de Lisboa, publicado *in Diário da República* 2ª série – N.º 209 - 30 de Outubro de 2006, esclareço que participei integralmente na concepção e execução do trabalho experimental, na interpretação dos resultados e na redacção do manuscrito.

2) Porque nesta tese está integrado um artigo científico publicado na revista *Developmental Dynamics* (Campos-Baptista MI, Holtzman NG, Yelo D and Schier AF - Nodal signaling promotes the speed and directional movement of cardiomyocytes in zebrafish. *Developmental Dynamics*, 237:3624 – 3633; 2008 - Capítulo II), a redacção dos capítulos subsequentes foi efectuada de acordo com as normas dessa mesma revista. Os capítulos III e IV correspondem a uma compilação de resultados considerados relevantes para esta tese, ainda não publicados.

CONTENTS

I would like to thank Alex Schier for outstanding supervision. For teaching me how to do real, honest, high-quality science and being the pier I look up to and the kind of scientist I want to be. For being not only my boss but also my friend. For allowing me the privilege of learning from him and enjoying such intellectually stimulating scientific atmosphere. Thanks Alex for being my true Father in science.

I thank Deborah Yelon for great collaboration and support and all the Schier and Yelon lab members for the great work atmosphere and thoughtful discussions.

I thank Sólveig Thorsteinsdottir for internal supervision, prompt help with all the details of writing and submitting a thesis and for all the input, critic and comments. More importantly, I thank Sólveig for being that special teacher that inspired me during classes and showed me how beautiful and amazing Developmental Biology is.

I thank all my friends, without whom going through my PhD would have been unbearable. So many friends, I cannot take the risk of trying to enumerate them all. They know who they are! I could not not mention though my dearest Sarita, for all the late nights in the lab, for crying and laughing with me (tu não é os Shawn!?; Maria Albertina!!), for always being there. Lu, Vitor, Sara, Daniel, Janicos, Vera, Zezito, Flávia, Tiago, Bernardo, Maurício (gajo!), Horácio, Sónia, Laura, Edgar, Claúdia, Patrick, Rita, Miguel, Joana, Kika, Cátia, Rogério, Paula, Bruno, Steve, Si… so many and so many more. As I said, I shouldn't risk trying to name them all. Thank you, thank you all!

I would like to thank my piers, my foundation, my "porto-de-abrigo", my origins, the reason of my existence and the genesis of who I am: my Family.

I thank David, my best friend, my companion, metade-da-minha-laranja, my husband. For always being there for me, with extreme love, tenderness, understanding and patience.

I thank my sister Eduarda for her constant uplifting personality, for always making me laugh and bringing sunshine when clouds seem to persist. For the precious gift that is having Clara, my sweet little niece, in my life. Obrigada mana!

I thank Tai-Tai, Duarte, Mané, Sara, Tono, Nary, Pi, Joana, Mimi, Ivone, Susana, Zezinha, João, Nanda, Kiki for the constant support and always making distance seem smaller with all their love and bem-querer.

Last but not least, I thank my parents. My parents! I should reformulate this phrase: I TRY to thank my parents, today and always, for words fail me… there will never be a tangible way to thank them. Love you!

Embora externamente os vertebrados se apresentem como organismos simétricos, esta aparência é enganadora. Os vertebrados desenvolveram a capacidade de distinguir o lado direito do lado esquerdo do corpo e existem assimetrias óbvias na maneira como os seus órgãos internos se dispõem no interior da cavidade corporal e são formados. No adulto estas assimetrias são facilmente observáveis aquando da análise de órgãos como o coração, o estômago e os intestinos e estes apresentam características morfológica e estruturalmente assimétricas. De igual forma, os órgãos internos distribuem-se assimetricamente dentro da cavidade corporal e assumem posições unilaterais, como sejam o coração e o estômago do lado esquerdo e o fígado do lado direito, por exemplo. A forma como os órgãos internos se dispõem dentro da cavidade corporal é conservada em todos os vertebrados e é necessária para o funcionamento correcto e adequado desses órgãos.

Para que o eixo esquerdo-direito (ED) se forme é necessário que os eixos anterior-posterior (AP) e dorsal-ventral (DV) já tenham sido estabelecidos. Só então é que os órgãos internos se podem distribuir correctamente no interior do organismo. Quando os órgãos internos se dispõem de forma correcta dentro da cavidade corporal, o organismo apresenta *situs solitus*. Se ocorrerem anomalias na distribuição dos órgãos internos o *situs* do organismo é afectado e pode levar a diferentes tipos de distribuição dos órgãos internos. Nos casos de *situs inversus* o eixo ED está invertido relativamente aos outros dois eixos e os órgãos internos ocupam uma posição diametralmente oposta ‘aquela que normalmente exibiriam. Pode suceder de os órgão internos se distribuírem de forma discordante, sendo que alguns se encontram na posição correcta, enquanto que outros estão mal posicionados. Estes casos denominam-se de *situs ambiguous* ou heterotaxia e dois exemplos de heterotaxia são o isomerismo esquerdo e o isomerismo direito. Nestes casos particulares os órgãos internos exibem dois lados esquerdos ou dois lados direitos, respectivamente. 1 em 8000 adultos nascem com deficiências causadas

pelo estabelecimento incorrecto do eixo ED, deficiências essas que comportam graves implicações para a saúde do indivíduo. Das possíveis anomalias de assimetria, *situs inversus* é a única classe cujos efeitos não afectam a saúde do indivíduo, uma vez que os órgãos internos continuam a funcionar normalmente, pese embora a sua disposição invertida. Por outro lado, isomerismos, casos de inversão individual (por exemplo, dextrocardia, em que apenas o coração está incorrectamente posicionado, no lado direito) ou outros tipos de heterotaxia, são frequentemente letais ou fonte de graves problemas. Por exemplo, dextrocardia está associada com malformações cardíacas dramáticas tais como defeitos no septo ventricular, formação de apenas um ventrículo, etc. E', portanto, um problema fundamental perceber como é que nos vertebrados o plano corporal, inicialmente simétrico, adquire uma assimetria ED estereotípica.

Embora os biólogos já se interessem pelo estabelecimento da assimetria esquerda-direita há bastantes anos, só recentemente é que se começou a perceber em mais detalhe como é que este processo decorre, nomeadamente ao nível genético e molecular. Com base nesse conhecimento, os estabelecimento da assimetria ED divide-se em 4 passos: quebra de simetria ao nível do nódulo, transferência dos sinais de assimetria do nódulo para a placa mesodérmica lateral (PML), expressão assimétrica de moléculas-sinal (tais como moléculas da família dos TGF-ß e morfogénese assimétrica dos órgãos internos, induzida por essas moléculas-sinal. Para o propósito desta tese, o *focus* da nossa pesquisa incide no último passo de estabelecimento da assimetria ED, ou seja, na indução de morfogénese assimétrica por parte de moléculas-sinal expressas unilateralmente na PML. Por forma a abordar este problema, recorremos ao estudo do estabelecimento de assimetria no coração do peixe-zebra e 'a análise de como esta é induzida pela cascada genética Nodal.

Nodals são membros da família de factores de crescimento de transformação (TGF-ß), secretados extracelularmente e necessários para a formação de mesoderme e endoderme, bem como para os estabelecimento de assimetria ED em vertebrados. A cascada genética activada por Nodal sinaliza para o interior da célula através de receptores e co-receptores do tipo EGF-CFC (tal como *one-eyed pinhead*,

oep, no peixe) e induz a expressão assimétrica de vários genes no lado esquerdo da PML, tais como *lefty2* (antagonista da cascada genética) e *pitx2* (gene alvo de Nodal). Estudos em pacientes com defeitos congénitos de assimetria demonstraram que os genes Nodal são necessários para o estabelecimento correcto da assimetria em humanos. No peixe-zebra, o gene Nodal *southpaw* (*spaw*) é expresso no lado esquerdo da PLM, sendo que este é também o tecido no qual o coração de forma.

O coração é o primeiro órgão a formar-se e a funcionar durante a embriogénese dos vertebrados e, no peixe-zebra, este órgão inicia a sua formação através da diferenciação de precursores cardíacos na placa mesodérmica lateral anterior (PMLA), do lado esquerdo e do lado direito do embrião. Os precursores cardíacos correspondem a células do miocárdio e do endocárdio que, após diferenciados, migram em direcção 'a linha mediana do embrião e se fundem, para formar uma estrutura simétrica, o cone cardíaco. O cone cardíaco corresponde a um disco, formado por células do miocárdio, centrado num lúmen, formado por células do endocárdio, inicialmente orientado ao longo do eixo DV. Rapidamente, o cone cardíaco reorienta-se e inicia um processo de extensão que leva 'a formação do tubo cardíaco e posiciona a base do cone (que vai formar a região venosa) do lado esquerdo da linha mediana. O apex deste cone vai originar a região arterial do coração. Posteriormente, o tubo cardíaco inicia uma série de dobras e movimentos rotacionais que transformam a estrutura inicialmente linear em duas câmaras cardíacas: o átrio e o ventrículo.

Por forma a que o cone cardíaco, uma estrutura simétrica, dê origem ao tubo cardíaco, assimetricamente posicionado do lado esquerdo da linha mediana, têm que decorrer uma série de eventos morfogenéticos que quebrem a simetria inicial. Existem vários fenómenos, visualmente perceptíveis, que ocorrem nesta fase inicial de quebra de simetria: rotação, no sentido horário, do cone cardíaco; deslocamento do lúmen para o lado esquerdo da linha mediana; extensão das células anteriores posicionadas no lado esquerdo para a esquerda; involução das células posicionadas no lado direito em direcção ao lado esquerdo.

O gene Nodal *spaw* é expresso do lado esquerdo da PMLA, num domínio adjacente ao cone cardíaco e, na altura em que a simetria é quebrada, o gene *lefty2* já foi

activado na porção esquerda do cone cardíaco. Desta forma, na altura em que a estrutura cardíaca inicia a aquisição de assimetria, a cascada genética Nodal está presente, tanto na placa mesodérmica lateral como no próprio cone cardíaco. Como é que a expressão assimétrica de Nodal induz a morfogénese assimétrica do coração ao nível celular?

Os nossos estudos confirmaram, através da análise de embriões mutantes para o co-receptor de Nodal *oep*, as observações anteriores de que, na ausência de Nodal, o cone cardíaco não exibe os processos morfogenéticos indicativos de quebra de simetria. Recorrendo a microscopia confocal de alta resolução obtivemos filmes do desenvolvimento inicial do coração do peixe-zebra que, quando reconstruídos em 3-dimensões e analisados, nos permitiram caracterizar pormenorizadamente as características cinéticas destas células. Quantificámos a velocidade, deslocamento, ângulo de movimento e outros componentes relevantes na deslocação dos cardiomiócitos. Os nossos estudos revelaram que, na ausência da cascada genética Nodal, as células cardíacas perdem a capacidade de se mover. A velocidade exibida pelas células é altamente reduzida quando comparada com aquela obtida para o tipo-selvagem. Da mesma maneira, enquanto que no tipo-selvagem as células exibem um movimento determinado, linear e direccionado para o lado esquerdo, nos mutantes LZ*oep* o pouco movimento efectuado pelos cardiomiócitos é aleatório e não direccionado.

Em linhas gerais, o nosso trabalho demonstra que Nodal é responsável pela promoção do movimento e da velocidade dos cardiomiócitos, ao mesmo tempo que introduz informação direccional para que esta deslocação seja feita para o lado esquerdo do embrião. Estas observações foram subsequentemente confirmadas pelo estudo e análise de embriões com diferentes interferências ao nível da cascada genética Nodal, nomeadamente por a exibirem bilateralmente ou apenas no lado direito da placa mesodérmica.

Preliminarmente, também tentámos perceber qual é o primeiro processo, dos vários visualmente perceptíveis, a ocorrer durante a quebra de simetria no coração do peixe. Os nosso resultados sugerem que a deslocação do lúmen para o lado esquerdo do embrião seja o primeiro sinal visível de assimetria no coração e que a rotação do

cone cardíaco e a extensão das células do lado esquerdo continuem o processo assimétrico. A involução das células do lado direito parece decorrer somente após estes três processos já terem decorrido.

Palavras-chave: coração, esquerdo-direito, assimetria, nodal, peixe-zebra.

Although externally bilaterally symmetric, vertebrates display asymmetry in the way their internal organs are shaped and distributed within the body cavity. The Nodal signaling pathway has long been implicated in the establishment of left-right asymmetry in vertebrates. Nodals are members of the TGF-β super-family that signal to the interior of the cell to activate downstream targets, such as *Nodal* itself and *lefty2*, a pathway inhibitor. Many of the genes in the Nodal-signaling pathway have a conserved asymmetric expression pattern in the left lateral plate mesoderm (LPM). Little is known on how this asymmetric gene expression translates into asymmetric morphogenesis. To address this question I studied the process of asymmetry acquisition in the zebrafish heart. The heart is the first organ to form and function in vertebrates. Initially, the bilateral fields of cardiomyocytes on the left and right LPM migrate toward the midline to fuse and form the heart cone, a symmetric ring-shaped structure centered in a lumen. The cone tilts and extends to form the heart tube. During heart tube formation symmetry is broken and the cardiac structure develops toward the left of the embryo. The Nodal gene *southpaw* is expressed adjacently to the cardiomyocytes, whereas *lefty2* is expressed in the left side of the heart.

In this thesis I analyzed how Nodal expression instructs cells to break organ symmetry. Studies on embryos lacking Nodal signaling (LZ*oep* mutants) revealed that Nodal promotes the speed and directional movement of cardiomyocytes (Chapter II). Analyses of embryos with bilateral Nodal expression (*ntl* morphants) or Nodal expressed solely in the right LPM (*polaris* morphants) confirmed and extended these results (Chapter III). Preliminary results suggest that asymmetry initiates with a leftward displacement of the lumen (Chapter IV). Taken together, my results indicate that asymmetric Nodal signaling regulates the speed and guides the movement of heart cells and thus establishes left-right asymmetry during organogenesis.

Keywords: heart, left-right, asymmetry, nodal, zebrafish.

.

ALPM	Anterior Lateral Plate Mesoderm
AVE	Anterior Visceral Endoderm
Bmp	Bone morphogenetic protein
Cmlc2	Cardiac myosin light chain 2
DFC	Dorsal Forerunner Cells
ES	Embryonic Stem
FR	Fasciculus Retroflexus
Hpf	Hours-post-fertilization
IFT	Intra-Flagellar Transport
KV	Kupffer's Vesicle
Lft2	Lefty2
LPM	Lateral Plate Mesoderm
LR	Left-Right
LZoep	Late Zygotic one-eyed-pinhead
Ntl	No tail
NVP	Nodal Vesicular Parcel
Oep	One-eyed-pinhead
PFP	Prospective Floor-Plate
PCD	Primary Ciliary Dyskinesia
Pol	Polaris
RNA	Ribonucleic Acid
Shh	Sonic hedgehog
Smo	Smoothened
Spaw	Southpaw
Sqt	Squint
YSL	Yolk Syncytial Layer

Chapter I

- Introduction -

1. Left-Right Asymmetry in Vertebrates

Although vertebrates originate from an initially bilaterally symmetrical embryo, they developed the ability to differentiate left and right-handedness. Left-right (LR) asymmetries are evident, especially in the development and disposition of internal organs. Asymmetries along the LR axis are readily apparent in the adult, where internal organs such as the heart, stomach, and intestines all have a characteristic asymmetric structure and are asymmetrically positioned within the body cavity. These and other organs form during development by following complex patterns of loops and turns that result in stereotyped positioning (reviewed by Fujinaga, 1997). Interestingly, the direction of these loops and turns and the relative positioning of organs within the body cavity appear to be conserved in all vertebrates, suggesting that this particular asymmetric structure and arrangement is necessary for the normal function of the internal organs. For example, the asymmetric development of the digestive system (which is particularly complex in vertebrates) allows it to be packed more efficiently within the body cavity. Likewise, the heart has to be asymmetric for proper and efficient blood pumping.

1.1. Left-Right Axis Organization

The vertebrate body plan is organized according to the establishment of three body axes: antero-posterior (AP), dorso-ventral (DV) and left-right (LR), the latter being the last to be determined. Although all three axes are associated with morphological asymmetry, LR asymmetry provides a unique opportunity to address cellular and molecular mechanisms underlying asymmetry generation, for several reasons. First, it is possible to study this process from the initial symmetry-breaking step to the final stages, including asymmetric organogenesis. Second, being the last axis to be determined, the LR axis is more accessible and the more amenable to experimental manipulation. Finally, defects arising from abnormal LR patterning are less severe than those originating from abnormal AP or DV patterning, which makes experimental approaches easier.

1.1.1. *Situs solitus*, *Situs inversus* and Heterotaxia

Correct placement of the internal organs inside the body cavity is known as *situs solitus* (Figure 1.1A). Deviations in LR axis determination during embryogenesis result in a wide spectrum of abnormal laterality phenotypes, generally classified as either *situs inversus* or *situs ambiguous*. *Situs inversus* is a condition in which the LR axis is reversed in alignment with the other two body axes, resulting in a mirror image of normal body and organ *situs* (Figure 1.1D). *Situs ambiguous*, also known as heterotaxia, is a much broader category that refers to any combination of discordant normal and abnormal LR asymmetries. An example of heterotaxia is left and right isomerism, where internal organs are placed as if there were two right or two left sides (Figure 1.1B and 1.1C).

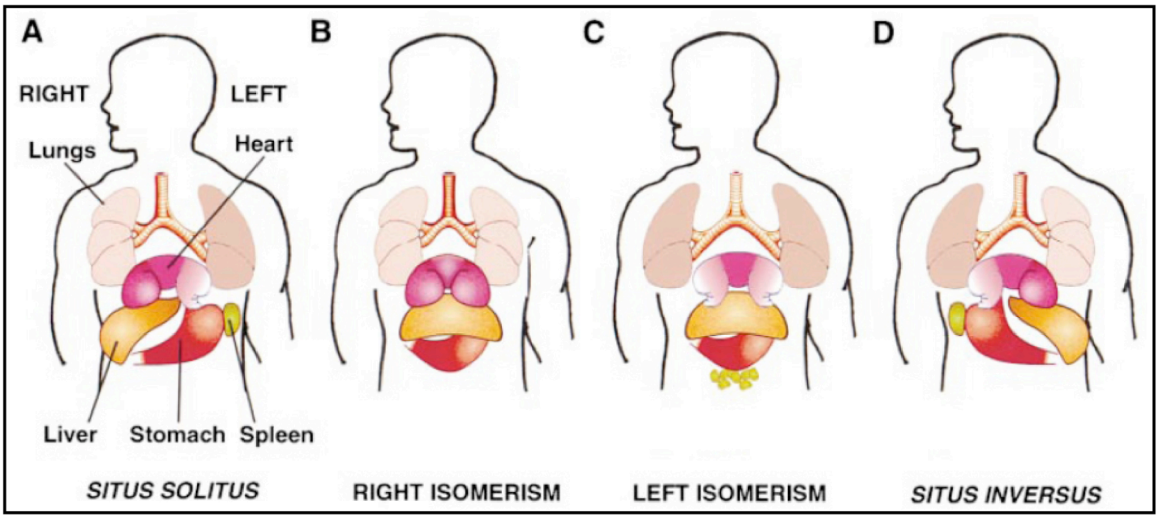

Figure 1.1. Asymmetric disposition of visceral organs in humans. The normal disposition of organs is called *situs solitus* **(A)**. The right lung has three lobes, whereas the left lung (indicated in a different color for clarity) has two. In addition, the apex of the heart points to the left side, the liver is on the right side, and the stomach and the spleen are on the left side. Although not shown in the figure, the gut coils counterclockwise in the abdominal cavity. In right isomerism **(B)**, also called asplenia syndrome, the heart and lungs are double-right (as indicated by the structure of the heart chamber and by both lungs having three lobes), as is the liver, which is generally found in a midline position. The stomach may be located on either side or in the midline, and the spleen is absent. In left isomerism **(C)**, also called polysplenia syndrome, the heart and lungs are double-left, the liver may be double-left, located in a midline position, or normal, and the stomach is usually found in a midline position. There is always more than one spleen (termed splenules), although multilobulated single spleen may also occur. *Situs inversus* refers to the complete mirror-image reversal of organ asymmetry **(D)**. Since laterality defects are highly variable, the figure depicts simplified cases, and is not intended to portray accurately the whole range of possible defects. The term *situs inversus* and right and left isomerism can also be used to describe laterality defects in individual organs, even if

they are not included in specific syndromes. Adapted from Brown and Anderson, 1999. From Capdevila et al., 2000.

Altered LR asymmetry is at the base of several human birth defects (1 in 8000 live births) with significant implications for the health of the individual (reviewed in Casey and Hackett, 2000). Of these, *situs inversus* is the only class with no major effects on the health of the individual. In contrast, isomerism (symmetrical organ *situs*), single organ inversions (such as dextrocardia) or heterotaxia often have serious consequences. For instance, isolated dextrocardia with the abdominal viscera normally positioned is associated with various combinations of severe cardiac malformations (ventricular septal defects, single ventricle, etc). Understanding how the body-plan switches from initial symmetry to a stereotyped LR asymmetry in vertebrates is a fundamental problem.

1.2. Early Steps of Left-Right Asymmetry

Although LR asymmetry has fascinated biologists for many years, only recently progress has been made toward understanding this process at the genetic and molecular levels. In general terms, establishment of left-right asymmetry can be divided into four steps: initial breaking of LR symmetry in or near the node, transfer of LR-biased signals from the node to the lateral plate mesoderm (LPM), LR asymmetric expression of signaling molecules, such as transforming growth factor-β (TGF-β) related molecules, and LR morphogenesis of the visceral organs induced by these signaling molecules (Figure 1.2). Studies on different vertebrates have contributed for this view of the establishment of LR asymmetry. *Xenopus laevis* and chick misexpression studies provided important insights while studies in zebrafish and mouse have helped develop important models.

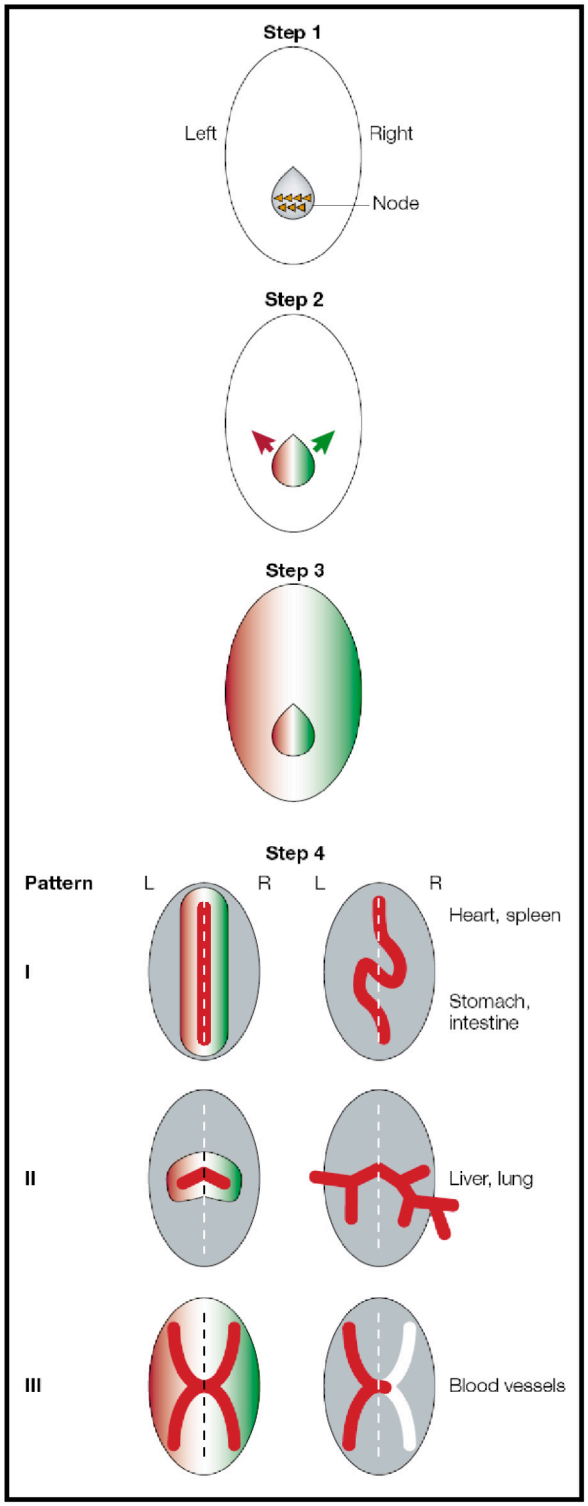

Figure 1.2. Four steps of left-right asymmetric morphogenesis.
In the first step, initial symmetry is broken in a process that might involve nodal flow (the node is represented in grey; direction of the flow is indicated with red arrows). In the second step, LR asymmetric signals are transferred (arrows) from the node to the LPM. Asymmetric expression of *nodal* and *lefty* in the LPM is established in the third step. The last step involves asymmetric morphogenesis. Three distinct patterns can result from asymmetric morphology: directional looping of a tube (pattern I), differential lobation (pattern II) and one-sided regression of a structure (pattern III). Red and green represent LR asymmetric signals; grey represents parts of the embryo that are LR asymmetric. Adapted from Hamada et al, 2002.

1.2.1. Brown and Wolpert: the F-Molecule Model

In the early 1990s, Wolpert and colleagues proposed a theoretical solution for the breaking of symmetry and generation of LR asymmetry, known as the F molecule model (Brown and Wolpert, 1990). They postulated that a chiral protein, the F-molecule, is tethered with respect to the AP and DV axes and thus automatically aligns the LR axis along with the other two main axes. According to this model, in the absence of such molecule, symmetry should be maintained.

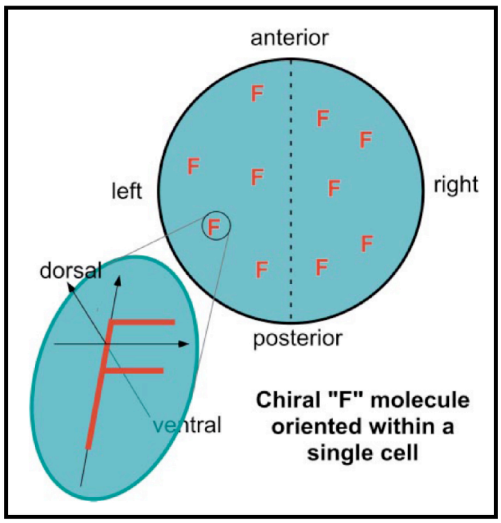

Figure 1.3 – The Brown and Wolpert (1990) model. A chiral molecule (schematized by an F) tethered with respect to the other axes can orient the direction of the LR axis. Adapted from Mercola and Levin, 2001.

However, observations that in the absence of symmetry break the result was random asymmetry and not symmetry, lead to other hypothesis, depicted below. Interestingly, the F-molecule model is supported by recent observations (see section 1.4.1.1).

1.3. Structures Involved in Left-Right Asymmetry Determination

Recent observations suggest that the rotational movement of cilia in the node might be involved in breaking symmetry in vertebrates.

1.3.1. Monocilia and the Node

Cilia are projections from the apical cell surface, derived from a basal body, the centriole, and membrane bound. They possess a microtubule cytoskeleton, named the ciliary axoneme, wrapped by a ciliary membrane. The ciliary axoneme consists of a ring of nine doublet microtubules surrounding a central pair or a missing pair of microtubules and acts as a rail for the transport of membrane organelles and protein complexes over long distances.

In the animal kingdom, depending on the presence or absence of the central pair of microtubules, axonemes fall into two major groups: 9+2, in which the nine doublet microtubules surround a central pair of singlet microtubules, and 9+0, in which the central pair is missing (Porter, 1957; Satir, 2005). The molecular motors responsible for ciliary movement are the axonemal dyneins and these are missing in the 9+0 cilia (Figure 1.4).

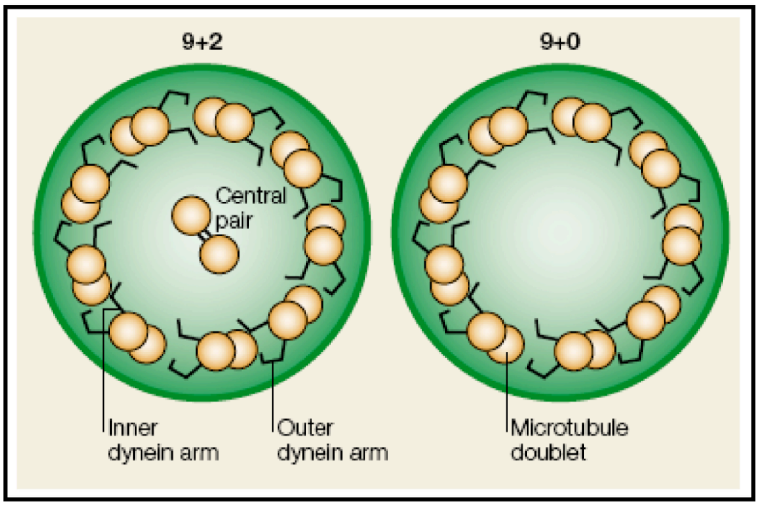

Figure 1.4 – Two types of cilium. 9+2 cilia contain a ring of nine peripheral doublets of microtubules plus a pair of central microtubules, whereas 9+0 cilia, also known as primary cilia or monocilia, lack the central pair of microtubules. 9+2 cilia are typically found in the respiratory epithelium, reproductive system (for example, the oviduct) and central nervous system (for example, ependyma). 9+0 cilia are found in various organs, including skin (keranocytes), kidney (renal tubular epithelial cells) and blood vessels (in endothelial cells). 9+0 cilia are also found in early mouse embryos, in particular on the cells of the midline structures, such as prechordal plate, node and notochordal plate (Sulik et al., 1994). Adapted from Hamada et al., 2002.

Contrary to 9+2 cilia, 9+0 cilia are immotile. Whereas epithelial cells may possess several hundred 9+2 motile cilia, 9+0 are usually solitary, being also known as primary cilia or monocilia. They have a widespread distribution among the cells of

the body and can be found on epithelial cells, such as the kidney tubule, the bile duct, the endocrine pancreas and the thyroid, and in non-epithelial cells such as the chondrocytes, fibroblasts, smooth muscle cells, neurons and Schwann cells.

In Kartagener's syndrome, a relatively rare human genetic disorder in ciliary structure and function, also known as primary ciliary dyskinesia (PCD), the dynein arms are missing from the microtubules of the molecular motors. Half of the patients have their organs with reverse orientation, immotile sperm and defective cilia in their airway. This phenotype indicated a possible link between cilia and LR asymmetry determination (Afzelius, 1976), although it was not known which cilia were relevant for this process.

Because 9+0 cilia are in general immotile, it was surprising to find that unique motile 9+0 cilia are present in the transient, liquid-filled midline structure, formed during gastrulation, the embryonic node (Sulik et al., 1994).

The mouse embryonic node is the equivalent to the Spemann organizer in amphibians, the Hensen's node in chick and the Kupffer's vesicle in zebrafish.

The mouse node arises after the DV and AP axes have been defined and, as in primary cilia, only one cilia exists per node cell, with 9+0 axonemes. However, node monocilia possess dynein arms with LR dynein (Supp et al., 1997; Supp et al., 1999) and are motile. The ventral monocilia project into the extra-embryonic space and rotate rapidly, in a clockwise direction (when viewed from the ventral side) (Nonaka et al., 1998). The rotational movement of nodal monocilia is unique, since most motile cilia and flagella only move back and forth.

The particular kinetics of the nodal monocilia generates a leftward flow of the extra-embryonic fluid around the node – a phenomenon called "nodal flow" - and might transport an unknown molecule that could act as a left-side determinant.

1.4. Nodal Flow

Several studies suggested the "nodal flow" to be important for LR determination (Harvey, 1998).

The nodal flow is impaired in several mouse mutants, such as those deficient in the kinesin super-family proteins KIF3a or KIF3b. KIFs move various cargo and the KIF3 complex is composed of a heterodimer of the motorproteins KIF3a and KIF3b, and an associated protein KAP3. These motorproteins are essential for ciliogenesis in the node cells and *Kif3a* and *kif3b* knockout mice either completely lack cilia or have very short cilia, only found sporadically in the ventral node. These mice showed randomized *situs* (Nonaka et al., 1998; Marszalek et al., 1999; Takeda et al., 1999).

Left-right dynein (Lrd), a mouse axonemal dynein gene, has been identified as the gene responsible for the *inversus viscerum* (*iv*) phenotype, consisting of randomization of LR determination. In *iv* homozygous mice embryos, the nodal cilia seldom move and appear very rigid (Okada et al., 1999). Nodal cilia cannot rotate because of the mutation in *Lrd* and thus cannot generate the leftward nodal flow necessary for LR determination.

Polaris, a gene directly involved in the microtubule-dependent transport process called intra-flagellar transport (IFT), is required for the maintenance of cilia integrity (Murcia et al., 2000). *Polaris* mutant mice lack the primary cilia in the node and exhibit LR randomization (Murcia et al., 2000).

Other experiments have supported the involvement of the nodal flow in LR determination. Local injection of methylcellulose to increase the viscosity of the extracellular node fluid leads to LR defects, in *Xenopus* (Schweickert et al., 2007).

Culturing mouse embryos under conditions of artificial nodal flow, to the right, reversed LR asymmetry indicating that the direction of the flow of the extra-embryonic fluid determines the subsequent LR asymmetry of the mouse embryos (Nonaka et al., 2002).

1.4.1. Generation of the Nodal Flow

How the clockwise motion of the node monocilia drives a leftward flow in the node is an intriguing question. In the mouse, the node is a roughly pear-shaped depression on the surface of the embryo, when viewed from the ventral side, covered by the Reichert's membrane, which makes it a closed structure. It is filled

with extra-embryonic liquid and arrayed over its base are a few tens of monocilia. When viewed from above (ventral view) these monocilia rotate clockwise (Figure 1.5). Since the node is a closed structure, how does the fluid re-circulate inside the node, as it must, in order to generate the observed leftward flow?

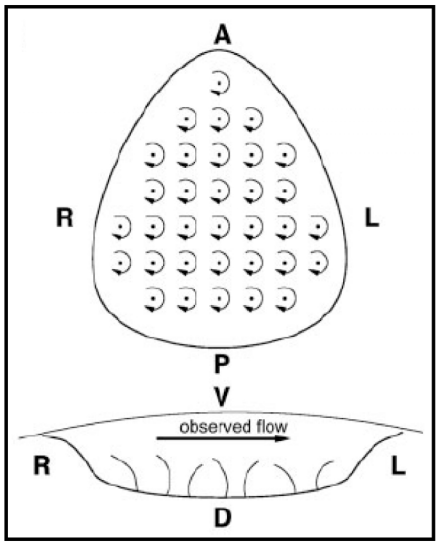

Figure 1.5 – Mouse Node. Ventral and posterior sketch views of the node of the mouse embryo, and its rotating cilia, showing also the experimentally observed leftward nodal flow. Adapted from Cartwright et al., 2004.

1.4.2. Theoretical Model for Nodal Flow Generation

Cartwright and colleagues approached this problem, and established a model for the fluid-dynamical basis of the embryonic development of LR asymmetry in the mouse node. If the monocilia were to rotate around its vertical axes (Figure 1.6A), a set of vortices would be generated, one per cilium, and not a directional flow in the fluid above. Instead, the resulting flow would consist of a cellular network of vortices, in which general circulation would only occur at the edges of the network of cilia (Figure 1.6A). Elsewhere other than the edges the movement would be vortical. This scenario does not correspond to the general leftward flow above the cilia that has been experimentally observed. It has been suggested that the elongated pear-shape of the node is the key factor, defining the leftward nodal flow (Nonaka et al., 1998; Nonaka et al., 2002). A triangle is the geometric shape that most resembles the node shape. However, switching from a rectangular array of

cilia to a triangular array of cilia does not qualitatively change the flow field (Figure 1.6B). The flow field is still vortical within the triangular array, with a general circulation only at the edges, as described for the rectangular array.

One other possible way to generate a leftward nodal flow could relay on the shape of the cilia. A directional flow would be produced if cilia were shaped like oars and feathered during part of the rotation. This does not seem to be the case since cilia are cylindrical in cross section. To hypothesize how a directed and circulating flow within the node can be produced by cylindrical cilia, one can use the analogy of a kitchen blender. When the blender is held vertically in the fluid it is mixing, with the blades rotating in a horizontal plane, this utensil generates a surface flow that corresponds to a vortex around the stem. If the blender is tilted, then a general flow is generated, in the direction in which the blades are turning when they are closest to the surface. If one considers this scenario in the node, all cilia would be tilted in the same direction, inclined and forming an angle to the horizontal. When sweeping out circles, the tilted cilia would generate a directional flow across the chamber above them, due to the fluid overhead being entrained in their direction of rotation (Figure 1.6D). The greater the tilt of the cilia, the stronger the directional flow above the vortices. In order to obtain the observed leftward flow, and considering the cilia rotate clockwise, the monocilia have to be tilted toward the posterior end of the embryo.

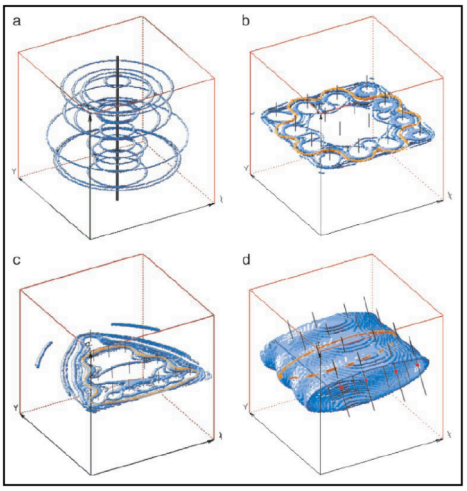

Figure 1.6 – Flow generated by different models of cilia positioning. (A) Vortical flow structure produced by a single rotlet. **(B)** Rectangular array of rotlets with vertical axes, showing cellular structure of vortices with a general circulation only occurring at the edges. **(C)** Triangular array of rotlets with vertical axes, to correspond more closely to the shape of the node. As in **(B)**, general circulation is observed only at the edges. **(D)** Results of tilting the rotlet axes: array of tilted rotlets with a tilt angle of approximately 24°, showing directional flow above and below the array. Adapted from Cartwright et al., 2004.

Cartwright and colleagues proposed that the monocilia tilt at an angle ranging from 5° to 25° from the vertical. Recent studies revealed that the monocilia in the node have an axis of rotation tilted of 10° to 40° to the posterior from the vertical angle (Buceta et al., 2005). It is worth noticing that the posterior tilting of the node cilia allows the cilia to orient along the anterior-posterior and dorsal-ventral axes, fulfilling one central condition of the F molecule model, proposed by Brown and Wolpert. The clockwise rotation of the cilia is an intrinsic chiral activity and thus the cilia have been proposed as an F structure in vertebrates (Nonaka et al., 2005; Okada et al., 2005). The cilia make a leftward swing away from the surface and a rightward sweep near the surface. According to hydrodynamics, a stationary surface retards the movement of fluids by shear resistance. Thus, the rightward sweep is lees effective than the leftward swing in generating fluid movement (Figure 1.8).

It has been shown that the cilia in the mouse node rotate in a clockwise direction, when viewed from the ventral side, and that these cilia are tilted toward the posterior end of the embryos (Nonaka et al., 2005; Okada et al., 2005). The net flow at the node is from the right to left side and is driven by the effective stroke of the tilted cilia.

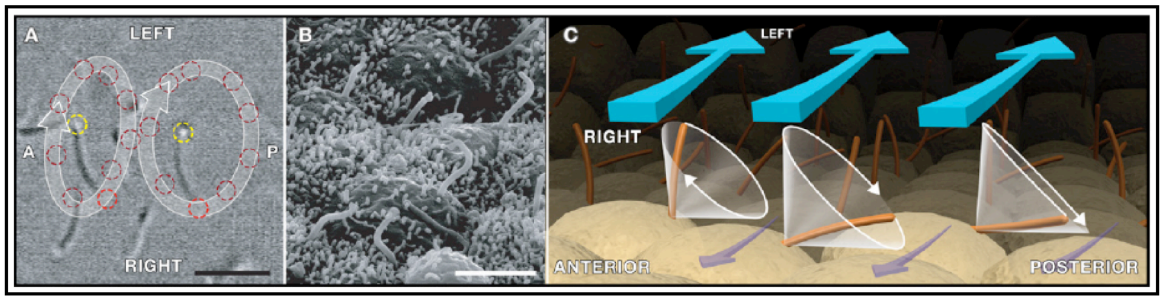

Figure 1.8 – Leftward flow is generated by the posterior tilt of nodal cilia.
(A) The trajectory of the tips of nodal cilia (red circles on the white ellipse) is shifted toward the posterior when compared to the root of the cilia (yellow circles). **(B)** A scanning electron micrograph of ciliated cells of the ventral node of the rabbit embryo is shown. The root of a cilium is most frequently found toward the posterior of the cell. Bar, 5µm. **(C)** A hydrodynamic mechanism generates the leftward flow. Due to a gradient of shear resistance, a cilium cannot efficiently drive the extra-embryonic fluid when it makes a rightward movement in the proximity of the surface. These figures are modified from Okada et al, 2005. Adapted from Hirokawa et al., 2006.

This nodal flow has been demonstrated in *Xenopus* (Schweickert et al., 2007), medaka, *Oryzias latipes*, (Tanaka et al., 2005; Blum et al., 2007) zebrafish and rabbit (Okada et al., 2005) and it is thus proposed to be the initial break of LR asymmetry for all vertebrates (Nonaka et al., 1998; Nonaka et al., 2002; Okada et al., 2005).

1.4.3. Nodal Flow in the Zebrafish Kupffer's Vesicle

In zebrafish, the Kupffer's vesicle (KV) is assumed to be the analogous structure to the mouse node in terms of LR patterning (Essner et al., 2002). KV is a transient ciliated organ derived from the dorsal forerunner cells (DFCs) (Cooper and D'Amico, 1996; D'Amico and Cooper, 1997), a group of cells that remains at the margin while the dorsal blastoderm involutes, during gastrulation. While the ciliated surface at the ventral floor of the mouse is relatively flat, KV is a hollow sphere containing cilia that project both from the dorsal roof and the ventral floor (Amack et al., 2007; Kreiling et al., 2007). Several studies reported that cilia rotate counterclockwise when viewed from the apical side (Figure 1.7B), which is the opposite of what is observed in the mouse node (Figure 1.7A and A') (Kramer-Zucker et al., 2005; Shu et al., 2007).

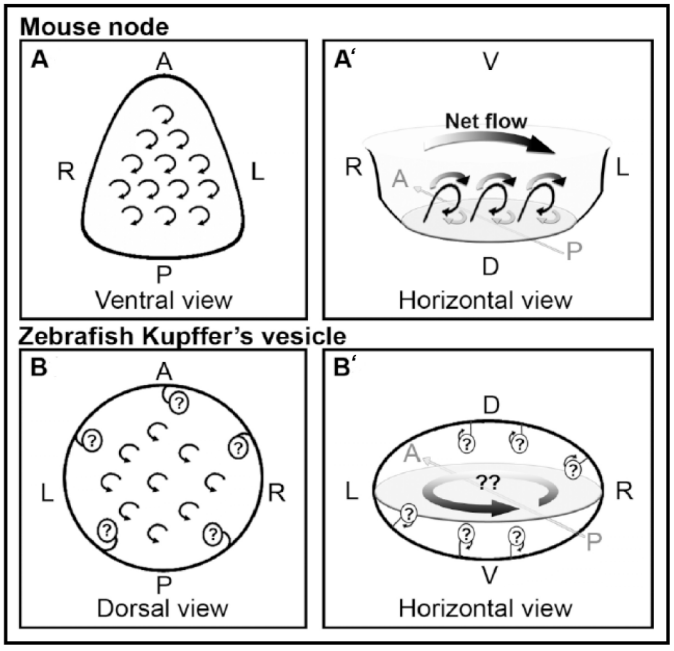

Figure 1.7 – Models for the net flow inside zebrafish Kupffer's vesicle compared with the planar mouse node. A, A', B, B': Schematic diagrams of predicted nodal flow at the mouse node, and in zebrafish Kupffer's vesicle. **(A)** The ventral view of the mouse node showing clockwise rotation of the cilia (as viewed from the apical side of the cells). **(A')** Horizontal view of the mouse node (as viewed from the posterior side of the embryo) showing the posterior tilted cilia (thin, black arrows), which cause the dominant leftward flow (thick black arrows) and diminish the rightward flow (thick, gray arrows) due to the surface interactions. The net flow results in unidirectional flow from right to left (gradient arrow). **(B)** Dorsal view of zebrafish Kupffer's vesicle showing counterclockwise

rotation of the cilia (as viewed from the dorsal side of the vesicle). **(B')** Horizontal view of the zebrafish Kupffer's vesicle assuming counterclockwise rotation of the cilia (as viewed from the posterior side of the embryo). Flow inside Kupffer's vesicle would be predicted to be counterclockwise (gradient arrows). However, this illustrates how conflicting flow paths would be produced if cilia on all surfaces rotate similarly. A, anterior; D, dorsal; L, left; R, right; P, posterior; V, ventral. Adapted from Baker et al., 2008.

This was puzzling, since it suggested that the mechanism for LR determination was not conserved in zebrafish. Likewise, the fluid dynamics inside the zebrafish Kupffer's vesicle was not completely understood.

Having the two ciliated surfaces of the dorsal roof and the ventral floor facing each other, with cilia rotating in the same direction would not generate the strong leftward flow (Kramer-Zucker et al., 2005), circular and counterclockwise at the center of the vesicle, as observed by bead movement and computational analysis (Figure 1.7B') (Essner et al., 2005; Kawakami, 2005; Ellertsdottir et al., 2006; Kreiling et al., 2007; Shu et al., 2007).

Recent studies have shown that cilia on all cells in Kupffer's vesicle rotate clockwise, when viewed from the apical side of the cells (Okabe et al., 2008). This seems to differ from the previous report (Kramer-Zucker et al., 2005) but cilia on the dorsal roof were observed from the basal side of the cells, making the rotation appear different from those on the ventral floor. Thus, all cilia in Kupffer's vesicle rotate clockwise similar to what is observed in the mouse node (Nonaka et al., 2002; Okada et al., 2005). Although cilia rotate in opposite directions at the dorsal roof and the ventral floor, the dominant flow inside the zebrafish Kupffer's vesicle is counterclockwise (when viewed from the dorsal side of the KV). This correlates with cilia movement on the dorsal roof structure, since cilia are more numerous at the dorsal roof (Kreiling et al., 2007; Okabe et al., 2008).

The current model for fluid flow in the zebrafish Kupffer's vesicle is reasonably comparable to the descriptions of flow within the mouse node, making the nodal flow as the initial break of LR asymmetry a conserved mechanism to all vertebrates.

1.5. Interpreting the Nodal Flow

As mentioned earlier, after left-right symmetry is disrupted in or near the node and left-right asymmetry is initiated, it is necessary to transfer the left-right biased signals from the node to the lateral plate mesoderm. Although the nodal flow has been widely accepted to be the mechanism breaking symmetry in all vertebrates, it is not yet well understood how the nodal flow directs left-right asymmetry. Two non-mutually exclusive models have been proposed to explain how the information from the leftward nodal flow is interpreted at the level of the lateral plate mesoderm: the chemical gradient model and the "two cilia"/physical stimulation model.

1.5.1. Chemical Gradient Model

The chemical gradient model appeared first and, as the name suggests, is based on the formation of chemical gradients. It proposes that the directional flow transports particles/molecules (morphogens) and produces a concentration gradient along the ventral node (Nonaka et al., 1998; Okada et al., 2005). The chemical morphogen(s) accumulate only on the left side. In this model, simply by sensing the morphogen the cells can tell whether they are on the left side of the embryo. There are phenotypic differences between mouse mutant embryos lacking cilia and those with immotile cilia. Mutant mice with immotile cilia exhibit a complex pattern of expression of genes that are normally specific to the left side while mice without cilia have a higher tendency to exhibit bilateral patterns of gene expression in the LPM (Nonaka et al., 1998; Marszalek et al., 1999; Takeda et al., 1999; Murcia et al., 2000). In the chemical gradient model these differences can be explained if some (or all) node monocilia serve as the sensor for the chemical morphogen. Recent studies reported the presence of membrane-sheated vesicles in the node that could correspond to the chemical morphogen. These particles, coined Nodal Vesicular Parcels (NVPs), bud from the node cells and have a diameter of 0.3-5μm. Due to the mechanism by which NVPs are released and then caught, such big particles avoid circling within the ventral node (Tanaka et al., 2005). NVPs appear as

if they are leaving the tip of a bending rod (perhaps a microvilium) much like a whip. Ultra-structurally, NVPs seem to comprise multiple lipophilic granules bounded by a membrane. NVPs are actively released from all regions of the ventral node into the middle of the laminar fluid flow, several micrometers above the ciliated surface, where the flow rate is fastest. This allows NVP to avoid being hit by rotating cilia in the initial phase. They are transported to the left side by the nodal flow and then hit the ciliated surface, burst and are fragmented. NVPs are absorbed by the surface of nodal crown cells on the left side and release their content, namely Shh and retinoic acid (RA), two molecules involved in LR asymmetry determination (Schilling et al., 1999; Tsukui et al., 1999; Wang et al., 2004), and shown to be present in NVPs (Tanaka et al., 2005). Cilia contain *shh* receptor, Smoothened (Smo). Because the turnover of NVPs seems to be delayed in *Kif3a* mutants (that lack cilia) compared with the *iv/iv* mutant (that has immotile cilia) it is plausible that a physical interaction between an NVP and a cilium is essential for the burst of the vesicles to occur. Studies on a hypomorphic allele of *fibroblast-growth-factor 8* (*Fgf8*) in mouse implicated FGFs in left sidedness promotion (Meyers and Martin, 1999). Blocking of FGFs with pharmacological and biochemical methods blocked the production of NVPs (Tanaka et al., 2005), suggesting that FGF signaling in the node is required for the production of NVPs (Figure 1.9).

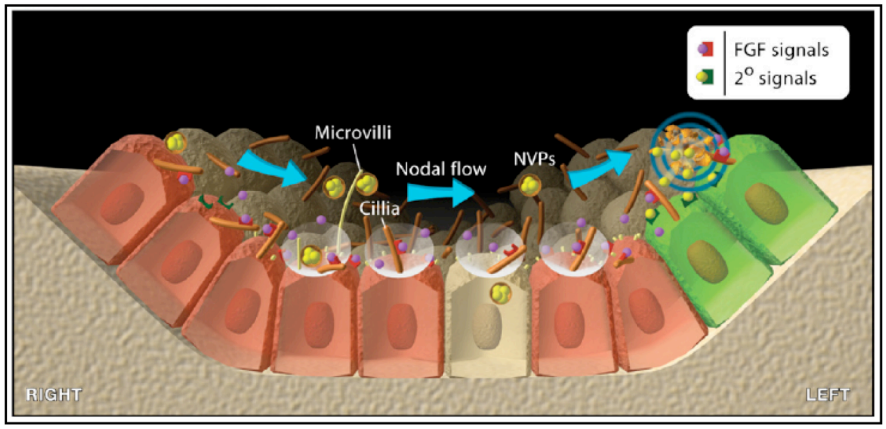

Figure 1.9 – The flow of NVPs
Protruding microvillum picks up an NVP and releases it into the nodal flow. This event is stimulated by FGFR signaling. The NVP is transported to the left by the fluid flow and is hit by the ciliated surface on the left periphery of the node, releasing its contents onto the surface of nodal crown cells. Figure was modified from Tanaka et al, 2005 and adapted from Hirokawa et al, 2006.

As with most novel findings, this work provides possible explanations and raises several questions. This model respects the original idea of a morphogen being made in the node and carried to the left. It also presents a plausible mechanism to explain FGF function in mouse LR determination. NVPs, as presented in this work, provide a mechanism that could deliver asymmetric hedgehog signaling at the mouse node. However, no asymmetric hedgehog expression has ever been reported, as one would expect from the proposed model. Patched-1 expression (up-regulated by hedgehog) is symmetrical in the mouse node (Zhang et al., 2001). Mice lacking *shh* exhibit bilateral Nodal expression due to defects on the midline (Tsukui et al., 1999) rather than at the node, suggesting that *shh* is not the only LR morphogen in NVPs. These are a few questions showing that the precise relationship between hedgehog signaling and NVPs is still far from being clear.

1.5.2. Two-Cilia Model

The physical stimulation model considers a second type of non-motile nodal cilia, placed in the peripheral region of the central node, expressing polycystin-2 and having mechanosensory properties.

It has been suggested that these immotile cilia could act as a sensor for the direction of the flow upon physical stimulation. This model is now commonly known as the "two-cilia" model, since one type of cilia generates the flow and the other senses it (Tabin and Vogan, 2003).

Upon monocilia physical stimulation, the information of flow direction is relayed by the induction of an asymmetric, left-sided elevation of the intracellular of Ca^{2+} on the left periphery of the ventral node (McGrath et al., 2003). Propagation of the increased Ca^{2+} concentration through the LPM may affect the balance of Lefty/Nodal TGF-β signaling, establishing the "leftness" of the LPM and inducing left-side specific gene cascades. However, the detailed molecular mechanism of these signal transduction events is still under investigation.

The "two-cilia" hypothesis appeared in order to explain the differences between

mutant embryos with immotile cilia and those lacking cilia. These exhibit a complex expression pattern of genes that are normally specific to the left side of the LPM or tend to have bilateral gene expression patterns, respectively (Nonaka et al., 1998; Marszalek et al., 1999; Takeda et al., 1999; Murcia et al., 2000). This model is based on the idea that some nodal cilia would have sensory function, but this does not necessarily imply that the nodal cilia sense mechanical stimulus by flow.

The monocilia may serve as the sensor for chemical molecules. Both scenarios are supported: the cilia of the nasal epithelium sense chemical molecules. However, early LR signaling is disrupted by mutations in human polycystic disease (PKD) genes that are involved in mechanosensation by the monocilia of the renal epithelial cells (Murcia et al., 2000; Pennekamp et al., 2002).

Some conceptual issues remain unanswered for the two-cilia hypothesis.

In this model, each ciliated cell should detect the directionality of flow by using the monocilium as a sensor. However, because of the symmetrical shape of the ventral node, the node cells on both sides can similarly sense the flow coming from the right side. It is thus not possible to convey global information on laterality. Further information, such as communication with surrounding cells, would be required to know whether they are on the left or on the right side of the node.

1.5.3. NVPs and Ca^{2+} Concentration

A connection between the release of NVPs and elevation of Ca^{2+} concentration on the left periphery of the ventral node was established by pharmacological studies.

Treatment of mice embryos with an FGFR inhibitor not only completely suppresses NVPs release as it also abolishes Ca^{2+} elevation. It did not perturb the leftward nodal flow, indicating that the flow by itself is insufficient for left specific Ca^{2+} elevation.

Treatment with either Indian hedgehog (Ihh), retinoic acid (RA) or Shh (all factors symmetrically present within the embryonic node), was able to rescue calcium signaling at the node. Intriguingly, Shh and RA specifically rescued left-sided Ca^{2+}

signaling, while Ihh stimulated bilateral Ca^{2+} signaling. Analysis of the production of NVPs revealed that Shh and RA rescued the production of NVPs that were carried by the nodal flow toward the left side but, strangely, Ihh did not rescue the production of NVPs. These results suggest that Ihh specifically stimulates Ca^{2+} while Shh and RA activated left-sided Ca^{2+} signaling through their rescue of NVP production.

Antibodies against Shh and RA detect both Shh and RA in NVPs being released from floor of the node. The precise role of Shh and RA in NVP production is unclear. The ability of Ihh, but not Shh, to bilaterally activate Ca^{2+} signaling is also difficult to explain. Both molecules are capable of activating the LR pathway in chick (Pathi et al., 2001), albeit *ihh* less efficiently than *shh*. Both are expressed at the mouse node and loss of both genes, or of their common receptor smoothened (*Smo*), results in loss of the left-sided nodal cascade (Zhang et al., 2001). Still many questions remain to be answered and further investigation in the field is necessary.

1.6. Asymmetry Before the Nodal Flow

Although the leftward flow of NVPs presents itself as a good candidate for the initial mechanism breaking left-right asymmetry in mouse embryos, this does not seem to be the case in other organisms (reviewed by Levin, 2005). Monocilia in the ventral node or its counterpart structures are evolutionarily conserved (Essner et al., 2002) but the leftward nodal flow might not be the event breaking symmetry in some vertebrates, such as frog, birds and fish.

In frog, the establishment of the left-right axis is linked to the formation of the dorsal-ventral axis, thus happening very early during development. The DV axis is initiated by sperm entry during fertilization, followed by a cytoplasmic rotation during the first cells cycle (Gerhart et al., 1989). Thus, laterality has already been generated 2 hours after fertilization in frog eggs. During the initial cleavages of fertilized eggs the maternal RNA of H^+/K^+- ATPase is already localized asymmetrically and this localization is essential for left-right determination (Levin et al., 2002).

In chick, the Hensen's node is morphologically tilted before the neurulation stage (Kölliker, 1879), being the first morphological asymmetry in the embryo. These left-right asymmetries are established before the formation of monociliated cells on the ventral midline.

In zebrafish, the nodal flow exists in Kupffer's vesicle and is required for the Ca^{2+} elevation on the left periphery of the ventral node (Essner et al., 2005; Kramer-Zucker et al., 2005). However, if eggs are treated with an H^+/K^+- ATPase inhibitor during the cleavage period, embryos develop left-right patterning defects without disturbing the leftward flow in the Kupffer's vesicle (Kawakami, 2005).

These observations suggest that at least two different and independent symmetry-breaking events might exist during fish development: one is dependent on H^+/K^+-ATPase during early-cleavage stages of embryogenesis, the other requires nodal fluid flow later on.

The leftward direction of the nodal flow is autonomously defined without referring to the left-right asymmetry at the early-cleavage stage. On the other hand, nodal flow is not sufficient for the subsequent development of left-right asymmetry of the visceral organs such as the heart, gut and liver. This means that the earlier symmetry breaking is most likely the principal determining factor.

The ventral node might be necessary for the downstream signaling pathway that may relay/amplify the information established during the early-cleavage stage for proper accomplishment of the subsequent developmental processes in the mesoderm (Raya and Belmonte, 2004).

To date, no biased asymmetrical events have been found in mouse embryos earlier than the stage of nodal flow. This assumption is strongly supported by the experiments in mice using artificial flow (Nonaka et al., 2002) demonstrating that the breaking of asymmetry by nodal flow dominates the earlier polarity information. The fact that differences relative to the earliest events in left-right determination exist among species but that all species possess a ventral node or the equivalent structure involved in left-right establishment, suggests that the ventral node is a converging point for redundant asymmetry-breaking processes (Figure 1.10).

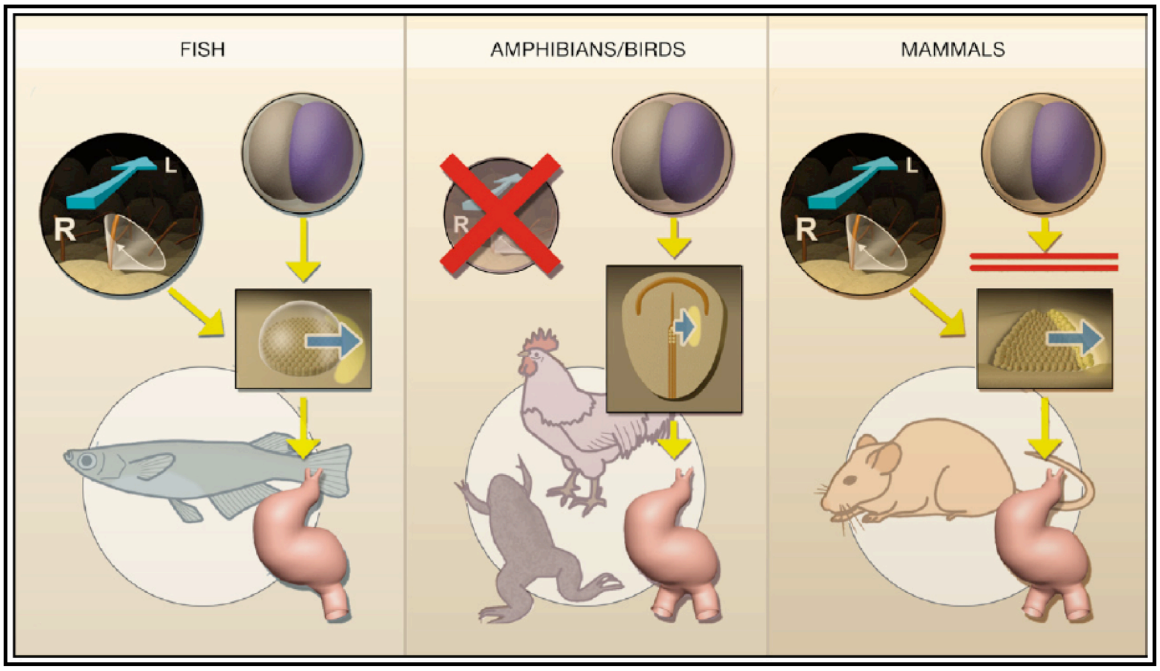

Figure 1.10 – Breaking of LR asymmetry in vertebrates. Fish might be the best archetype for the breaking of LR asymmetry in vertebrates. They have two independent sources of LR asymmetry: the first occurs with the initial cleavage of fertilized egg, and the second is created by the leftward nodal flow. The ventral node serves as the "knot" tying these sources of information together and is necessary for relaying information to the left LPM, where a well-conserved left-right signaling pathway for asymmetrical development takes place. This figure was adapted from Hirokawa et al, 2006 and it is not completely accurate. **It has recently been demonstrated that a cilia-leftward flow determines laterality in *Xenopus* (Schweickert A et al, 2007)**.

1.7. Asymmetric Cascade of Gene Expression

Once the orientation of LR asymmetry has been determined relative to the AP and DV axes, distinct left and right-sided signaling cascades reinforce and transmit this information to tissues, in order to form asymmetric organs. Independently of how LR orientation is initially established in different species, the intermediate part of the process converges on Nodal signaling on the left side of the embryo.

1.7.1. Nodal signaling Pathway

The *Nodal* gene, a member of the TGF-β super-family of signaling molecules was initially discovered in the early 90's in genetic studies in the mouse (Conlon et al., 1991; Zhou et al., 1993; Conlon et al., 1994) and identification of *Nodal*-related ligands ensued in other species (Jones et al., 1995; Levin et al., 1995; Rebagliati et al., 1998a). It was of great importance to clone this gene since *Nodal* is essential for mammalian gastrulation and studies in *Xenopus* at the time had suggested that TGF-β signals, such as activin, Vg1, or related molecules, might serve as the long-sought vertebrate mesoderm inducers (Smith et al., 1995; Schier and Shen, 2000; Whitman, 2001). Recent studies have shown that, indeed, *Xenopus* Vg1 plays a role in mesoderm and endoderm formation (Birsoy et al., 2006). The fact that the Nodal signals Cyclops and Squint are required for germ-layer formation in zebrafish (Feldman et al., 1998) and the isolation of *Nodal* genes in other vertebrates (Jones et al., 1995; Rebagliati et al., 1998a; Rebagliati et al., 1998b; Sampath et al., 1998) reiterated the idea that Nodals are *bona fide* mesendoderm (mesoderm and endoderm) inducers. Currently, it is generally assumed that Nodals serving as mesendoderm inducers is highly conserved and applicable to all vertebrates.

In addition to mesendoderm induction, Nodals play another very important role, namely in the establishment left-right asymmetry (Burdine and Schier, 2000; Capdevila et al., 2000; Mercola and Levin, 2001; Hamada et al., 2002). This was suggested by the finding that some Nodal genes are expressed asymmetrically in the left side of the lateral plate mesoderm (Levin et al., 1995; Collignon et al., 1996; Lowe et al., 1996). Studies of patients with congenital left-right defects implicate Nodal signaling in the establishment of left-right asymmetry in humans (Bamford et al., 2000).

Several components of the Nodal signaling pathway (Figure 1.11) were isolated. The related activities of activin and Nodal suggest that Nodals act via activin receptors, Smad transcription factors and associated factors such as FoxH1 (Schier and Shen, 2000; Whitman, 2001). Studies in zebrafish and mouse revealed that extracellular-attached EGF-CFC proteins, such as one-eyed-pinhead and Cripto, respectively, are

required for Nodal signaling during gastrulation (Gritsman et al., 1999). These proteins act as Nodal co-receptors (Reissmann et al., 2001; Yeo and Whitman, 2001; Chen and Shen, 2004). Lefty proteins, a very divergent group of TGF-β signals, were isolated and led to the discovery of extracellular inhibitors of Nodal signaling (Meno et al., 1996; Meno et al., 1999; Thisse and Thisse, 1999). Likewise, Cerberus, the forebrain inducer, was identified as an antagonist of Nodals (Piccolo et al., 1999). More recently, several novel modulators of Nodal signaling have been found, ranging from convertases responsible for regulating the generation of the active signal to factors that regulate the response to the signal, such as Arkadia and DRAP1 (Episkopou et al., 2001; Niederlander et al., 2001; Beck et al., 2002; Iratni et al., 2002).

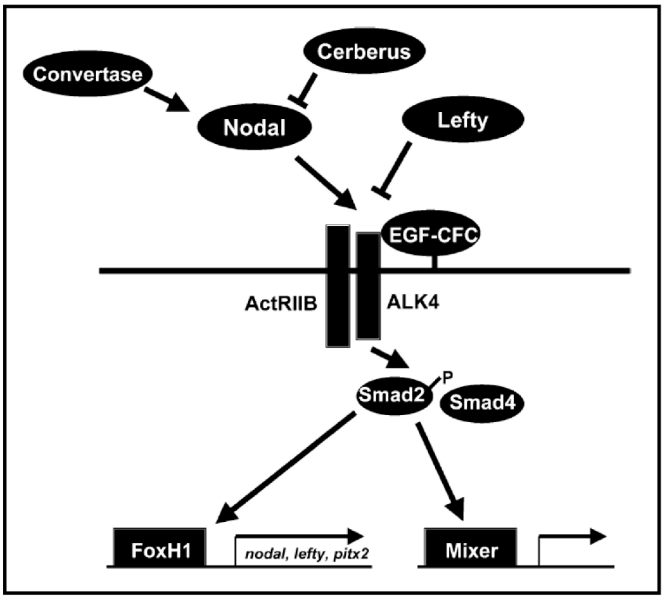

Figure 1.11 – The Nodal signaling pathway. Nodal signaling is activated by the interaction of Nodals with activin receptors (ActRIIB, ALK4) and EGF-CFC co-receptors. Nodal signaling is inhibited by Leftys and Cerberus. Convertases process Nodal pro-proteins. Nodal signaling is transmitted intra-cellularly by phosphorylation of Smad2 and its association with Smad4 and transcription factors (FoxH1, Mixer) that determine which genes are regulated by P-Smad2. Adapted from Schier, 2003.

Detailed studies on how Nodals pattern embryonic tissues suggest four major aspects of Nodal signaling. First, Nodal signaling in the mouse has an unexpected early role in the positioning of the anterior-posterior axis of the embryo (Ding et al., 1998; Waldrip et al., 1998; Brennan et al., 2001). Second, the activity and propagation of Nodal signaling is regulated by complex auto-regulatory interactions (Saijoh et al., 2000; Brennan et al., 2001; Whitman, 2001; Brennan et al., 2002; Chen

and Schier, 2002; Feldman et al., 2002; Dougan et al., 2003). Third, Nodals can act locally or act as morphogens, directly at the distance, in a concentration-dependent manner (Chen and Schier, 2001; Gurdon and Bourillot, 2001; Meno et al., 2001; Green, 2002). Fourth, Nodal signaling is restricted both spatially and temporally by the feedback inhibitor Lefty (Bisgrove et al., 1999; Meno et al., 1999; Agathon et al., 2001; Meno et al., 2001; Branford and Yost, 2002; Chen and Schier, 2002; Feldman et al., 2002).

1.7.2. Components of the Nodal signaling Pathway

Genetic and biochemical studies have dissected the Nodal signaling pathway, being the most common read-out of an active Nodal signaling pathway the induction of mesendodermal genes and tissues, phosphorylation of the downstream effector Smad2 and the development of the left-right axis. Nodal signaling is transmitted via components that are shared with other TGF-β signals, such as activin receptors and Smads. However, several proteins have been found to be more specific for Nodal signaling, namely EGF-CFC co-receptors and Lefty antagonists.

1.7.2.1. Nodals

Nodals constitute a group within the TGF-β super-family that seemed to be restricted to deuterostomia. However, although to date no Nodals have been found in flies or nematodes, recent work has reported the existence of a Nodal orthologue in a non-deuterostomia group, the Lophotrocozoa (Grande and Patel, 2008), suggesting that Nodal was present in the common ancestor of all bilaterians. In chordates, Nodals include the mouse Nodal, the zebrafish Cyclops, Squint and Southpaw, the *Xenopus* Xnr1, 2, 4, 5 and 6, the amphioxus AmphiNodal and a Nodal in ascidians.

In general terms, Nodals are secreted extra-cellularly and the signaling pathway is activated by the interaction of Nodals with activin receptors and EGF-CFC co-

receptors in the membrane (Figure 1.11). Nodal signaling is transmitted intra-cellularly by phophorylation of Smad2 and association with Smad4 and transcription factors, to then activate downstream targets. Nodal activates its own expression, as well as the expression of *lefty* genes (antagonists of the Nodal signaling pathway) and *pitx2* (bicoid-type homeobox transcription factor). *Lefty2* is induced in the left lateral plate mesoderm and *lefty1* in the left midline (Saijoh et al., 2000). Nodals have similar biochemical activities and the functional specificity is mostly controlled by the regulation of the expression of Nodal genes. However, Nodals can also differ in some activities. For example, the putative Nodal receptor ALK7 seems to interact with Xnr1 and Nodal, but not with Xnr2 and Xnr4 (Reissmann et al., 2001). Additionally, Nodals appear to differ in their range of activity *in vivo* (Jones et al., 1996; Chen and Schier, 2001; Niederlander et al., 2001). For instance, Squint and Cyclops have similar activity in inducing downstream genes, but only Squint activates the pathway in cells distant to the source (Chen and Schier, 2001). Nodal ligands can heterodimerize with other members of the TFG-ß super-family, such as Derriére and Bmp4, forming signaling factors with reduced or distinct activities (Yeo and Whitman, 2001; Eimon and Harland, 2002).

1.7.2.2. Convertases

As most TGF-β super-family members, Nodals are synthesized as pro-proteins that are proteolytically processed by subtilisin-like pro-protein convertases. Spc1 (Furin) and Spc4 (Pace4/Pcsk6) are the two convertases directly implicated in the maturation of Nodal (Beck et al., 2002) although, due to the ability for other convertases to cleave Nodal pro-proteins *in vitro*, other convertases might be involved in the maturation of Nodal *in vivo*. Although most TGF-β ligands do not exhibit signaling activity as pro-proteins, mutant pro-proteins that cannot be cleaved, such as Xnr2 and Nodal, retain their activity *in vivo* (Eimon and Harland, 2002; Ben-Haim et al., 2006).

1.7.2.3. Receptors

After maturation, the TGF-β ligands assemble a receptor complex consisting of type I and type II receptors that function as serine/threonine kinases (Attisano and Wrana, 2002; Shi and Massague, 2003). The type II receptor activates and phosphorylates the type I receptor, that in turn phosphorylates the downstream Smads. Nodal and activin have similar activities when over-expressed in *Xenopus*, suggesting that Nodals might act via the activin receptors ActRIB (ALK4), ActRIIA and ACtRIIB. Indeed, genetic studies have shown that activin receptors are involved in Nodal signaling (Oh and Li, 1997; Gu et al., 1999; Song et al., 1999) and *in vitro* studies demonstrate that Nodals can be part of a complex with activin receptors (Reissmann et al., 2001; Yeo and Whitman, 2001; Bianco et al., 2002; Sakuma et al., 2002; Yan et al., 2002). Although the type I receptor ALK7 is able to transduce Nodal signaling in the absence of EGF-CFC co-receptor (Reissmann et al., 2001) there is no evidence supporting that ALK7 is required for Nodal activity *in vivo* (Jornvall et al., 2004; Andersson et al., 2006).

1.7.2.4. Co-Receptors

Co-receptors are important components of the Nodal signaling pathway, namely EGF-CFC proteins. These are extra-cellular, GPI-linked proteins and EGF-CFC genes include the zebrafish *one-eyed pinhead*, the frog *FRL-1*, *XCR-1* and *XCR-2*, the chick *CFC* and the mouse and human c*ripto* and *cryptic* (Shen and Schier, 2000; Dorey and Hill, 2006). EGF-CFC proteins confer specificity for the type 1 receptor ALK4 (Yeo and Whitman, 2001; Yan et al., 2002). Zebrafish embryos lacking both maternal and zygotic one-eyed pinhead activity appear identical to *cyclops*; *squint* double mutants and do not respond to Nodals (Gritsman et al., 1999). In contrast, if the receptor ALK4 is activated, aspects of the *one-eyed pinhead* phenotype are rescued. Cripto mutants also share some phenotypic characteristics with Nodal mutants (Ding et al., 1998). The activity of EGF-CFC proteins is regulated both transcriptionally and post-translationally. The zebrafish *one-eyed pinhead*, chick

CFC, and mouse *cryptic* are expressed in the lateral plate mesoderm and overlap with regions where Nodals are assumed to determine left-right laterality. Misexpression of EGF-CFC proteins in chick can induce left-right defects (Schlange et al., 2001) being thus important to have a restricted expression pattern for these proteins. At the post-translation level, EGF-CFC activity can be modulated by O-linked fucose modification at Thr-88, as observed for the human Cripto (Schiffer et al., 2001; Yan et al., 2002). Site mutation results in weaker signaling activity. In certain contexts, EGF-CFC proteins can play distinct roles. For instance, mouse Cripto can act as a secreted trans-acting factor to mediate Nodal signaling, both *in vivo* and *in vitro* (Yan et al., 2002; Chu et al., 2005), whereas the Ras/Raf/MAPK and PI3K/Akt pathways can be activated in mammary epithelial cells in a Nodal-independent manner by soluble human Cripto protein (Bianco et al., 2002; Bianco et al., 2003).

1.7.2.5. Antagonists

Lefty is the antagonist of Nodal signaling and genetic studies have revealed important roles for this inhibitor. Lefty molecules are divergent members of the TGF-β super-family, ranging from a single *lefty* gene in ascidians to two *lefty* genes in mouse and zebrafish, namely *lefty1* and *lefty2* (also called antivins in zebrafish). Unlike other TGF-β-related factors, Leftys lack a cysteine residue necessary for the formation of covalently linked dimers and appear to be monomeric (Sakuma et al., 2002). Lefty proteins are secreted and antagonize Nodal signaling by interacting with EGF-CFC proteins and Nodal ligands, impeding the formation of receptor complexes (Chen and Shen, 2004; Cheng et al., 2004). These proteins do not function as competitive inhibitors of ALK4 and ActRIIB receptors since interactions with these receptors have not been found (Chen and Shen, 2004; Cheng et al., 2004). Over-expression of Leftys in zebrafish induces phenotypes very similar to *cyclops*; *squint* double mutants and maternal-zygotic *one-eyed pinhead* mutants (Bisgrove et al., 1999; Meno et al., 1999; Thisse and Thisse, 1999; Thisse et al., 2000). If Lefty is

lost, Nodal signaling is enhanced during mesendoderm induction and left-right development (Meno et al., 1999; Agathon et al., 2001; Meno et al., 2001; Branford and Yost, 2002; Chen and Schier, 2002; Feldman et al., 2002). Leftys activity is controlled at the transcriptional level. *Lefty* genes are frequently downstream targets of Nodal signaling, generating a negative-feedback mechanism (Meno et al., 1999; Branford and Yost, 2002; Feldman et al., 2002; Hamada et al., 2002).

In addition to secreted inhibitors, is has been proposed that several membrane-associated proteins are pathway antagonists, such as Tomoregulin-1 and Nicalin (Harms and Chang, 2003; Haffner et al., 2004). The relationship between these proteins and Nodal function *in vivo* remains to be clarified. At the intracellular level, several putative mechanisms for down-regulating the pathway activity have been described. For example, Dapper2 (Dpr2) functions as an antagonist of Activin/Nodal signaling pathway during zebrafish mesoderm formation by binding the endocytosed ALK4/ALK5 receptors and facilitating their degradation (Zhang et al., 2004).

1.7.2.6. Cytoplasmic and Nuclear Factors

As most TGF-β signals, Nodal signaling induces the phosphorylation of regulatory Smads, Smad2 and possibly Smad3 (Kumar et al., 2001; Lee et al., 2001; Yeo and Whitman, 2001). After being phosphorylated, Smads associate with the common mediator-(co-Smad) Smad4 (Massague et al., 2005), translocate into the nucleus and regulate downstream genes by interactions with specific transcription factors. However, other proteins may provide a co-Smad function: *in vivo* gene substitution experiments, in mouse, have shown that *smad3* can functionally replace *Smad2* (Dunn et al., 2005) and the phenotype of *smad4*-null mutants is less severe than that of *Nodal* or *Smad2*;*Smad3* double mutants (Chu et al., 2004).

FoxH1 and the Mixer subclass of homeodomain proteins are winged-helix transcription factors associated with P-Smad2/Smad3, leading to the formation of active transcription complexes on the enhancers of Nodal pathway target genes

(Germain et al., 2000; Whitman, 2001; Randall et al., 2004). Several enhancer elements, including those in *lefty2*, *Nodal*, *mix2* and *pitx2*, respond to Nodal signaling via FoxH1/P-smad2. However, it is not well understood how Nodal signaling regulates downstream targets. Genetic analyses in zebrafish indicate that FoxH1 and Mixer do not fully account for Nodal-mediated transcriptional events (Kunwar et al., 2003).

1.7.3. Upstream and Downstream of Nodal signaling

The upstream activators and downstream effectors of the Nodal signaling pathway are strongly depend on context, as for most signaling pathways.

Direct upstream activators of Nodals, in addition to Nodals themselves, include components of the Wnt signaling pathway, T-box transcription factors and Notch signaling. Several transcription factors and signaling molecules are included in the downstream effector genes but it is unclear if they are direct or indirect targets of the Nodal signaling pathway. The only gene that appears to be an effector of Nodal signaling both in mesendoderm induction and left-right patterning, besides Nodals and Leftys, is the *pitx2* homeobox gene. *Pitx2* is expressed in mesendoderm progenitors in *Xenopus* and zebrafish and in the left lateral plate mesoderm in all vertebrates studied so far (Burdine and Schier, 2000; Essner et al., 2000; Faucourt et al., 2001; Shiratori et al., 2001). Mice lacking *pitx2* exhibit a subset of left-right defects, including right pulmonary isomerism (Burdine and Schier, 2000), associated with anomalies in Nodal signaling. Cardiac looping appears to be initially unaffected in these mice, suggesting that there might exist other downstream targets of Nodal signaling during left-right development. In general, the Nodal signaling pathway is a self-regulatory cassette that is activated by diverse upstream regulators and regulates diverse downstream genes.

1.7.4. Nodal Signaling in Development

The Nodal signaling pathway is important for several aspects of development, namely mesendorderm induction, development of left-right axis and neural patterning.

1.7.4.1. Mesendoderm Induction

Genetic studies in mouse and zebrafish and inhibitor experiments in frog and chick established Nodals to be crucial for the induction of most mesendodermal and endodermal cell types. If Nodal signaling is absent in zebrafish, the embryos lack all head and trunk endoderm and mesoderm, including notochord, heart, kidney, blood, liver, pancreas and gut (Feldman et al., 1998; Gritsman et al., 1999). With the exception of some somites in the most posterior region of the embryo, Nodals are also required for the induction of all mesendodermal cell types. In *Xenopus*, Xnr1 in the vegetal region leads to a DV graded Nodal signal that induces a dose-dependent mesendoderm formation in the marginal zone (Agius et al., 2000; Kimelman, 2006).
Endoderm formation can be induced by over-expression of four of seven Mixer-related homeoproteins (Kofron et al., 2004). Mouse Nodal mutants do not form a primitive streak, which normally forms from mesendodermal progenitors (Zhou et al., 1993; Conlon et al., 1994). Ectopic expression of Nodal in the presumptive ectoderm can induce cells to become mesoderm or endorderm (Schier and Shen, 2000; Whitman, 2001).
Depending on the strength of Nodal signaling the formation of mesendoderm occurs in a greater or lesser extent. Mutations in mouse *lefty2* lead to a dramatically enlarged primitive streak (Meno et al., 1999). Likewise, blocking Lefty1 and Lefty2 function in zebrafish results in the formation of an expanded domain of mesendoderm progenitors and an enlarged germ ring (structure analogous to the mouse primitive streak) (Agathon et al., 2001; Chen and Schier, 2002; Feldman et al., 2002). Gene expression and fate map studies in zebrafish indicated that Nodal signaling acts before gastrulation to specify the progenitors of mesoderm and

endoderm. When Nodal signaling is missing the progenitors acquire fates that do not correspond to their position (Feldman et al., 2000; Carmany-Rampey and Schier, 2001).

1.7.4.2. Neural Patterning

Because Nodals are mesendoderm inducers, it is necessary that these signals are blocked in the prospective neuroectoderm for the nervous system to form (Piccolo et al., 1999; Thisse et al., 2000). This is achieved by the local generation of Nodals and the inhibition by Nodal antagonists. However, Nodal signaling is required for the specification of ventral cell types in the zebrafish nervous system during later stages of development (Schier and Talbot, 2001). Zebrafish mutants lacking the Nodal signal Cyclops and partial loss of the co-receptor one-eyed pinhead do not form the medial floor plate or the ventral forebrain. This results in cyclopic embryos (Hatta et al., 1991; Schier et al., 1997; Strahle et al., 1997). Some of these defects are not indirectly caused by defects in the development of the underlying axial mesoderm or endoderm but, instead, by a direct requirement for Nodal signaling in neural cells. During the establishment of the medial floor plate in the spinal cord and the posterior-ventral hypothalamus in the forebrain Nodal signaling is required in a cell-autonomous fashion (Strahle et al., 1997; Mathieu et al., 2002). Hypomorphic mutations of mouse *Nodal* and *FoxH1* mutations also results in the absence of ventral CNS fates. High levels of Nodal activity in the posterior epiblast are necessary to form the prechordal plate and anterior endoderm (Vincent et al., 2003), which in turn are required for ventral patterning of the neural tube and maintenance of the anterior forebrain. Loss or reduction of Nodal signaling can lead to phenotypes resembling human holoproencephaly, as observed in zygotic *oep* zebrafish or hypomorphic *Cripto* mouse mutants (Schier et al., 1997; Chu et al., 2005).

1.7.4.3. Left-Right Axis Determination

Nodal genes exhibit a conserved asymmetric expression pattern in the left side of the LPM that ranges from snails (*nodal*), ascidians (*HrNodal*), zebrafish (*cyclops* and *southpaw*) and *Xenopus* to rabbit, chick and mouse (*nodal*). Several studies highlight the requirement for Nodal during left-right patterning. During LR axis specification the Nodal pathway is required both in the node and in the left LPM (Raya and Belmonte, 2006; Shiratori and Hamada, 2006). Ectopic expression of Nodal in the right can induce the expression of left-side specific genes in the right. Also, hypomorphic Nodal mutations in mouse (Lowe et al., 2001; Norris et al., 2002) and depletion of the Nodal protein Southpaw in zebrafish (Long et al., 2003) lead to left-right defects. Despite the conserved asymmetric expression pattern in the left side of the LPM of *Nodal*, it is important to notice that these observations do not demonstrate without a doubt that Nodal is required in the left. *Nodal* and *southpaw* are expressed no only in the left LPM as also in additional regions, suggesting that they might act indirectly during left-right development. Removal of Nodal specifically in the left lateral plate mesoderm is required to fully establish its role in the left.

The Nodal signaling pathway is not required for the asymmetric development of organs *per se*, however it controls the laterality of asymmetry (Burdine and Schier, 2000; Hamada et al., 2002). Organ asymmetry becomes randomized or isomeric when Nodal is absent. For instance, the parapineal organ in the zebrafish brain, namely in the diencephalon, is normally located on the left. When Nodal signaling is absent the parapineal is located on the right side in approximately half of the mutants (Concha et al., 2000). Likewise, mouse *cryptic* (Nodal co-receptor) mutants present right isomerism by having the left lung mirror image the right one (Gaio et al., 1999; Yan et al., 1999). Because the downstream targets of the Nodal signaling pathway during left-right development remain to be discovered, with the exception of *pitx2*, it is largely unknown how Nodal signaling directs left-right morphogenesis.

The regulatory cascade controlling asymmetric Nodal expression resembles the interactions occurring during the early stages of development: Nodal starts by

being induced in the node in a Notch signaling-dependent way (Krebs et al., 2003; Przemeck et al., 2003; Raya et al., 2003) and is then induced in the left lateral plate mesoderm. Asymmetric induction of Nodal requires Nodal in the node, intact cilia and fluid flow (Nonaka et al., 1998; Brennan et al., 2002; Saijoh et al., 2003; Raya and Belmonte, 2006; Shiratori and Hamada, 2006) and, as mentioned earlier (see Chapter 1, section 1.5) two non-mutually exclusive models have been proposed to explain how the information from the leftward nodal flow is interpreted at the level of the lateral plate mesoderm: the chemical gradient model and the "two cilia"/physical stimulation model.

Nodal signaling in the lateral plate mesoderm plate induces *lefty2* in the left LPM and *lefty1* in the left midline (Saijoh et al., 2000; Yamamoto et al., 2003), thus inducing both locally and at a distance. The relationship between Lefty2 and Nodal during mouse left-right development resembles the roles of Leftys and Squint during mesendoderm induction. In the absence of Lefty2, *Nodal* expression erroneously remains and the downstream genes, including *Nodal* itself, are expressed on the right side (Meno et al., 2001). The relationship of *lefty1* and *lefty2* expression with the site of Nodal activity during the formation of the left-right axis is also very similar to their expression during mesendoderm formation in mouse. In this context, *lefty2* is expressed in the same domain as *Nodal*, whereas *lefty1* is expressed at a distance in the visceral endoderm. In both cases, Lefty1 and Lefty2 are involved in restricting Nodal signaling to a specific region of the embryo.

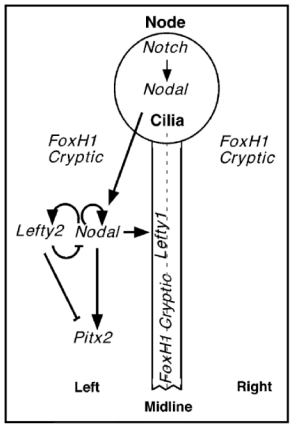

Figure 1.12 – A regulatory cascade establishes left-right asymmetry. Notch signaling induces *Nodal* expression in the mouse node. Nodal in the node is required for *Nodal* expression in the left lateral plate mesoderm. Cilia in the node are required for the left-side-specific activation of *Nodal*. Nodal in the left lateral plate auto-regulates, activates *pitx2* and *lefty2*, and induces *lefty1* in the left midline. The co-receptor cryptic and the phospho-Smad2 associated transcription factor FoxH1 are expressed symmetrically and in the midline to allow Nodal signaling in these regions. Adapted from Schier AF, 2003.

1.7.4.4. Body Axis Rotation and Body Wall Closure

The left-right cascade of asymmetric gene expression controls not only the asymmetry of visceral organs but also two other important processes: body axis rotation and body wall closure.

The rotation of the body axis, also known as "axial turning", follows the rightward looping of the heart tube. The rotation of the embryo from a dorsally flexed to a ventrally flexed position always happens in the same direction, resulting in several asymmetries, as revealed by the placement of the chorioallantoic placenta, tail and umbilical vessels to the right side and vitelline vessels to the left side of the embryo (reviewed by Fujinaga, 1997). This is true for the mouse, rat and many other mammals. A similar "body rotation" occurs in chick, between stages 11 and 20. It is suggested that "body rotation" is directed by asymmetric cell proliferation in the embryonic body and extra-embryonic membrane.

Pitx2 might be involved in this process due to its activities in the body wall mesoderm and amnion. In the mouse, *Pitx2* is expressed in both the left and the right distal ends of the lateral body wall mesoderm at E9-9.5, exhibiting a stronger expression in the left side, similar to the pattern observed in chick. *Pitx2*-defficient mice embryos fail to close the body wall and the abdominal and thoracic organs are extruded toward the left side (Gage et al., 1999; Kitamura et al., 1999; Lin et al., 1999; Lu et al., 1999), most likely due to the failure of the left lateral body wall to turn inward to meet the right lateral body wall. The mesoderm and the amnion appear to thicken on the left side of the embryo through an increase in cell proliferation, which creates physical constrains to the movement of the left body wall and the rotation of the posterior part of the embryos (Gage et al., 1999; Kitamura et al., 1999; Lin et al., 1999; Lu et al., 1999).

Although it may seem intuitive to assume that alterations in *situs* of abdominal organs should always follow alterations of *situs* of thoracic organs, this is not always the case. In fact, there are several situations where thoracic and abdominal *situs* are uncoupled. In some rare human syndromes, normal thoracic *situs* is accompanied by abdominal *situs inversus* or *ambiguous*, suggesting left-right development alterations

specific to the abdominal organs, probably involving alterations of gene expression in the posterior LPM.

In *lefty1*- deficient mice the laterality defects are restricted to thoracic organs, while *situs* of abdominal organs is normal (Meno et al., 1998). Studies on the regulatory sequences of mouse *lefty2* genes revealed that he left-specific enhancer of *lefty2* is composed of tow distinct elements, one for the anterior lefty LPM and another for the posterior left LPM (Saijoh et al, 1999), supporting the idea that the expression of key regulators of left-right development may be controlled independently in the thorax and abdomen.

1.7.4.5. Neurological Asymmetries

While the majority of molecular studies of left-right patterning have been interested in the asymmetry of visceral organs, one should be aware that the brain possesses its own asymmetry.

Nervous system lateralization is spread throughout evolution (Andrew, 2000), with significant implications for cognition (Harnad, 1977; McManus, 1999) . Anatomical differences between the left and the right hemispheres have been implicated in many aspects of brain function and dysfunction, such as the developmental disorders of schizophrenia, depression, autism and dyslexia (Morgan and Hynd, 1998; Steffens and Krishnan, 1998; Petty, 1999; Hendren et al., 2000; Robichon et al., 2000; Herbert et al., 2002; Pujol et al., 2002).

For long hemispheric specialization has been recognized: ancient Greeks knew that injuries specific to one side of the head lead to different symptoms from those occurring on the opposite side (Changeaux, 1985). Back in the 19th century, studies of patients presenting selective language deficits after stroke or a localized injury in the head allowed cognitive tasks to be assigned to particular brain regions (McManus, 2002).

While some animals often exhibit paw preference, the consistent preference among all individuals only approaches high levels in man (approximately 90% for right-handedness).

The genetic basis of handedness in man is still highly controversial (McManus, 1992; McManus, 1995). Left-handedness is transmitted weakly along the family since almost half of all left-handers have no known left-handed relatives (McManus, 1995). Monozygotic twins often differ in their handedness. Interestingly, certain neurological or behavioral asymmetries do not correlate with visceral asymmetry (Kennedy et al., 1999; Tanaka et al., 1999). For instance, when individuals present complete *situs inversus* they still have language lateralization and hand preference in 95% of normal right-handed individuals.

The incidence of left-handedness is the same in *situs inversus* individuals as in the rest of the population (Cockayne, 1938; Torgersen, 1950).

These observations seem to indicate that the mechanisms establishing the laterality of the brain are different from those determining the sidedness of visceral organs, during some early point of left-right determination.

Human patients with ciliary dyskenesia, or Kartagener's syndrome, and the attendant heterotaxia, do not show reversals in the normal prevalence of right-handedness (McManus, 2002). This means that at least some aspects of laterality in humans are indeed upstream of mutations affecting ciliary function. However, there are several studies supporting that the Nodal signaling pathway regulates some of the brain asymmetries.

There is symmetric expression in the brain of genes encoding EGF-CFC and FAST genes (Zhang et al., 1998; Concha et al., 2000; Pogoda et al., 2000) and asymmetric expression of *nodal* homologues and Pitx2 isoforms (Rebagliati et al., 1998a; Rebagliati et al., 1998b; Sampath et al., 1998; Thisse and Thisse, 1999; Concha et al., 2000; Essner et al., 2000). Also, the Nodal signaling pathway regulates anatomical asymmetry in the habenulae and pineal complex in zebrafish (Rebagliati et al., 1998a; Rebagliati et al., 1998b; Sampath et al., 1998; Thisse and Thisse, 1999; Concha et al., 2000; Essner et al., 2000; Liang et al., 2000).

In zebrafish, as in many lower vertebrates, the dorsal dienchephalic region of the forebrain, the epithalamus, is organized asymmetrically. It contains the pineal complex and the bilaterally paired dorsal habenular nuclei.

The habenulae display LR asymmetry in size, neurohistochemistry, cytoarchitectonic organization and connectivity. For example, in the lamprey, the right habenular nucleus is considerably larger than the left one (Yanez and Anadon, 1994). In amphibians, the habenulae are divided into major dorsal and ventral nuclei and asymmetries have been described between the dorsal nuclei (Braitenberg and Kemali, 1970; Kemali et al., 1990). At the cell morphology level, amphibians and reptiles exhibit asymmetries in the sub-nuclear organization of the habenulae and these asymmetries are also present in fish (Signore et al., 2008). In terms of neurohistochemistry, a discrete serotonin-immunoreactive sub-nucleus is found exclusively within the left habenulae of the coho salmon (Ekstrom and Ebbesson, 1988). The medial subnucleus of the left dorsal habenulae of the frog displays high levels of melatonin binding (Wiechmann and Wirsig-Wiechmann, 1993) and calretinin immunoreativity (Guglielmotti et al., 2004). Connectivity-wise left-right differences between the habenulae are associated with asymmetries in the major efferent pathway from the dorsal dienchephalon, the fasciculus retroflexus (FR). For instance, in both the lamprey and the Syberian sturgeon, the larger right habenula is associated with a thicker right FR, and in the sturgeon the right-sided axons have larger calibre than those in the left (Adrio et al., 2000).

The pineal complex often consists of two parts: the medial pineal (or epiphysis) and the frontal organ (amphibians), parietal organ (reptiles) or parapineal organ (fish) (Butler, 1996) (Figure 1.13).

The parapineal is asymmetrically positioned in the fish diencephalon (van Veen et al., 1980; Borg, 1983; Yanez and Anadon, 1994; Yanez and Anadon, 1996) and numerous morphological, biochemical and physiological left-right habenular differences have been discovered in a variety of vertebrates (Wehrmaker, 1969; Braitenberg and Kemali, 1970; Morgan et al., 1973; Kemali and Guglielmotti, 1977; Kemali and Guglielmotti, 1982; Guglielmotti and Fiorino, 1999; Concha et al., 2000; Concha and Wilson, 2001; Concha et al., 2003; Signore et al., 2008). The parapineal is originates at 28 hpf from the bilateral precursor cells, on either side of the midline, that begin to migrate toward the left habenula (Concha et al., 2003).

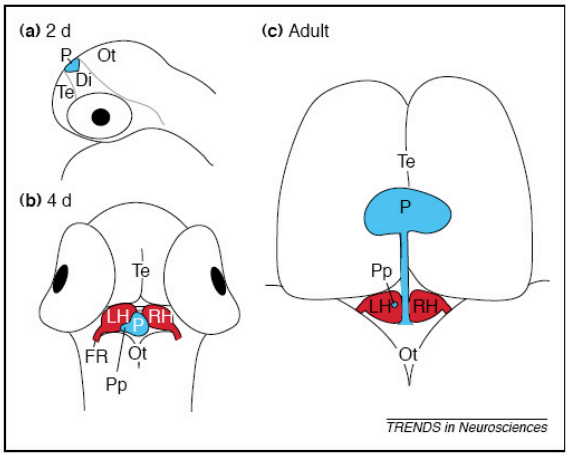

Figure 1.13 – Zebrafish epithalamic development. **(A)** Schematic side view of a 2-day-old zebrafish larval head, showing the pineal domain (P, blue) in the dorsal diencephalon (Di). **(B)** In a 4-day-old larva (dorsal view), the pineal complex consists of the pineal anlage (P) and the left-sided parapineal (Pp). The adjacent diencephalic nuclei, the left and right dorsal habenulae (LH and RH, respectively; red), are connected by a prominent commissure and send efferents through the fasciculus retroflexus (FR) to the midbrain. **(C)** In the adult epithalamus (dorsal view), the photoreceptive pineal end-vesicle (P) is connected to a stalk emerging from the diencephalic roof; the small parapineal remains closely apposed to the left habenulae. Ot, optic tectum; Te, telencephalon. Adapted from Halpern et al., 2003.

This asymmetric migration represents one of the earliest signs of asymmetry in the dorsal dienchephalon and is dependent on *fgf* signaling. Parapineal cells in zebrafish mutants for *fgf8* fail to migrate away from the midline (Regan et al., 2009). In teleosts, parapineal axons terminate in a defined rostro-dorsal region of the left habenula (Concha et al., 2003; Signore et al., 2008).

Expression studies have shown that genes encoding the Nodal-related factor Cyclops, Pitx2 and the Nodal-related antagonist Lefty1 are all transiently expressed on the left side of the bilateral pineal anlage (Liang et al., 2000) (Figure 1.14). The Nodal co-receptor *one-eyed pinhead* and *schmalspur*, which encodes a FoxH1 transcription factor that is active in Nodal receptive cells, are transcribed in a partially overlapping domain. Thus, the left diencephalon of the zebrafish embryo possesses the same inter-cellular signaling cassette as the left lateral plate mesoderm. Asymmetries in the epithalamus appear to be intimately connected with the morphogenesis of the pineal complex. When *cyclops*, *lefty1* and *pitx2* are bilaterally expressed, as observed in mutants with disrupted midline (Rebagliati et al., 1998a; Rebagliati et al., 1998b; Sampath et al., 1998; Thisse and Thisse, 1999; Bisgrove et al., 2000; Essner et al., 2000; Liang et al., 2000), the parapineal develops either to the left or right of the pineal. Conversely, mutations inactivating Nodal

signaling or reception inhibit left-sided gene expression in the pineal anlage (Concha et al., 2000; Gamse et al., 2003). Asymmetric Nodal signaling is not required for morphogenesis of the pineal. Instead, it positions outgrowth of the anlage along the left-right axis of the diencephalon (Liang et al., 2000). Additionally, Nodal signal influences parapineal position and habenular laterality (Concha et al., 2000; Gamse et al., 2002; Gamse et al., 2003). Recent studies have shown that, in order to repress Nodal signaling during gastrulation, proper regulation of Wnt/Axin/β-catenin signaling and function of Six3 proteins is required (Carl et al., 2007; Inbal et al., 2007). This is an essential prerequisite to allow later unilateral activation of the pathway exclusively on the left side of the brain.

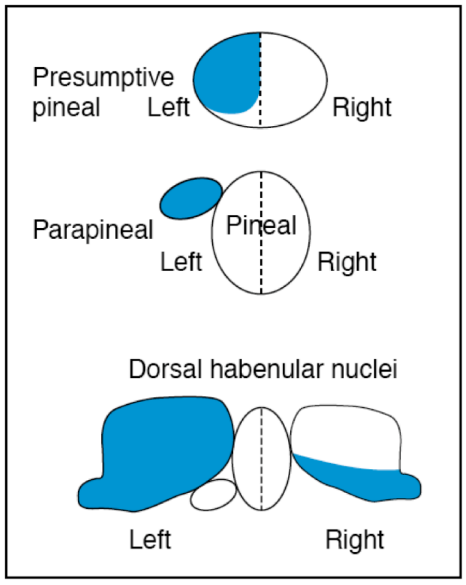

Figure 1.14 – Sequential appearance of epithalamic asymmetry from 20hpf to 2-days and 4 days. *Cyclops*, *lefty1* and *pitx2* (blue) are briefly transcribed on the left side of the presumptive pineal (20hpf). The parapineal forms to the left of the pineal (2-days). The dorsal habenular nuclei exhibit a characteristic left-right pattern (4-days). Adapted from Halpern et al, 2003.

The left habenula has higher density of neuropil than the right habenula (Concha et al., 2000) and several molecular markers are also expressed asymmetrically, such as the members of the potassium channel tetramerization domain-containing family *leftover* (*lov*), *right-on* (*ron*) and *dexter* (*dex*) (Gamse et al., 2003; Gamse et al., 2005). *Lov* is expressed more strongly on the left, whereas *ron* and *dex* are expressed more extensively in the right habenula. Asymmetry also exists in the afferent and efferent connectivities of the larval zebrafish habenulae. For instance, recent studies have

shown that a subset of neurons, on both sides of the brain, project axons that asymmetrically innervate the habenulae and terminate within a small medial domain of the right habenula (Hendricks and Jesuthasan, 2007).

Regardless of the sidedness, laterality of the parapineal and habenulae always correspond, suggesting that they are coordinately regulated (Concha et al., 2000; Gamse et al., 2002; Gamse et al., 2003).

The fact that brain asymmetry and visceral organ asymmetry can either rely or not on the same pathways might suggest that both visceral organ and neurological asymmetries may depend on the same symmetry breaking event but the pathways may diverge later such that some neurological asymmetries might depend on a novel regulatory cascade.

1.7.4.6. Novel Roles for the Nodal signaling Pathway

Unexpected functions to the Nodal pathway continue to emerge over recent studies. It has been proposed that maternal transcripts for the Nodal ligand *sqt* act as dorsal determinants in zebrafish (Gore et al., 2005). However, it was not clear what the significance of these findings was since the phenotype of maternal-zygotic *sqt* mutants resembles that of zygotic *sqt* mutants (Aoki et al., 2002), suggesting that maternal *sqt* transcripts are not required for dorsal specification. Indeed, work from Bennet et al. (2007) has shown that maternal *sqt* is not required for dorsal axis specification or for any other aspect of embryogenesis.

Nodal has also been implicated in the formation of the AP axis, in mouse, namely in the formation and directional movement of the AVE (anterior visceral endoderm). For instance, if Nodal is absent, the AVE does not form and there is no apparent AP axis (Brennan et al., 2001; Norris et al., 2002). The activity of the mouse Nodal pathway ligand Gdf3 is also necessary for AVE induction and movement because both processes are affected in *Gdf3*-null mutants (Chen et al., 2006).

Recent studies suggest that the Nodal signaling pathway is required for the maintenance of undifferentiated human and mouse embryonic stem (ES) cells. Over-

expression of Nodal in human ES cells inhibits mesoderm differentiation within embryoid bodies, maintains cells undifferentiated and promotes visceral endoderm differentiation (Vallier et al., 2004). These observations are consistent with findings that Nodal *in vivo* required for epiblast pluripotency maintenance and to prevent early neural differentiation (Ding et al., 1998; Brennan et al., 2001; Camus et al., 2006; Mesnard et al., 2006).

These are a few examples of some of the novel functions that have been suggested for Nodal. The extent to which there are conserved along evolution is currently unknown and further studies will be necessary.

1.7.5. Midline Barrier Model

The same way the Nodal signaling pathway is expressed in the left side of the embryo, there are pathways being expressed in the right lateral plate mesoderm. For instance, during the early stages of chick gastrulation, FGF-8 and BMP4 are expressed in the right side of the Hensen's node, establishing right-sided identity in the LPM (Boettger et al., 1999; Monsoro-Burq and Le Douarin, 2000).

Once local asymmetric signals in and around the node have been converted into broad domains of asymmetric gene expression with the LPM, it is crucial that the genes that have been activated either on the left or on the right side of the embryo remain confined to their original positions. Failure to maintain distinct domains of side-specific gene expression can result in a wide variety of laterality defects. In order to keep these extensive domains of asymmetrically expressed signals on the right and on the left sides of the embryo, there has to be a mechanism keeping them separate from each other.

Earlier studies suggested the existence of a barrier at the level of the embryonic dorsal midline, preventing signaling on one side of the embryo from interfering with cascades on the other. It has long been known, for instance, that twins conjoined at the level of the trunk often exhibit laterality disturbances and that the defects reside primarily in the right sibling. Similar effects are observed in spontaneous chick

conjoined twins or experimentally induced *Xenopus* conjoined twins (Levin et al., 1997; Nascone and Mercola, 1997).

Molecular genetic analyses revealed that the defects observed in the right twin are not due to an intrinsic error in the orientation of the left-right axis but instead a result of the interference from signals originating from the right flank of the left twin.

Mouse and zebrafish mutants with defects in the axial midline structures frequently display left-right patterning defects in conjunction with abnormal expression of left-side specific genes (Danos and Yost, 1996; Chen et al., 1997; Lohr et al., 1997; Dufort et al., 1998; King et al., 1998; Melloy et al., 1998; Izraeli et al., 1999). Surgical removal of midline structures from *Xenopus* embryos randomizes the heart looping and gut coiling, leading to bilateral expression of the *Nodal*-related genes (Danos and Yost, 1996; Lohr et al., 1997) .

Together, these observations led to the proposal that the midline barrier exists and that it prevents the contra-lateral diffusion of long-range, asymmetric signals either physically, biochemically or both (Levin et al., 1996; Meno et al., 1998).

1.7.5.1. Involvement of *Lefty1* in the Midline Barrier

Analysis of *lefty1* deficient mice provided valuable insight into the midline barrier problem. In the mouse, as in chick, *lefty1* is expressed in the left side of the node and the left half of the prospective floor plate (PFP) (Meno et al., 1996; Meno et al., 1997). Although the midline structures, including the notochord and the floorplate, develop normally, in the absence of *lefty1* the mouse embryos exhibit typical midline barrier defects, such as bilateral expression of *nodal*, *lefty2* and *pitx2* (left-side-specific genes) and pulmonary left isomerism (Meno et al., 1998). *Shh*, *SIL* and *nt* (no turning) mutant mice all show bilateral expression of left-side-specific genes as well as they all lack *Lefty1* expression in the prospective floorplate (Melloy et al., 1998; Izraeli et al., 1999; Meyers and Martin, 1999; Tsukui et al., 1999). These phenotypes indicate that Lefty1 induces/functions at the midline barrier,

preventing an unknown left-side-specific signaling molecule from crossing the midline.

Recent studies have shown that it is possible to disrupt asymmetric gene expression and still have normal *lefty1* expression in the midline (Ishimura et al., 2008). Man1, an inner nuclear membrane protein, regulates TGF-β signaling by interacting with receptor-associated Smads. In *man1*-deficient embryos, vascular remodeling is perturbed and embryos exhibit abnormal heart morphogenesis. Left side-specific genes responsible for LR asymmetry (*nodal*, *lefty2*, and *pitx2*) are expressed bilaterally in the LPM and notably, *lefty1* is maintained in the midline of *man1* mutants. In this study it is also suggested that Man1 regulates LR asymmetry by controlling Nodal signaling in a node-independent manner (Ishimura et al., 2008). Thus, *lefty1* expression is not being activated by Nodal in the node.

In such cases, how does *lefty1* function as the midline barrier?

1.7.5.2. Role of *Lefty1* in the Midline Barrier

In order to function as such, the barrier would have to restrict the passage of a signal (factor-X) across the midline. In the simplest model, Lefty1 protein could physically interact with that signal to prevent its diffusion. It has been suggested that Caronte might be the factor-X.

Caronte is a long-range signal identified in chick that can induce *Nodal* expression. It inhibits BMP and relays left-right information from the node to the left lateral plate mesoderm (Rodriguez Esteban et al., 1999; Yokouchi et al., 1999). The putative binding of Lefty1 to Caronte would prevent Caronte from interfering with the BMP-mediated repression of *Nodal* on the right side of the LPM. However, up until now there is no evidence for a direct interaction between the Caronte and the Lefty1 proteins. Another possibility is that Nodal itself is the factor-X, since Nodal is a long-range-acting molecule (Chen and Schier, 2001; Meno et al., 2001). Lefty1 from the floor plate might bind to Nodal receptors in the adjacent area and prevent Nodal activity from being propagated across the midline.

1.7.5.3. Production of *Lefty1* in the Midline

Asymmetric expression of *Nodal* in the left lateral plate mesoderm is controlled by ASE, a left-side specific enhancer (Adachi et al., 1999; Norris and Robertson, 1999; Norris et al., 2002), the most critical elements of which ate two FoxH1-binding sites (Adachi et al., 1999; Saijoh et al., 2000). These binding sites act as a Nodal-responsive element. FoxH1 is normally expressed bilaterally in the lateral plate mesoderm and in the midline and conditional knockout mice lacking FoxH1 specifically in the mesoderm lack the left-sided expression of *Nodal*, *Lefty2* and *Pitx2* in the lateral plate mesoderm. This reveals the requirement for FoxH1 to induce the expression of *Nodal* in the left lateral plate mesoderm. FoxH1 mutant mice also lack the expression of *Lefty1* in the prospective floor plate, although both *Nodal* and *Lefty1* expression are preserved in the node. These mice show various left-right defects with right isomerism as the major phenotype, resembling what is observed in cryptic mutant mice (Yan et al., 1999), consistent with a lack of Nodal. The fact that the expression of *Lefty1* was lost in the prospective floor plate was unexpected given that *FoxH1* is preserved in the midline structure, including the prospective floor plate. These observations suggest that *Lefty1* expression in the floor plate might be induced by Nodal produced in the lateral plate mesoderm. Indeed, transplantation and electroporation studies in mice confirm that *Lefty1* expression in the prospective floor plate is directly induced by Nodal produced in the lateral plate mesoderm (Yamamoto et al., 2003). Nodal in the LPM diffuses over to the PFP and induces *Lefty1* consistent with the notion that Nodal is able to act over a long distance (Chen and Schier, 2001; Meno et al., 2001). *Lefty1* expression in the left floor plate initiates slightly later than that of *Nodal* expression in the left LPM, suggesting that the midline barrier might be required only when the left-side signals, such as Nodal and Lefty2, are already present.

When Lefty1 is absent, the ectopic expression of the left-side-specific genes occurs mainly in the anterior region of the right side of the LPM (Meno et al., 1998), suggesting that the anterior and the posterior portions of the midline barrier are formed and/or maintained by distinct mechanisms. While Lefty1 might be a

component of the anterior midline barrier, the posterior portion of the midline barrier might involve a different process. This idea is supported by the fact that the posterior border of *Lefty1* expression ends at the node. The nature of the posterior midline barrier that lies posterior to the node remains unclear. However, it is known that excessive retinoic acid specifically perturbs the posterior midline function (Chazaud et al., 1999; Wasiak and Lohnes, 1999).

1.7.5.4. Cell death and the midline barrier

Kelly et al, 2002 addressed if specific components of the midline could be at the base of left-right expression maintenance. They showed that, in the chick embryo, the midline is formed from a distinct population of cells within the primitive streak. The cells in the dorsal midline of the primitive streak express the gastrulation markers *fgf8* and *brachury* and are fated to die. These dead cells remain in the midline throughout gastrulation. If cell death is inhibited in the midline the early expression of left-sided genes, such as *shh* and *nodal*, is disrupted. The expression of *shh* is significantly down-regulated and expanded into the right side of the node. Although still expressed asymmetrically, *nodal* expression is also down-regulated. These embryos exhibited randomized heart looping suggesting that cell death along the primitive streak midline might be a novel mechanism involved in the regulation of LR asymmetry during early embryogenesis (Kelly et al., 2002).

1.7.6. Asymmetric organ development

Shortly after asymmetric Nodal expression in the left lateral plate mesoderm and the mechanisms outlined above provide a specific, consistent bias to the organogenetic process, situs-specific morphogenesis is initiated in response to Nodal signaling. Organ primordia develop by performing a stereotyped choreography of loops and turns that lead to the normal disposition of organs.

1.7.6.1. *Pitx2*

An important factor acting downstream of Nodal signaling in the left lateral plate mesoderm is the bicoid-type homeobox transcription factor *Pitx2* (Logan et al., 1998; Piedra et al., 1998; Ryan et al., 1998; St Amand et al., 1998; Yoshioka et al., 1998; Campione et al., 1999; Gage et al., 1999; Kitamura et al., 1999; Lin et al., 1999; Lu et al., 1999; Essner et al., 2000; Schweickert et al., 2000).

Three differently spliced *Pitx2* transcripts correspond to the three different protein isoforms in the mouse (*Pitx2a*, *Pitx2b*, *Pitx2c*) and a fourth one *(Pitx2d*) has been identified in *Xenopus* (Essner et al., 2000; Schweickert et al., 2000; Faucourt et al., 2001). Of these, *Pitx2c* is expressed asymmetrically in the left lateral plate mesoderm of *Xenopus* and mouse. Zebrafish show a more complex pattern of expression, with *Pitx2c* left-sided in the developing gut mesoderm, and *Pitx2a* left-sided in the pre-cardiac mesoderm. Unlike other left-specific genes that are expressed in the lateral plate mesoderm, *Pitx2* is also expressed at subsequent stages in the left side of several organ primordia such as the main blood vessels, the sinus venosus, the vitelline vein and the cardinal vein, the common atrial chamber of the heart, the septum transversus (which will contribute to the liver) and the foregut region that corresponds to the lung bud. All these organs will lie on the left side of the body. Asymmetric *pitx2* expression is conferred by an enhancer containing three FoxH1-binding sites and a biding site for the homeobox transcription factor Nkx2 (Shiratori et al., 2001). The FoxH1-binding sites are essential for the initiation of the asymmetric expression, whereas the Nkx2-binding site is only necessary for the maintenance of late-stage expression. Therefore, Nodal initiates the left-sided expression of *Pitx2* and Nkx2 maintains it.

Pitx2 is responsible for generating left-side morphology of at least some of the visceral organs. Ectopic *Pitx2* expression can lead to laterality defects in several vertebrates (Logan et al., 1998; Ryan et al., 1998; Campione et al., 1999; Essner et al., 2000). Mouse embryos lacking *Pitx2* fail to achieve ventral body wall closure and exhibit arrested embryonic turning, probably due to a thickening of the mesoderm and amnion on the left side of the embryo (Gage et al., 1999; Kitamura et al., 1999;

Lin et al., 1999; Lu et al., 1999). Importantly, these mice also presented right pulmonary isomerism such that both the left and the right lungs frequently had four lobes, rather than the usual pattern of a single left and four right lobes. Involvement of *Pitx2* in heart asymmetry, although evident was less obvious than it might have been anticipated from the over-expression studies. Although complex defects resembling right atrial isomerism were observed, the hearts looped rightward and had normal expression of markers of asymmetric development. The direction of heart looping becomes randomized when asymmetric *pitx2c* function is depleted with antisense oligonucleotides (chick and *Xenopus*) or an engrailed repressor-Pitx2c fusion protein (chick) (Yu et al., 2001). It appears that asymmetric morphogenesis of the heart and the lung strongly depends on the dosage of Pitx2c (Liu et al., 2001). Because the *Pitx2*-null mutants have additional severe defects, the left-right defects in other visceral organs such as the stomach, gut, liver, spleen and vascular system have not been analyzed. Thus, it is not clear yet whether Pitx2 is required for normal development of all the asymmetric organs or only a subset.

In chick, *pitx2* leads to the counterclockwise coiling of the intestines by regulating left-right asymmetry changes in the architecture of the dorsal mesentery of the gut (Davis et al., 2008). *Pitx2* promotes asymmetry in both extra-cellular matrix and cell:cell adhesion (Kurpios et al., 2008).

Pitx2 has also been shown to regulate gonad morphogenesis. Although in most vertebrates the urogenital system is symmetrical and bilateral in both genders, in birds the bilateral development of paired gonads is sex-dependent (Kinsky, 1971). Female chick embryos undergo asymmetrical gonad morphogenesis that results in only one functional ovary, the left one. The right gonad degenerates at later stages of development. *Pitx2c* is expressed only in the left gonad and influences gonad shape and size by controlling somatic cell morphology, extra-cellular composition, spindle orientation and cell proliferation (Rodriguez-Leon et al., 2008).

1.7.6.2. *SnR* and *Nkx3.2*

Snail-related (SnR) and Nkx3.2 are two other transcription factors downstream of Nodal in the lateral plate mesoderm that are likely to influence left-right asymmetry development of organ primordia.

Nkx3.2 encodes a homeodomain protein that is left-sided in the chick and right sided in the mouse (Rodriguez Esteban et al., 1999; Schneider et al., 1999). In chick it is repressed by Nodal, but it is activated in the mouse. Mutant mice lacking *Nkx3.2* do not have obvious situs defects (Tribioli and Lufkin, 1999; Akazawa et al., 2000; Lettice et al., 2001) but they lack a spleen and have morphological abnormalities of the gastroduodenal portion of the gut. This phenotype might be regarded as left-right positional defects.

Snail-related encodes a zinc finger protein and is initially expressed in the anterior lateral plate mesoderm of streak-stage chick and mouse embryos in a bilateral pattern (Isaac et al., 1997; Sefton et al., 1998). The left-sided *SnR* expression disappears in both species shortly after *nodal* transcripts appear in the left lateral plate mesoderm and becomes stronger in the right lateral plate mesoderm. In chick, *Nodal* acts as a repressor of *SnR* and as an activator of *Nkx3.2*. Treatment of chick embryos with specific antisense oligonucleotides for *SnR* depletes *SnR* RNA and leads to bilateral expression of *Pitx2* and randomization of heart *situs* (Isaac et al., 1997). This observation suggests that SnR functions as a repressor of *Pitx2* and that *Nodal* activates *Pitx2* in the left lateral plate mesoderm through the repression of *SnR*. In addition, *SnR* also seems to act independently in the right side to influence the direction of heart looping (Patel et al., 1999).

1.7.6.3. Other Asymmetrically Expressed Genes

In addition to *Pitx2*, *SnR* and *Nkx3.2*, other genes exist that display side-specific expression patters in the heart, gut or stomach primordia. In zebrafish, *BMP4* is expressed predominantly in the left side of the heart tube and is required for normal cardiac left-right patterning (Chen et al., 1997; Schilling et al., 1999).

Rtk2 encodes an ephrin receptor and is expressed on the right side of the gut primordia. The adhesion protein DM-GRASP is expressed on the right side in the hepatic diverticulum (Schilling et al., 1999). In chick, the extra-cellular matrix proteins Flectin (Tsuda et al., 1998) and hLAMP (Smith et al., 1999) are expressed on the left side of the heart tube, whereas Fibrilin-2 is expressed in the right side (Smith et al., 1997). Despite all these observations, very little is known about how asymmetric organ development is controlled at the cellular level.

The first organ to exhibit left-right asymmetry is the heart, followed by asymmetric lobe formation in the lungs, rotation and coiling of the digestive tract and regression of parts of the vascular system on one side. The liver and the pancreas occupy asymmetric positions relative to the midline and the intestine bends and folds in a complex pattern in order to fit into the abdominal cavity. The asymmetric development of the intestine appears to depend on increased growth rate in two specific places: the duodenum and the central part of the primitive loop. In zebrafish, the first leftward bend in the developing intestine arises through a morphogenetic process known as gut looping and recent studies propose that a dynamic asymmetric migration of the LPM causes the initial leftward bend (Horne-Badovinac et al., 2003). Similarly, it is known that the left side of the stomach primordia has an increased growth rate that results in the so-called "great curvature" of the stomach and, secondarily, in the correct positioning of the spleen in the left upper side of the abdominal cavity. In *Xenopus*, the tissue that gives rise to the spleen is initially located in symmetric domains on both sides of the embryo. Only cells on the left side go on to form the mature spleen, in a process that does not appear to involve either differential cell death or cell migration (Patterson et al., 2000). It is therefore clear that local processes involving differential control of cell proliferation and/or cell death, as well as instructive changes in cell fate and behavior are likely to be involved in directing asymmetric development of specific organs. However, clear links between the activity of particular genes and specific morphogenetic or proliferative functions in organ primordia are still poorly known.

1.7.7. Heart asymmetric morphogenesis

Because the main focus of thesis main is the zebrafish heart, the following lines are intended to give an overview on what is known about general cardiac morphogenesis in this organism.

In vertebrates, the heart is the first organ to form and function during embryogenesis. In zebrafish, the heart is initially composed of two concentric layers, an outer muscular layer (the myocardium) and an inner endothelial layer (the endocardium), that together form a simple, linear tube, just before circulation is established. Later, the two-layered tube loops and is subdivided into two major chambers, the atrium and the ventricle, with unidirectional blood flow (Figure 1.15). Although at a first glance the heart seems to bear an uncomplicated architecture, complex aspects underlay its formation. The first step involves pattern formation events for the specification of the cell types essential for cardiac development. These include endocardial and myocardial lineages and separate ventricular and atrial myocardial lineages. However, they have distinct embryonic origins: cardiac muscle cells originate from the anterior lateral plate mesoderm whereas skeletal muscle cells derive from the paraxial mesoderm. Endothelial cells line the entire vascular system, including the lumen of the heart. Differentiation of cardiac precursor cells begins around 16 hours-post-fertilization (hpf) and takes place in the anterior lateral plate mesoderm (ALPM) of both the right and the left side of the embryo (Figure 1.15C). Then, the cells migrate and converge to the embryonic midline (i.e., primitive streak in mouse and chick, and dorsal midline in fish and frog), where they form the linear heart tube, in concert with the medial movement of the entire ALPM (Figure 1.15E). Cardiac migration appears to be organized, with the medially located ventricular precursors advancing first than the laterally located atrial precursors (Yelon et al., 1999). One key pre-requisite for myocardial cells to migrate is proper myocardial differentiation, since all zebrafish mutations causing myocardial deficiencies lead to *cardia bifida* (two separate hearts form in lateral positions) (Chen et al., 1996; Stainier et al., 1996; Alexander et al., 1998). However, normal myocardial differentiation is not sufficient to drive cardiac migration. Correct

differentiation of the closely juxtaposed endodermal precursors is also required (Schier et al., 1997; Alexander and Stainier, 1999; Reiter et al., 1999; Kikuchi et al., 2000; Dickmeis et al., 2001; Kikuchi et al., 2001). Once the myocardial precursors have reached the midline, they fuse, in a process known as cardiac fusion (Yelon et al., 1999). The first contact occurs between the two populations of ventricular precursors, at a relative posterior point, followed by junction of the myocardiocytes posterior to the initial junction.

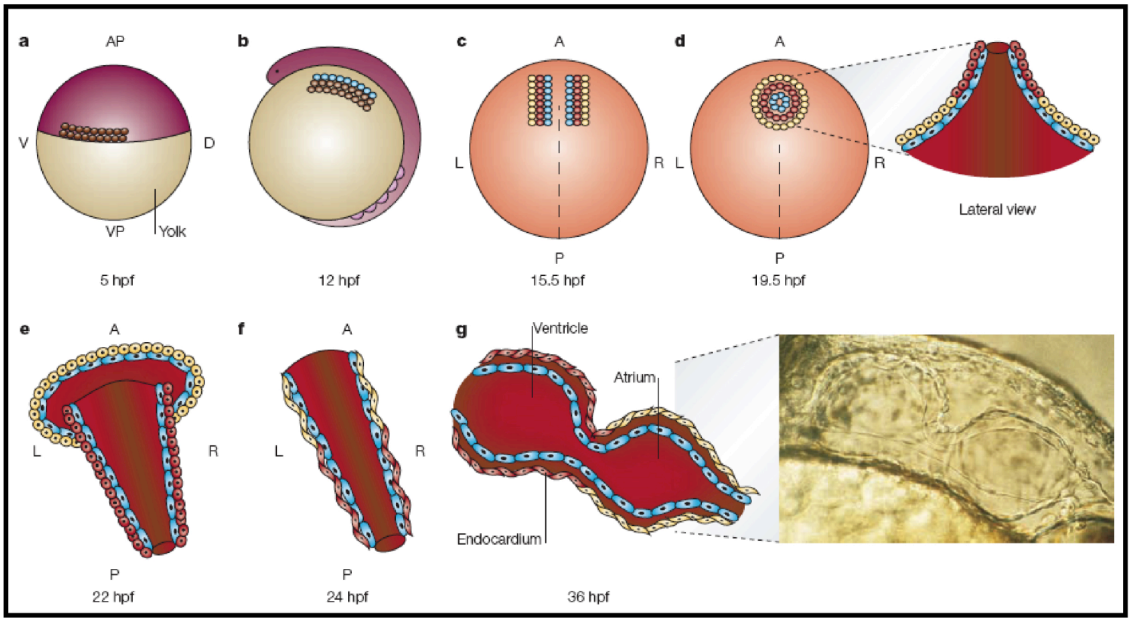

Figure 1.15 – Zebrafish heart development. (A) Just before gastrulation, 5 hours post-fertilization (hpf), the heart progenitor cells are located throughout the ventral and lateral regions of the embryo. **(B)** After involution, these cells converge toward the embryonic axis and reach their destination at the level of the future hindbrain by the five-somite stage (~ 12 hpf). Three rows of cells are represented at this stage, the endocardial precursors (blue) lie most medially and the myocardial precursors most laterally (Alexander and Stainier, 1999). **(C)** By the 13-somite stage (15.5 hpf), the myocardial precursors have segregated into pre-ventricular (red) and pre-atrial (Yellow) groups, although this segregation might well happen earlier (Yelon et al, 1999). **(D)** starting at 19 hpf, the myocardial precursors merge posteriorly to form a horseshoe-shaped structure. By 19.5 hpf, as anterior cells migrate medially, the horseshoe transforms into a cone with the ventricular cells (red) and its centre and apex, an the atrial cells (yellow) at its base. The endocardial cells (blue) line in the inside of the cone. **(E)** Next, the cone telescopes out to form a tube, The ventricular end of the heart tube assembles first, followed by the atrial end. **(F)** By24 hpf, the tube lies along the anterior-posterior axis with the atrial end to the left of the midline. Subsequently, by 30 hpf, visibly distinct ventricular and atrial chambers form. **(G)** By 36 hpf, the heart undergoes looping morphogenesis and, by 48 hpf, functional valves are formed. (A, anterior; AP, animal pole; D, dorsal; P, posterior; V, ventral; VP, vegetal pole; L, left; R, right). Adapted from Stainier, 2001.

This creates a v-shaped structure that, upon connection of the most anterior populations, generates a ring centered in a lumen.

A complex series of morphogenetic events have to take place in order to properly assemble the heart tube at the embryonic midline. One of the critical events leading to heart tube formation in zebrafish is the assembly of the heart cone (Figure 1.15D) (Stainier et al., 1993; Yelon et al., 1999). The apex of this cone will become the arterial (ventricular) end of the heart, whereas the base of the cone will become the venous (atrial) end. Initially, the cone orients along the dorso-ventral axis but then rapidly reorients by 90°, to extend and lie along the anterior-posterior axis and position the venous end of the heart to the left of the midline. Between 24 and 48 hpf, the linear heart tube gradually bends at the boundary between the ventricle and the atrium in a process called cardiac lopping and creates a S-shaped loop. The ventricle then lies to the right of the atrium. The cardiac tube undergoes a series of bending and rotational movements in looping morphogenesis, necessary to establish structural asymmetry within the heart and to establish proper organ placement within the body. As soon as the heart tube forms it begins to function and drive circulation with regular, peristaltic contractions by 24 hpf (Warren and Fishman, 1998). Cardiac differentiation and morphogenesis continues while the heart is working, building on the foundation of the initial embryonic tube to produce the final form of the adult heart. In addition to cardiac looping, aspects of cardiac remodeling include valve formation, thickening of the ventricular wall and formation of ventricular trabeculae (Hu et al., 2000; Hu et al., 2001).

The heart can be more easily observed and manipulated than other internal organs and is thus one of the first organs to be investigated in many model organisms. Because the zebrafish has several advantages as a genetic and embryological model organism for studying vertebrate developmental processes, it is of great application to the study of cardiac development. Zebrafish embryos are small, easy to care for, have a fast generation time and external fertilization thus developing outside of the mother. The transparency and optical clarity of the embryos allows high-resolution visualization of the heart during its fast

development. Because of their small size, zebrafish embryos are not completely dependent on a functional cardiovascular system. Even in the total absence of blood circulation, they receive enough oxygen by passive diffusion to survive and continue to develop in a relatively normal fashion for several days, allowing a detailed analysis of animals with severe cardiovascular defects (by contrast, avian and mammalian embryos die rapidly in the absence of a functional cardiovascular system). Moreover, the fish is a vertebrate, and therefore its genetic program is more similar to that of mammals than invertebrate models.

2. Aims and Structure of the Thesis

As described, in zebrafish, the heart tube is composed of two concentric layers: the myocardium (outer muscular layer) and the endocardium (inner endothelial layer), and gradually progresses to form two discrete chambers, a ventricle and an atrium. In higher vertebrates the two chambers are later divided by a septum, originating four chambers (Harvey, 2002; Moorman and Christoffels, 2003). Defects occurring during left-right patterning of the embryo heart result in congenital heart defects such as transposition of the great arteries or double-outlet-right-ventricle, having major consequences for proper heart function after birth (Ramsdell, 2005). It is thus of great importance to understand the mechanisms by which left-right signals control asymmetric cardiac development. For instance, *Pitx2* is essential for situs-specific remodeling of the branchial arch arteries, inducing dynamic morphological changes in the outflow tract and generating a differential distribution of blood flow that maintains the aortic arch on the left side (Yashiro et al., 2007). Although several genes are expressed asymmetrically on the left side of the lateral plate mesoderm already prior to the formation of the heart tube, such as *spaw*, *lefty1*, *lefty2* and *pitx2*, it remains unclear how the Nodal signaling pathway correlates with the events taking place during the early asymmetric morphogenesis of the heart. The cellular mechanisms underlying left-right asymmetric organogenesis are still largely elusive. The zebrafish presents itself as a high-resolution model to address the regulation of vertebrate heart asymmetry

acquisition. Analysis of cell movements, shapes and rearrangements during cardiac development, in wild type and mutants for the genes involved in asymmetric organogenesis, will shed some light upon this field and bring a deeper understanding (Horne-Badovinac et al., 2003; Yashiro et al., 2007; Davis et al., 2008; Kurpios et al., 2008; Rohr et al., 2008; Smith et al., 2008).

The results presented during the next chapters aim to address how the Nodal signaling pathway regulates the acquisition of asymmetry during the early morphogenesis of the zebrafish heart, particularly at the cellular level. Our first approach was to perform high resolution time-lapse imaging of the initial steps of heart development in fish, taking advantage of the *cmlc2:*GFP transgenic zebrafish embryos. These fish express GFP specifically in the cardiac cells. 3D reconstructions of such time-lapse movies allowed us to characterize the overall movement of the cardiac structure as well as to assess aspects of individual cell migration during this process, such as speed variation, displacement rate, meandering index, relative position, neighbor relationships and direction of movement. Atrial and ventricular cell populations were also analyzed and compared base on these criteria in order to address if a correlation exists between cell type fate and cell type behavior. After careful characterization of the cellular movements in the wild type heart, we aimed to understand how the cell movements were affected in the absence of *Nodal* signal. In order to address this question we performed the same set of imaging and analyzes procedures in LZ*oep* mutants, lacking the co-receptor for Nodal and thus deficient for the Nodal signaling pathway (Chapter II – published in *Developmental Dynamics* 237:3624 – 3633, 2008). In order to confirm and reinforce the results obtained from the analyzes of *LZoep* fish we next addressed how cellular speed variation, displacement rate, meandering index, relative position, neighbor relationships and direction of movement vary when the Nodal signaling pathway is bilaterally expressed or expressed in the right lateral plate mesoderm, contrary of being expressed in the left LPM as it normally happens in the wild type. We used morpholinos to abolish the expression of *no tail* and thus induce bilateral expression of *Nodal* in the LPM. Likewise, morpholinos were also used against *polaris* in order

to obtain embryos expressing *Nodal* in the right LPM (Chapter III – unpublished data). Overall, our results show that the Nodal signaling pathway governs asymmetry acquisition in the zebrafish heart by promoting the speed and directional movement of cardiomyocytes in zebrafish.

During our studies it became evident that the first morphological visible sign of asymmetry during the early formation of the zebrafish heart is not yet clear. Throughout the first steps of heart development, the initially symmetrical cardiac structure undergoes several events that are amenable of breaking symmetry and making it asymmetric. These include a clockwise rotation of the heart cone, a leftward displacement of the prospective endocardium (the lumen at the center of the cardiac structure), involution of the right cells toward the left side and expansion of the left-anterior most cells toward the left. These morphological landmarks have been observed and reported by us and by other groups (Smith et al, 2008; Rohr et al, 2008, unpublished observations) but not yet addressed regarding its order of appearance or if these events are coupled, if at all. We undertook this question and performed double-fluorescent *in situ* hybridization in wild type embryos fixed during the early onset of heart development. Confocal analyzes of the heart features relative to the midline (landmark defining the center) and 3D reconstructions/spatial rotations seem to indicate that lumen displacement is the first visible sign of asymmetry during cardiac formation (Chapter IV – unpublished data). Finally, Chapter V congregates the conclusions from Chapter II, III and IV and integrates/discusses them at the light of the general knowledge in the field.

3. REFERENCES

Adachi H, Saijoh Y, Mochida K, Ohishi S, Hashiguchi H, Hirao A, Hamada H. 1999. Determination of left/right asymmetric expression of nodal by a left side-specific enhancer with sequence similarity to a lefty-2 enhancer. Genes Dev 13:1589-1600.

Adrio F, Anadon R, Rodriguez-Moldes I. 2000. Distribution of choline acetyltransferase (ChAT) immunoreactivity in the central nervous system of a chondrostean, the siberian sturgeon (Acipenser baeri). J Comp Neurol 426:602-621.

Afzelius BA. 1976. A human syndrome caused by immotile cilia. Science 193:317-319.

Agathon A, Thisse B, Thisse C. 2001. Morpholino knock-down of antivin1 and antivin2 upregulates nodal signaling. Genesis 30:178-182.

Agius E, Oelgeschlager M, Wessely O, Kemp C, De Robertis EM. 2000. Endodermal Nodal-related signals and mesoderm induction in Xenopus. Development 127:1173-1183.

Akazawa H, Komuro I, Sugitani Y, Yazaki Y, Nagai R, Noda T. 2000. Targeted disruption of the homeobox transcription factor Bapx1 results in lethal skeletal dysplasia with asplenia and gastroduodenal malformation. Genes Cells 5:499-513.

Alexander J, Stainier DY. 1999. A molecular pathway leading to endoderm formation in zebrafish. Curr Biol 9:1147-1157.

Alexander J, Stainier DY, Yelon D. 1998. Screening mosaic F1 females for mutations affecting zebrafish heart induction and patterning. Dev Genet 22:288-299.

Amack JD, Wang X, Yost HJ. 2007. Two T-box genes play independent and cooperative roles to regulate morphogenesis of ciliated Kupffer's vesicle in zebrafish. Dev Biol 310:196-210.

Andersson O, Reissmann E, Jornvall H, Ibanez CF. 2006. Synergistic interaction between Gdf1 and Nodal during anterior axis development. Dev Biol 293:370-381.

Andrew R. 2000. The earliest origins and subsequent evolution of lateralisation. Rogers, L.J., Andrew, R.J. (Eds.), Comparative vertebrate lateralisation. Cambridge University Press, Cambridge.

Aoki TO, Mathieu J, Saint-Etienne L, Rebagliati MR, Peyrieras N, Rosa FM. 2002. Regulation of nodal signalling and mesendoderm formation by TARAM-A, a TGFbeta-related type I receptor. Dev Biol 241:273-288.

Attisano L, Wrana JL. 2002. Signal transduction by the TGF-beta superfamily. Science 296:1646-1647.

Baker K, Holtzman NG, Burdine RD. 2008. Direct and indirect roles for Nodal signaling in two axis conversions during asymmetric morphogenesis of the zebrafish heart. Proc Natl Acad Sci U S A 105:13924-13929.

Bamford RN, Roessler E, Burdine RD, Saplakoglu U, dela Cruz J, Splitt M, Goodship JA, Towbin J, Bowers P, Ferrero GB, Marino B, Schier AF, Shen MM, Muenke M, Casey B. 2000. Loss-of-function mutations in the EGF-CFC gene CFC1 are associated with human left-right laterality defects. Nat Genet 26:365-369.

Beck S, Le Good JA, Guzman M, Ben Haim N, Roy K, Beermann F, Constam DB. 2002. Extraembryonic proteases regulate Nodal signalling during gastrulation. Nat Cell Biol 4:981-985.

Ben-Haim N, Lu C, Guzman-Ayala M, Pescatore L, Mesnard D, Bischofberger M, Naef F, Robertson EJ, Constam DB. 2006. The nodal precursor acting via activin receptors induces mesoderm by maintaining a source of its convertases and BMP4. Dev Cell 11:313-323.

Bianco C, Adkins HB, Wechselberger C, Seno M, Normanno N, De Luca A, Sun Y, Khan N, Kenney N, Ebert A, Williams KP, Sanicola M, Salomon DS. 2002. Cripto-1 activates nodal- and ALK4-dependent and -independent signaling pathways in mammary epithelial Cells. Mol Cell Biol 22:2586-2597.

Bianco C, Strizzi L, Rehman A, Normanno N, Wechselberger C, Sun Y, Khan N, Hirota M, Adkins H, Williams K, Margolis RU, Sanicola M, Salomon DS. 2003. A Nodal- and ALK4-independent signaling pathway activated by Cripto-1 through Glypican-1 and c-Src. Cancer Res 63:1192-1197.

Birsoy B, Kofron M, Schaible K, Wylie C, Heasman J. 2006. Vg 1 is an essential signaling molecule in Xenopus development. Development 133:15-20.

Bisgrove BW, Essner JJ, Yost HJ. 1999. Regulation of midline development by antagonism of lefty and nodal signaling. Development 126:3253-3262.

Bisgrove BW, Essner JJ, Yost HJ. 2000. Multiple pathways in the midline regulate concordant brain, heart and gut left-right asymmetry. Development 127:3567-3579.

Blum M, Andre P, Muders K, Schweickert A, Fischer A, Bitzer E, Bogusch S, Beyer T, van Straaten HW, Viebahn C. 2007. Ciliation and gene expression

distinguish between node and posterior notochord in the mammalian embryo. Differentiation 75:133-146.

Boettger T, Wittler L, Kessel M. 1999. FGF8 functions in the specification of the right body side of the chick. Curr Biol 9:277-280.

Borg B. 1983. The parapineal organ of teleosts. Acta. Zool. 64:211-218.

Braitenberg V, Kemali M. 1970. Exceptions to bilateral symmetry in the epithalamus of lower vertebrates. J Comp Neurol 138:137-146.

Branford WW, Yost HJ. 2002. Lefty-dependent inhibition of Nodal- and Wnt-responsive organizer gene expression is essential for normal gastrulation. Curr Biol 12:2136-2141.

Brennan J, Lu CC, Norris DP, Rodriguez TA, Beddington RS, Robertson EJ. 2001. Nodal signalling in the epiblast patterns the early mouse embryo. Nature 411:965-969.

Brennan J, Norris DP, Robertson EJ. 2002. Nodal activity in the node governs left-right asymmetry. Genes Dev 16:2339-2344.

Brown NA, Wolpert L. 1990. The development of handedness in left/right asymmetry. Development 109:1-9.

Buceta J, Ibanes M, Rasskin-Gutman D, Okada Y, Hirokawa N, Izpisua-Belmonte JC. 2005. Nodal cilia dynamics and the specification of the left/right axis in early vertebrate embryo development. Biophys J 89:2199-2209.

Burdine RD, Schier AF. 2000. Conserved and divergent mechanisms in left-right axis formation. Genes Dev 14:763-776.

Butler AaH, W. 1996. Comparative vertebrate neuroanatomy: evolution and adaptation. Wiley-Liss.

Campione M, Steinbeisser H, Schweickert A, Deissler K, van Bebber F, Lowe LA, Nowotschin S, Viebahn C, Haffter P, Kuehn MR, Blum M. 1999. The homeobox gene Pitx2: mediator of asymmetric left-right signaling in vertebrate heart and gut looping. Development 126:1225-1234.

Camus A, Perea-Gomez A, Moreau A, Collignon J. 2006. Absence of Nodal signaling promotes precocious neural differentiation in the mouse embryo. Dev Biol 295:743-755.

Capdevila J, Vogan KJ, Tabin CJ, Izpisua Belmonte JC. 2000. Mechanisms of left-right determination in vertebrates. Cell 101:9-21.

Carl M, Bianco IH, Bajoghli B, Aghaallaei N, Czerny T, Wilson SW. 2007. Wnt/Axin1/beta-catenin signaling regulates asymmetric nodal activation, elaboration, and concordance of CNS asymmetries. Neuron 55:393-405.

Carmany-Rampey A, Schier AF. 2001. Single-cell internalization during zebrafish gastrulation. Curr Biol 11:1261-1265.

Cartwright JH, Piro O, Tuval I. 2004. Fluid-dynamical basis of the embryonic development of left-right asymmetry in vertebrates. Proc Natl Acad Sci U S A 101:7234-7239.

Casey B, Hackett BP. 2000. Left-right axis malformations in man and mouse. Curr Opin Genet Dev 10:257-261.

Changeaux J. 1985. Neuronal man: The biology of mind. Pantheon Books, New York.

Chazaud C, Chambon P, Dolle P. 1999. Retinoic acid is required in the mouse embryo for left-right asymmetry determination and heart morphogenesis. Development 126:2589-2596.

Chen C, Shen MM. 2004. Two modes by which Lefty proteins inhibit nodal signaling. Curr Biol 14:618-624.

Chen C, Ware SM, Sato A, Houston-Hawkins DE, Habas R, Matzuk MM, Shen MM, Brown CW. 2006. The Vg1-related protein Gdf3 acts in a Nodal signaling pathway in the pre-gastrulation mouse embryo. Development 133:319-329.

Chen JN, Haffter P, Odenthal J, Vogelsang E, Brand M, van Eeden FJ, Furutani-Seiki M, Granato M, Hammerschmidt M, Heisenberg CP, Jiang YJ, Kane DA, Kelsh RN, Mullins MC, Nusslein-Volhard C. 1996. Mutations affecting the cardiovascular system and other internal organs in zebrafish. Development 123:293-302.

Chen JN, van Eeden FJ, Warren KS, Chin A, Nusslein-Volhard C, Haffter P, Fishman MC. 1997. Left-right pattern of cardiac BMP4 may drive asymmetry of the heart in zebrafish. Development 124:4373-4382.

Chen Y, Schier AF. 2001. The zebrafish Nodal signal Squint functions as a morphogen. Nature 411:607-610.

Chen Y, Schier AF. 2002. Lefty proteins are long-range inhibitors of squint-mediated nodal signaling. Curr Biol 12:2124-2128.

Cheng SK, Olale F, Brivanlou AH, Schier AF. 2004. Lefty blocks a subset of TGFbeta signals by antagonizing EGF-CFC coreceptors. PLoS Biol 2:E30.

Chu GC, Dunn NR, Anderson DC, Oxburgh L, Robertson EJ. 2004. Differential requirements for Smad4 in TGFbeta-dependent patterning of the early mouse embryo. Development 131:3501-3512.

Chu J, Ding J, Jeays-Ward K, Price SM, Placzek M, Shen MM. 2005. Non-cell-autonomous role for Cripto in axial midline formation during vertebrate embryogenesis. Development 132:5539-5551.

Cockayne E. 1938. The genetics of transposition of the viscera. Quaterly J. Med. 31.

Collignon J, Varlet I, Robertson EJ. 1996. Relationship between asymmetric nodal expression and the direction of embryonic turning. Nature 381:155-158.

Concha ML, Burdine RD, Russell C, Schier AF, Wilson SW. 2000. A nodal signaling pathway regulates the laterality of neuroanatomical asymmetries in the zebrafish forebrain. Neuron 28:399-409.

Concha ML, Russell C, Regan JC, Tawk M, Sidi S, Gilmour DT, Kapsimali M, Sumoy L, Goldstone K, Amaya E, Kimelman D, Nicolson T, Grunder S, Gomperts M, Clarke JD, Wilson SW. 2003. Local tissue interactions across the dorsal midline of the forebrain establish CNS laterality. Neuron 39:423-438.

Concha ML, Wilson SW. 2001. Asymmetry in the epithalamus of vertebrates. J Anat 199:63-84.

Conlon FL, Barth KS, Robertson EJ. 1991. A novel retrovirally induced embryonic lethal mutation in the mouse: assessment of the developmental fate of embryonic stem cells homozygous for the 413.d proviral integration. Development 111:969-981.

Conlon FL, Lyons KM, Takaesu N, Barth KS, Kispert A, Herrmann B, Robertson EJ. 1994. A primary requirement for nodal in the formation and maintenance of the primitive streak in the mouse. Development 120:1919-1928.

Cooper MS, D'Amico LA. 1996. A cluster of noninvoluting endocytic cells at the margin of the zebrafish blastoderm marks the site of embryonic shield formation. Dev Biol 180:184-198.

D'Amico LA, Cooper MS. 1997. Spatially distinct domains of cell behavior in the zebrafish organizer region. Biochem Cell Biol 75:563-577.

Danos MC, Yost HJ. 1996. Role of notochord in specification of cardiac left-right orientation in zebrafish and Xenopus. Dev Biol 177:96-103.

Davis NM, Kurpios NA, Sun X, Gros J, Martin JF, Tabin CJ. 2008. The chirality of gut rotation derives from left-right asymmetric changes in the architecture of the dorsal mesentery. Dev Cell 15:134-145.

Dickmeis T, Mourrain P, Saint-Etienne L, Fischer N, Aanstad P, Clark M, Strahle U, Rosa F. 2001. A crucial component of the endoderm formation pathway, CASANOVA, is encoded by a novel sox-related gene. Genes Dev 15:1487-1492.

Ding J, Yang L, Yan YT, Chen A, Desai N, Wynshaw-Boris A, Shen MM. 1998. Cripto is required for correct orientation of the anterior-posterior axis in the mouse embryo. Nature 395:702-707.

Dorey K, Hill CS. 2006. A novel Cripto-related protein reveals an essential role for EGF-CFCs in Nodal signalling in Xenopus embryos. Dev Biol 292:303-316.

Dougan ST, Warga RM, Kane DA, Schier AF, Talbot WS. 2003. The role of the zebrafish nodal-related genes squint and cyclops in patterning of mesendoderm. Development 130:1837-1851.

Dufort D, Schwartz L, Harpal K, Rossant J. 1998. The transcription factor HNF3beta is required in visceral endoderm for normal primitive streak morphogenesis. Development 125:3015-3025.

Dunn NR, Koonce CH, Anderson DC, Islam A, Bikoff EK, Robertson EJ. 2005. Mice exclusively expressing the short isoform of Smad2 develop normally and are viable and fertile. Genes Dev 19:152-163.

Eimon PM, Harland RM. 2002. Effects of heterodimerization and proteolytic processing on Derriere and Nodal activity: implications for mesoderm induction in Xenopus. Development 129:3089-3103.

Ekstrom P, Ebbesson SO. 1988. The left habenular nucleus contains a discrete serotonin-immunoreactive subnucleus in the coho salmon (Oncorhynchus kisutch). Neurosci Lett 91:121-125.

Ellertsdottir E, Ganz J, Durr K, Loges N, Biemar F, Seifert F, Ettl AK, Kramer-Zucker AK, Nitschke R, Driever W. 2006. A mutation in the zebrafish Na,K-ATPase subunit atp1a1a.1 provides genetic evidence that the sodium potassium pump contributes to left-right asymmetry downstream or in parallel to nodal flow. Dev Dyn 235:1794-1808.

Episkopou V, Arkell R, Timmons PM, Walsh JJ, Andrew RL, Swan D. 2001. Induction of the mammalian node requires Arkadia function in the extraembryonic lineages. Nature 410:825-830.

Essner JJ, Amack JD, Nyholm MK, Harris EB, Yost HJ. 2005. Kupffer's vesicle is a ciliated organ of asymmetry in the zebrafish embryo that initiates left-right development of the brain, heart and gut. Development 132:1247-1260.

Essner JJ, Branford WW, Zhang J, Yost HJ. 2000. Mesendoderm and left-right brain, heart and gut development are differentially regulated by pitx2 isoforms. Development 127:1081-1093.

Essner JJ, Vogan KJ, Wagner MK, Tabin CJ, Yost HJ, Brueckner M. 2002. Conserved function for embryonic nodal cilia. Nature 418:37-38.

Faucourt M, Houliston E, Besnardeau L, Kimelman D, Lepage T. 2001. The pitx2 homeobox protein is required early for endoderm formation and nodal signaling. Dev Biol 229:287-306.

Feldman B, Concha ML, Saude L, Parsons MJ, Adams RJ, Wilson SW, Stemple DL. 2002. Lefty antagonism of Squint is essential for normal gastrulation. Curr Biol 12:2129-2135.

Feldman B, Dougan ST, Schier AF, Talbot WS. 2000. Nodal-related signals establish mesendodermal fate and trunk neural identity in zebrafish. Curr Biol 10:531-534.

Feldman B, Gates MA, Egan ES, Dougan ST, Rennebeck G, Sirotkin HI, Schier AF, Talbot WS. 1998. Zebrafish organizer development and germ-layer formation require nodal-related signals. Nature 395:181-185.

Fujinaga M. 1997. Development of sidedness of asymmetric body structures in vertebrates. Int J Dev Biol 41:153-186.

Gage PJ, Suh H, Camper SA. 1999. Dosage requirement of Pitx2 for development of multiple organs. Development 126:4643-4651.

Gaio U, Schweickert A, Fischer A, Garratt AN, Muller T, Ozcelik C, Lankes W, Strehle M, Britsch S, Blum M, Birchmeier C. 1999. A role of the cryptic gene in the correct establishment of the left-right axis. Curr Biol 9:1339-1342.

Gamse JT, Kuan YS, Macurak M, Brosamle C, Thisse B, Thisse C, Halpern ME. 2005. Directional asymmetry of the zebrafish epithalamus guides dorsoventral innervation of the midbrain target. Development 132:4869-4881.

Gamse JT, Shen YC, Thisse C, Thisse B, Raymond PA, Halpern ME, Liang JO. 2002. Otx5 regulates genes that show circadian expression in the zebrafish pineal complex. Nat Genet 30:117-121.

Gamse JT, Thisse C, Thisse B, Halpern ME. 2003. The parapineal mediates left-right asymmetry in the zebrafish diencephalon. Development 130:1059-1068.

Gerhart J, Danilchik M, Doniach T, Roberts S, Rowning B, Stewart R. 1989. Cortical rotation of the Xenopus egg: consequences for the anteroposterior pattern of embryonic dorsal development. Development 107 Suppl:37-51.

Germain S, Howell M, Esslemont GM, Hill CS. 2000. Homeodomain and winged-helix transcription factors recruit activated Smads to distinct promoter elements via a common Smad interaction motif. Genes Dev 14:435-451.

Gore AV, Maegawa S, Cheong A, Gilligan PC, Weinberg ES, Sampath K. 2005. The zebrafish dorsal axis is apparent at the four-cell stage. Nature 438:1030-1035.

Grande C, Patel NH. 2008. Nodal signalling is involved in left-right asymmetry in snails. Nature.

Green J. 2002. Morphogen gradients, positional information, and Xenopus: interplay of theory and experiment. Dev Dyn 225:392-408.

Gritsman K, Zhang J, Cheng S, Heckscher E, Talbot WS, Schier AF. 1999. The EGF-CFC protein one-eyed pinhead is essential for nodal signaling. Cell 97:121-132.

Gu Z, Reynolds EM, Song J, Lei H, Feijen A, Yu L, He W, MacLaughlin DT, van den Eijnden-van Raaij J, Donahoe PK, Li E. 1999. The type I serine/threonine kinase receptor ActRIA (ALK2) is required for gastrulation of the mouse embryo. Development 126:2551-2561.

Guglielmotti V, Cristino L, Sada E, Bentivoglio M. 2004. The epithalamus of the developing and adult frog: calretinin expression and habenular asymmetry in Rana esculenta. Brain Res 999:9-19.

Guglielmotti V, Fiorino L. 1999. Nitric oxide synthase activity reveals an asymmetrical organization of the frog habenulae during development: A histochemical and cytoarchitectonic study from tadpoles to the mature Rana esculenta, with notes on the pineal complex. J Comp Neurol 411:441-454.

Gurdon JB, Bourillot PY. 2001. Morphogen gradient interpretation. Nature 413:797-803.

Haffner C, Frauli M, Topp S, Irmler M, Hofmann K, Regula JT, Bally-Cuif L, Haass C. 2004. Nicalin and its binding partner Nomo are novel Nodal signaling antagonists. Embo J 23:3041-3050.

Halpern ME, Liang JO, Gamse JT. 2003. Leaning to the left: laterality in the zebrafish forebrain. Trends Neurosci 26:308-313.

Hamada H, Meno C, Watanabe D, Saijoh Y. 2002. Establishment of vertebrate left-right asymmetry. Nat Rev Genet 3:103-113.

Harms PW, Chang C. 2003. Tomoregulin-1 (TMEFF1) inhibits nodal signaling through direct binding to the nodal coreceptor Cripto. Genes Dev 17:2624-2629.

Harnad S. 1977. Lateralization in the nervous system. New York: Academic:537.

Harvey RP. 1998. Cardiac looping--an uneasy deal with laterality. Semin Cell Dev Biol 9:101-108.

Harvey RP. 2002. Patterning the vertebrate heart. Nat Rev Genet 3:544-556.

Hatta K, Kimmel CB, Ho RK, Walker C. 1991. The cyclops mutation blocks specification of the floor plate of the zebrafish central nervous system. Nature 350:339-341.

Hendren RL, De Backer I, Pandina GJ. 2000. Review of neuroimaging studies of child and adolescent psychiatric disorders from the past 10 years. J Am Acad Child Adolesc Psychiatry 39:815-828.

Hendricks M, Jesuthasan S. 2007. Asymmetric innervation of the habenula in zebrafish. J Comp Neurol 502:611-619.

Herbert MR, Harris GJ, Adrien KT, Ziegler DA, Makris N, Kennedy DN, Lange NT, Chabris CF, Bakardjiev A, Hodgson J, Takeoka M, Tager-Flusberg H, Caviness VS, Jr. 2002. Abnormal asymmetry in language association cortex in autism. Ann Neurol 52:588-596.

Hirokawa N, Tanaka Y, Okada Y, Takeda S. 2006. Nodal flow and the generation of left-right asymmetry. Cell 125:33-45.

Horne-Badovinac S, Rebagliati M, Stainier DY. 2003. A cellular framework for gut-looping morphogenesis in zebrafish. Science 302:662-665.

Hu N, Sedmera D, Yost HJ, Clark EB. 2000. Structure and function of the developing zebrafish heart. Anat Rec 260:148-157.

Hu N, Yost HJ, Clark EB. 2001. Cardiac morphology and blood pressure in the adult zebrafish. Anat Rec 264:1-12.

Inbal A, Kim SH, Shin J, Solnica-Krezel L. 2007. Six3 represses nodal activity to establish early brain asymmetry in zebrafish. Neuron 55:407-415.

Iratni R, Yan YT, Chen C, Ding J, Zhang Y, Price SM, Reinberg D, Shen MM. 2002. Inhibition of excess nodal signaling during mouse gastrulation by the transcriptional corepressor DRAP1. Science 298:1996-1999.

Isaac A, Sargent MG, Cooke J. 1997. Control of vertebrate left-right asymmetry by a snail-related zinc finger gene. Science 275:1301-1304.

Ishimura A, Chida S, Osada S. 2008. Man1, an inner nuclear membrane protein, regulates left-right axis formation by controlling nodal signaling in a node-independent manner. Dev Dyn 237:3565-3576.

Izraeli S, Lowe LA, Bertness VL, Good DJ, Dorward DW, Kirsch IR, Kuehn MR. 1999. The SIL gene is required for mouse embryonic axial development and left-right specification. Nature 399:691-694.

Jones CM, Armes N, Smith JC. 1996. Signalling by TGF-beta family members: short-range effects of Xnr-2 and BMP-4 contrast with the long-range effects of activin. Curr Biol 6:1468-1475.

Jones CM, Kuehn MR, Hogan BL, Smith JC, Wright CV. 1995. Nodal-related signals induce axial mesoderm and dorsalize mesoderm during gastrulation. Development 121:3651-3662.

Jornvall H, Reissmann E, Andersson O, Mehrkash M, Ibanez CF. 2004. ALK7, a receptor for nodal, is dispensable for embryogenesis and left-right patterning in the mouse. Mol Cell Biol 24:9383-9389.

Kawakami Y. 2005. [Mechanisms for establishment of vertebrate left-right asymmetry]. Tanpakushitsu Kakusan Koso 50:1609-1619.

Kelly KA, Wei Y, Mikawa T. 2002. Cell death along the embryo midline regulates left-right sidedness. Dev Dyn 224:238-244.

Kemali M, Guglielmotti V. 1977. An electron microscope observation of the right and the two left portions of the habenular nuclei of the frog. J Comp Neurol 176:133-148.

Kemali M, Guglielmotti V. 1982. Quantitative evaluation of the number of fibers in the right and left fasciculus retroflexus using horseradish peroxidase. Z Mikrosk Anat Forsch 96:750-754.

Kemali M, Guglielmotti V, Fiorino L. 1990. The asymmetry of the habenular nuclei of female and male frogs in spring and in winter. Brain Res 517:251-255.

Kennedy DN, O'Craven KM, Ticho BS, Goldstein AM, Makris N, Henson JW. 1999. Structural and functional brain asymmetries in human situs inversus totalis. Neurology 53:1260-1265.

Kikuchi Y, Agathon A, Alexander J, Thisse C, Waldron S, Yelon D, Thisse B, Stainier DY. 2001. casanova encodes a novel Sox-related protein necessary and sufficient for early endoderm formation in zebrafish. Genes Dev 15:1493-1505.

Kikuchi Y, Trinh LA, Reiter JF, Alexander J, Yelon D, Stainier DY. 2000. The zebrafish bonnie and clyde gene encodes a Mix family homeodomain protein that regulates the generation of endodermal precursors. Genes Dev 14:1279-1289.

Kimelman D. 2006. Mesoderm induction: from caps to chips. Nat Rev Genet 7:360-372.

King T, Beddington RS, Brown NA. 1998. The role of the brachyury gene in heart development and left-right specification in the mouse. Mech Dev 79:29-37.

Kinsky F. 1971. The consistent presence of paired ovaries in the Kiwi (Apteryx) with some discussion of this condition in other birds. Journal of Ornithology 112.

Kitamura K, Miura H, Miyagawa-Tomita S, Yanazawa M, Katoh-Fukui Y, Suzuki R, Ohuchi H, Suehiro A, Motegi Y, Nakahara Y, Kondo S, Yokoyama M. 1999. Mouse Pitx2 deficiency leads to anomalies of the ventral body wall, heart, extra- and periocular mesoderm and right pulmonary isomerism. Development 126:5749-5758.

Kofron M, Wylie C, Heasman J. 2004. The role of Mixer in patterning the early Xenopus embryo. Development 131:2431-2441.

Kölliker A. 1879. Entwicklungsgeschichte des menschen und höher-en thiere. Leipzig, Germany: wihelm engelmann.

Kramer-Zucker AG, Olale F, Haycraft CJ, Yoder BK, Schier AF, Drummond IA. 2005. Cilia-driven fluid flow in the zebrafish pronephros, brain and Kupffer's vesicle is required for normal organogenesis. Development 132:1907-1921.

Krebs LT, Iwai N, Nonaka S, Welsh IC, Lan Y, Jiang R, Saijoh Y, O'Brien TP, Hamada H, Gridley T. 2003. Notch signaling regulates left-right asymmetry determination by inducing Nodal expression. Genes Dev 17:1207-1212.

Kreiling JA, Williams G, Creton R. 2007. Analysis of Kupffer's vesicle in zebrafish embryos using a cave automated virtual environment. Dev Dyn 236:1963-1969.

Kumar A, Novoselov V, Celeste AJ, Wolfman NM, ten Dijke P, Kuehn MR. 2001. Nodal signaling uses activin and transforming growth factor-beta receptor-regulated Smads. J Biol Chem 276:656-661.

Kunwar PS, Zimmerman S, Bennett JT, Chen Y, Whitman M, Schier AF. 2003. Mixer/Bon and FoxH1/Sur have overlapping and divergent roles in Nodal signaling and mesendoderm induction. Development 130:5589-5599.

Kurpios NA, Ibanes M, Davis NM, Lui W, Katz T, Martin JF, Belmonte JC, Tabin CJ. 2008. The direction of gut looping is established by changes in the extracellular matrix and in cell:cell adhesion. Proc Natl Acad Sci U S A 105:8499-8506.

Lee MA, Heasman J, Whitman M. 2001. Timing of endogenous activin-like signals and regional specification of the Xenopus embryo. Development 128:2939-2952.

Lettice L, Hecksher-Sorensen J, Hill R. 2001. The role of Bapx1 (Nkx3.2) in the development and evolution of the axial skeleton. J Anat 199:181-187.

Levin M. 2005. Left-right asymmetry in embryonic development: a comprehensive review. Mech Dev 122:3-25.

Levin M, Johnson RL, Stern CD, Kuehn M, Tabin C. 1995. A molecular pathway determining left-right asymmetry in chick embryogenesis. Cell 82:803-814.

Levin M, Pagan S, Roberts DJ, Cooke J, Kuehn MR, Tabin CJ. 1997. Left/right patterning signals and the independent regulation of different aspects of situs in the chick embryo. Dev Biol 189:57-67.

Levin M, Roberts DJ, Holmes LB, Tabin C. 1996. Laterality defects in conjoined twins. Nature 384:321.

Levin M, Thorlin T, Robinson KR, Nogi T, Mercola M. 2002. Asymmetries in H+/K+-ATPase and cell membrane potentials comprise a very early step in left-right patterning. Cell 111:77-89.

Liang JO, Etheridge A, Hantsoo L, Rubinstein AL, Nowak SJ, Izpisua Belmonte JC, Halpern ME. 2000. Asymmetric nodal signaling in the zebrafish diencephalon positions the pineal organ. Development 127:5101-5112.

Lin CR, Kioussi C, O'Connell S, Briata P, Szeto D, Liu F, Izpisua-Belmonte JC, Rosenfeld MG. 1999. Pitx2 regulates lung asymmetry, cardiac positioning and pituitary and tooth morphogenesis. Nature 401:279-282.

Liu C, Liu W, Lu MF, Brown NA, Martin JF. 2001. Regulation of left-right asymmetry by thresholds of Pitx2c activity. Development 128:2039-2048.

Logan M, Pagan-Westphal SM, Smith DM, Paganessi L, Tabin CJ. 1998. The transcription factor Pitx2 mediates situs-specific morphogenesis in response to left-right asymmetric signals. Cell 94:307-317.

Lohr JL, Danos MC, Yost HJ. 1997. Left-right asymmetry of a nodal-related gene is regulated by dorsoanterior midline structures during Xenopus development. Development 124:1465-1472.

Long S, Ahmad N, Rebagliati M. 2003. The zebrafish nodal-related gene southpaw is required for visceral and diencephalic left-right asymmetry. Development 130:2303-2316.

Lowe LA, Supp DM, Sampath K, Yokoyama T, Wright CV, Potter SS, Overbeek P, Kuehn MR. 1996. Conserved left-right asymmetry of nodal expression and alterations in murine situs inversus. Nature 381:158-161.

Lowe LA, Yamada S, Kuehn MR. 2001. Genetic dissection of nodal function in patterning the mouse embryo. Development 128:1831-1843.

Lu MF, Pressman C, Dyer R, Johnson RL, Martin JF. 1999. Function of Rieger syndrome gene in left-right asymmetry and craniofacial development. Nature 401:276-278.

Marszalek JR, Ruiz-Lozano P, Roberts E, Chien KR, Goldstein LS. 1999. Situs inversus and embryonic ciliary morphogenesis defects in mouse mutants lacking the KIF3A subunit of kinesin-II. Proc Natl Acad Sci U S A 96:5043-5048.

Massague J, Seoane J, Wotton D. 2005. Smad transcription factors. Genes Dev 19:2783-2810.

Mathieu J, Barth A, Rosa FM, Wilson SW, Peyrieras N. 2002. Distinct and cooperative roles for Nodal and Hedgehog signals during hypothalamic development. Development 129:3055-3065.

McGrath J, Somlo S, Makova S, Tian X, Brueckner M. 2003. Two populations of node monocilia initiate left-right asymmetry in the mouse. Cell 114:61-73.

McManus C. 2002. Right hand, Left hand: The origins of asymmetry in brains, bodies, atoms and cultures. Harvard University Press.

McManus I. 1999. Handedness, cerebral lateralization and the evolution of language. The Descent of Mind: Psychological Perspectives on Hominid Evolution:194-217.

McManus IC. 1995. Familial sinistrality: the utility of calculating exact genotype probabilities for individuals. Cortex 31:3-24.

McManus IC, Bryden, MP. 1992. The genetics of handedness, cerebral dominance, and lateralization. Rapin, I., Segalowitz, S. (Eds.), Handbook of Neuropsychology 6 (10):115-144.

Melloy PG, Ewart JL, Cohen MF, Desmond ME, Kuehn MR, Lo CW. 1998. No turning, a mouse mutation causing left-right and axial patterning defects. Dev Biol 193:77-89.

Meno C, Gritsman K, Ohishi S, Ohfuji Y, Heckscher E, Mochida K, Shimono A, Kondoh H, Talbot WS, Robertson EJ, Schier AF, Hamada H. 1999. Mouse Lefty2 and zebrafish antivin are feedback inhibitors of nodal signaling during vertebrate gastrulation. Mol Cell 4:287-298.

Meno C, Ito Y, Saijoh Y, Matsuda Y, Tashiro K, Kuhara S, Hamada H. 1997. Two closely-related left-right asymmetrically expressed genes, lefty-1 and lefty-2: their distinct expression domains, chromosomal linkage and direct neuralizing activity in Xenopus embryos. Genes Cells 2:513-524.

Meno C, Saijoh Y, Fujii H, Ikeda M, Yokoyama T, Yokoyama M, Toyoda Y, Hamada H. 1996. Left-right asymmetric expression of the TGF beta-family member lefty in mouse embryos. Nature 381:151-155.

Meno C, Shimono A, Saijoh Y, Yashiro K, Mochida K, Ohishi S, Noji S, Kondoh H, Hamada H. 1998. lefty-1 is required for left-right determination as a regulator of lefty-2 and nodal. Cell 94:287-297.

Meno C, Takeuchi J, Sakuma R, Koshiba-Takeuchi K, Ohishi S, Saijoh Y, Miyazaki J, ten Dijke P, Ogura T, Hamada H. 2001. Diffusion of nodal signaling activity in the absence of the feedback inhibitor Lefty2. Dev Cell 1:127-138.

Mercola M, Levin M. 2001. Left-right asymmetry determination in vertebrates. Annu Rev Cell Dev Biol 17:779-805.

Mesnard D, Guzman-Ayala M, Constam DB. 2006. Nodal specifies embryonic visceral endoderm and sustains pluripotent cells in the epiblast before overt axial patterning. Development 133:2497-2505.

Meyers EN, Martin GR. 1999. Differences in left-right axis pathways in mouse and chick: functions of FGF8 and SHH. Science 285:403-406.

Monsoro-Burq A, Le Douarin N. 2000. Left-right asymmetry in BMP4 signalling pathway during chick gastrulation. Mech Dev 97:105-108.

Moorman AF, Christoffels VM. 2003. Cardiac chamber formation: development, genes, and evolution. Physiol Rev 83:1223-1267.

Morgan AE, Hynd GW. 1998. Dyslexia, neurolinguistic ability, and anatomical variation of the planum temporale. Neuropsychol Rev 8:79-93.

Morgan MJ, O'Donnell JM, Oliver RF. 1973. Development of left-right asymmetry in the habenular nuclei of Rana temporaria. J Comp Neurol 149:203-214.

Murcia NS, Richards WG, Yoder BK, Mucenski ML, Dunlap JR, Woychik RP. 2000. The Oak Ridge Polycystic Kidney (orpk) disease gene is required for left-right axis determination. Development 127:2347-2355.

Nascone N, Mercola M. 1997. Organizer induction determines left-right asymmetry in Xenopus. Dev Biol 189:68-78.

Niederlander C, Walsh JJ, Episkopou V, Jones CM. 2001. Arkadia enhances nodal-related signalling to induce mesendoderm. Nature 410:830-834.

Nonaka S, Shiratori H, Saijoh Y, Hamada H. 2002. Determination of left-right patterning of the mouse embryo by artificial nodal flow. Nature 418:96-99.

Nonaka S, Tanaka Y, Okada Y, Takeda S, Harada A, Kanai Y, Kido M, Hirokawa N. 1998. Randomization of left-right asymmetry due to loss of nodal cilia generating leftward flow of extraembryonic fluid in mice lacking KIF3B motor protein. Cell 95:829-837.

Nonaka S, Yoshiba S, Watanabe D, Ikeuchi S, Goto T, Marshall WF, Hamada H. 2005. De novo formation of left-right asymmetry by posterior tilt of nodal cilia. PLoS Biol 3:e268.

Norris DP, Brennan J, Bikoff EK, Robertson EJ. 2002. The Foxh1-dependent autoregulatory enhancer controls the level of Nodal signals in the mouse embryo. Development 129:3455-3468.

Norris DP, Robertson EJ. 1999. Asymmetric and node-specific nodal expression patterns are controlled by two distinct cis-acting regulatory elements. Genes Dev 13:1575-1588.

Oh SP, Li E. 1997. The signaling pathway mediated by the type IIB activin receptor controls axial patterning and lateral asymmetry in the mouse. Genes Dev 11:1812-1826.

Okabe N, Xu B, Burdine RD. 2008. Fluid dynamics in zebrafish Kupffer's vesicle. Dev Dyn 237:3602-3612.

Okada Y, Nonaka S, Tanaka Y, Saijoh Y, Hamada H, Hirokawa N. 1999. Abnormal nodal flow precedes situs inversus in iv and inv mice. Mol Cell 4:459-468.

Okada Y, Takeda S, Tanaka Y, Belmonte JC, Hirokawa N. 2005. Mechanism of nodal flow: a conserved symmetry breaking event in left-right axis determination. Cell 121:633-644.

Patel K, Isaac A, Cooke J. 1999. Nodal signalling and the roles of the transcription factors SnR and Pitx2 in vertebrate left-right asymmetry. Curr Biol 9:609-612.

Pathi S, Pagan-Westphal S, Baker DP, Garber EA, Rayhorn P, Bumcrot D, Tabin CJ, Blake Pepinsky R, Williams KP. 2001. Comparative biological responses to human Sonic, Indian, and Desert hedgehog. Mech Dev 106:107-117.

Patterson KD, Drysdale TA, Krieg PA. 2000. Embryonic origins of spleen asymmetry. Development 127:167-175.

Pennekamp P, Karcher C, Fischer A, Schweickert A, Skryabin B, Horst J, Blum M, Dworniczak B. 2002. The ion channel polycystin-2 is required for left-right axis determination in mice. Curr Biol 12:938-943.

Petty RG. 1999. Structural asymmetries of the human brain and their disturbance in schizophrenia. Schizophr Bull 25:121-139.

Piccolo S, Agius E, Leyns L, Bhattacharyya S, Grunz H, Bouwmeester T, De Robertis EM. 1999. The head inducer Cerberus is a multifunctional antagonist of Nodal, BMP and Wnt signals. Nature 397:707-710.

Piedra ME, Icardo JM, Albajar M, Rodriguez-Rey JC, Ros MA. 1998. Pitx2 participates in the late phase of the pathway controlling left-right asymmetry. Cell 94:319-324.

Pogoda HM, Solnica-Krezel L, Driever W, Meyer D. 2000. The zebrafish forkhead transcription factor FoxH1/Fast1 is a modulator of nodal signaling required for organizer formation. Curr Biol 10:1041-1049.

Porter K. 1957. The submicroscopic morphology of protoplasm. Harvey lectures 51:175-228
.

Przemeck GK, Heinzmann U, Beckers J, Hrabe de Angelis M. 2003. Node and midline defects are associated with left-right development in Delta1 mutant embryos. Development 130:3-13.

Pujol J, Cardoner N, Benlloch L, Urretavizcaya M, Deus J, Losilla JM, Capdevila A, Vallejo J. 2002. CSF spaces of the Sylvian fissure region in severe melancholic depression. Neuroimage 15:103-106.

Ramsdell AF. 2005. Left-right asymmetry and congenital cardiac defects: getting to the heart of the matter in vertebrate left-right axis determination. Dev Biol 288:1-20.

Randall RA, Howell M, Page CS, Daly A, Bates PA, Hill CS. 2004. Recognition of phosphorylated-Smad2-containing complexes by a novel Smad interaction motif. Mol Cell Biol 24:1106-1121.

Raya A, Belmonte JC. 2004. Sequential transfer of left-right information during vertebrate embryo development. Curr Opin Genet Dev 14:575-581.

Raya A, Belmonte JC. 2006. Left-right asymmetry in the vertebrate embryo: from early information to higher-level integration. Nat Rev Genet 7:283-293.

Raya A, Kawakami Y, Rodriguez-Esteban C, Buscher D, Koth CM, Itoh T, Morita M, Raya RM, Dubova I, Bessa JG, de la Pompa JL, Belmonte JC. 2003. Notch activity induces Nodal expression and mediates the establishment of left-right asymmetry in vertebrate embryos. Genes Dev 17:1213-1218.

Rebagliati MR, Toyama R, Fricke C, Haffter P, Dawid IB. 1998a. Zebrafish nodal-related genes are implicated in axial patterning and establishing left-right asymmetry. Dev Biol 199:261-272.

Rebagliati MR, Toyama R, Haffter P, Dawid IB. 1998b. cyclops encodes a nodal-related factor involved in midline signaling. Proc Natl Acad Sci U S A 95:9932-9937.

Regan JC, Concha ML, Roussigne M, Russell C, Wilson SW. 2009. An Fgf8-dependent bistable cell migratory event establishes CNS asymmetry. Neuron 61:27-34.

Reissmann E, Jornvall H, Blokzijl A, Andersson O, Chang C, Minchiotti G, Persico MG, Ibanez CF, Brivanlou AH. 2001. The orphan receptor ALK7 and the Activin receptor ALK4 mediate signaling by Nodal proteins during vertebrate development. Genes Dev 15:2010-2022.

Reiter JF, Alexander J, Rodaway A, Yelon D, Patient R, Holder N, Stainier DY. 1999. Gata5 is required for the development of the heart and endoderm in zebrafish. Genes Dev 13:2983-2995.

Robichon F, Levrier O, Farnarier P, Habib M. 2000. Developmental dyslexia: atypical cortical asymmetries and functional significance. Eur J Neurol 7:35-46.

Rodriguez Esteban C, Capdevila J, Economides AN, Pascual J, Ortiz A, Izpisua Belmonte JC. 1999. The novel Cer-like protein Caronte mediates the establishment of embryonic left-right asymmetry. Nature 401:243-251.

Rodriguez-Leon J, Rodriguez Esteban C, Marti M, Santiago-Josefat B, Dubova I, Rubiralta X, Izpisua Belmonte JC. 2008. Pitx2 regulates gonad morphogenesis. Proc Natl Acad Sci U S A 105:11242-11247.

Rohr S, Otten C, Abdelilah-Seyfried S. 2008. Asymmetric involution of the myocardial field drives heart tube formation in zebrafish. Circ Res 102:e12-19.

Ryan AK, Blumberg B, Rodriguez-Esteban C, Yonei-Tamura S, Tamura K, Tsukui T, de la Pena J, Sabbagh W, Greenwald J, Choe S, Norris DP, Robertson EJ, Evans RM, Rosenfeld MG, Izpisua Belmonte JC. 1998. Pitx2 determines left-right asymmetry of internal organs in vertebrates. Nature 394:545-551.

Saijoh Y, Adachi H, Sakuma R, Yeo CY, Yashiro K, Watanabe M, Hashiguchi H, Mochida K, Ohishi S, Kawabata M, Miyazono K, Whitman M, Hamada H. 2000. Left-right asymmetric expression of lefty2 and nodal is induced by a signaling pathway that includes the transcription factor FAST2. Mol Cell 5:35-47.

Saijoh Y, Oki S, Ohishi S, Hamada H. 2003. Left-right patterning of the mouse lateral plate requires nodal produced in the node. Dev Biol 256:160-172.

Sakuma R, Ohnishi Yi Y, Meno C, Fujii H, Juan H, Takeuchi J, Ogura T, Li E, Miyazono K, Hamada H. 2002. Inhibition of Nodal signalling by Lefty mediated through interaction with common receptors and efficient diffusion. Genes Cells 7:401-412.

Sampath K, Rubinstein AL, Cheng AM, Liang JO, Fekany K, Solnica-Krezel L, Korzh V, Halpern ME, Wright CV. 1998. Induction of the zebrafish ventral brain and floorplate requires cyclops/nodal signalling. Nature 395:185-189.

Satir P. 2005. Tour of organelles through the electron microscope: a reprinting of Keith R. Porter's classic Harvey Lecture with a new introduction. Anat Rec A Discov Mol Cell Evol Biol 287:1184-1185.

Schier AF. 2003. Nodal signaling in vertebrate development. Annu Rev Cell Dev Biol 19:589-621.

Schier AF, Neuhauss SC, Helde KA, Talbot WS, Driever W. 1997. The one-eyed pinhead gene functions in mesoderm and endoderm formation in zebrafish and interacts with no tail. Development 124:327-342.

Schier AF, Shen MM. 2000. Nodal signalling in vertebrate development. Nature 403:385-389.

Schier AF, Talbot WS. 2001. Nodal signaling and the zebrafish organizer. Int J Dev Biol 45:289-297.

Schiffer SG, Foley S, Kaffashan A, Hronowski X, Zichittella AE, Yeo CY, Miatkowski K, Adkins HB, Damon B, Whitman M, Salomon D, Sanicola M, Williams KP. 2001. Fucosylation of Cripto is required for its ability to facilitate nodal signaling. J Biol Chem 276:37769-37778.

Schilling TF, Concordet JP, Ingham PW. 1999. Regulation of left-right asymmetries in the zebrafish by Shh and BMP4. Dev Biol 210:277-287.

Schlange T, Schnipkoweit I, Andree B, Ebert A, Zile MH, Arnold HH, Brand T. 2001. Chick CFC controls Lefty1 expression in the embryonic midline and nodal expression in the lateral plate. Dev Biol 234:376-389.

Schneider A, Mijalski T, Schlange T, Dai W, Overbeek P, Arnold HH, Brand T. 1999. The homeobox gene NKX3.2 is a target of left-right signalling and is expressed on opposite sides in chick and mouse embryos. Curr Biol 9:911-914.

Schweickert A, Campione M, Steinbeisser H, Blum M. 2000. Pitx2 isoforms: involvement of Pitx2c but not Pitx2a or Pitx2b in vertebrate left-right asymmetry. Mech Dev 90:41-51.

Schweickert A, Weber T, Beyer T, Vick P, Bogusch S, Feistel K, Blum M. 2007. Cilia-driven leftward flow determines laterality in Xenopus. Curr Biol 17:60-66.

Sefton M, Sanchez S, Nieto MA. 1998. Conserved and divergent roles for members of the Snail family of transcription factors in the chick and mouse embryo. Development 125:3111-3121.

Shen MM, Schier AF. 2000. The EGF-CFC gene family in vertebrate development. Trends Genet 16:303-309.

Shi Y, Massague J. 2003. Mechanisms of TGF-beta signaling from cell membrane to the nucleus. Cell 113:685-700.

Shiratori H, Hamada H. 2006. The left-right axis in the mouse: from origin to morphology. Development 133:2095-2104.

Shiratori H, Sakuma R, Watanabe M, Hashiguchi H, Mochida K, Sakai Y, Nishino J, Saijoh Y, Whitman M, Hamada H. 2001. Two-step regulation of left-right asymmetric expression of Pitx2: initiation by nodal signaling and maintenance by Nkx2. Mol Cell 7:137-149.

Shu X, Huang J, Dong Y, Choi J, Langenbacher A, Chen JN. 2007. Na,K-ATPase alpha2 and Ncx4a regulate zebrafish left-right patterning. Development 134:1921-1930.

Signore IA, Guerrero N, Loosli F, Colombo A, Villalon A, Wittbrodt J, Concha ML. 2008. Zebrafish and medaka: model organisms for a comparative developmental approach of brain asymmetry. Philos Trans R Soc Lond B Biol Sci.

Smith CA, Andrews JE, Sinclair AH. 1997. Gonadal sex differentiation in chicken embryos: expression of estrogen receptor and aromatase genes. J Steroid Biochem Mol Biol 60:295-302.

Smith CA, Smith MJ, Sinclair AH. 1999. Expression of chicken steroidogenic factor-1 during gonadal sex differentiation. Gen Comp Endocrinol 113:187-196.

Smith DJ, Blake JR, Gaffney EA. 2008. Fluid mechanics of nodal flow due to embryonic primary cilia. J R Soc Interface 5:567-573.

Smith WC, McKendry R, Ribisi S, Jr., Harland RM. 1995. A nodal-related gene defines a physical and functional domain within the Spemann organizer. Cell 82:37-46.

Song J, Oh SP, Schrewe H, Nomura M, Lei H, Okano M, Gridley T, Li E. 1999. The type II activin receptors are essential for egg cylinder growth, gastrulation, and rostral head development in mice. Dev Biol 213:157-169.

St Amand TR, Ra J, Zhang Y, Hu Y, Baber SI, Qiu M, Chen Y. 1998. Cloning and expression pattern of chicken Pitx2: a new component in the SHH signaling pathway controlling embryonic heart looping. Biochem Biophys Res Commun 247:100-105.

Stainier DY. 2001. Zebrafish genetics and vertebrate heart formation. Nat Rev Genet 2:39-48.

Stainier DY, Fouquet B, Chen JN, Warren KS, Weinstein BM, Meiler SE, Mohideen MA, Neuhauss SC, Solnica-Krezel L, Schier AF, Zwartkruis F, Stemple DL, Malicki J, Driever W, Fishman MC. 1996. Mutations affecting the formation and function of the cardiovascular system in the zebrafish embryo. Development 123:285-292.

Stainier DY, Lee RK, Fishman MC. 1993. Cardiovascular development in the zebrafish. I. Myocardial fate map and heart tube formation. Development 119:31-40.

Steffens DC, Krishnan KR. 1998. Structural neuroimaging and mood disorders: recent findings, implications for classification, and future directions. Biol Psychiatry 43:705-712.

Strahle U, Jesuthasan S, Blader P, Garcia-Villalba P, Hatta K, Ingham PW. 1997. one-eyed pinhead is required for development of the ventral midline of the zebrafish (Danio rerio) neural tube. Genes Funct 1:131-148.

Sulik K, Dehart DB, Iangaki T, Carson JL, Vrablic T, Gesteland K, Schoenwolf GC. 1994. Morphogenesis of the murine node and notochordal plate. Dev Dyn 201:260-278.

Supp DM, Brueckner M, Kuehn MR, Witte DP, Lowe LA, McGrath J, Corrales J, Potter SS. 1999. Targeted deletion of the ATP binding domain of left-right dynein confirms its role in specifying development of left-right asymmetries. Development 126:5495-5504.

Supp DM, Witte DP, Potter SS, Brueckner M. 1997. Mutation of an axonemal dynein affects left-right asymmetry in inversus viscerum mice. Nature 389:963-966.

Tabin CJ, Vogan KJ. 2003. A two-cilia model for vertebrate left-right axis specification. Genes Dev 17:1-6.

Takeda S, Yonekawa Y, Tanaka Y, Okada Y, Nonaka S, Hirokawa N. 1999. Left-right asymmetry and kinesin superfamily protein KIF3A: new insights in determination of laterality and mesoderm induction by kif3A-/- mice analysis. J Cell Biol 145:825-836.

Tanaka S, Kanzaki R, Yoshibayashi M, Kamiya T, Sugishita M. 1999. Dichotic listening in patients with situs inversus: brain asymmetry and situs asymmetry. Neuropsychologia 37:869-874.

Tanaka Y, Okada Y, Hirokawa N. 2005. FGF-induced vesicular release of Sonic hedgehog and retinoic acid in leftward nodal flow is critical for left-right determination. Nature 435:172-177.

Thisse B, Wright CV, Thisse C. 2000. Activin- and Nodal-related factors control antero-posterior patterning of the zebrafish embryo. Nature 403:425-428.

Thisse C, Thisse B. 1999. Antivin, a novel and divergent member of the TGFbeta superfamily, negatively regulates mesoderm induction. Development 126:229-240.

Torgersen J. 1950. Situs inversus, asymmetry, and twinning. Am J Hum Genet 2:361-370.

Tribioli C, Lufkin T. 1999. The murine Bapx1 homeobox gene plays a critical role in embryonic development of the axial skeleton and spleen. Development 126:5699-5711.

Tsuda T, Majumder K, Linask KK. 1998. Differential expression of flectin in the extracellular matrix and left-right asymmetry in mouse embryonic heart during looping stages. Dev Genet 23:203-214.

Tsukui T, Capdevila J, Tamura K, Ruiz-Lozano P, Rodriguez-Esteban C, Yonei-Tamura S, Magallon J, Chandraratna RA, Chien K, Blumberg B, Evans RM, Belmonte JC. 1999. Multiple left-right asymmetry defects in Shh(-/-) mutant mice unveil a convergence of the shh and retinoic acid pathways in the control of Lefty-1. Proc Natl Acad Sci U S A 96:11376-11381.

Vallier L, Reynolds D, Pedersen RA. 2004. Nodal inhibits differentiation of human embryonic stem cells along the neuroectodermal default pathway. Dev Biol 275:403-421.

van Veen T, Ekstrom P, Borg B, Moller M. 1980. The pineal complex of the three-spined stickleback, Gasterosteus aculeatus L.: a light-, electron microscopic and fluorescence histochemical investigation. Cell Tissue Res 209:11-28.

Vincent SD, Dunn NR, Hayashi S, Norris DP, Robertson EJ. 2003. Cell fate decisions within the mouse organizer are governed by graded Nodal signals. Genes Dev 17:1646-1662.

Waldrip WR, Bikoff EK, Hoodless PA, Wrana JL, Robertson EJ. 1998. Smad2 signaling in extraembryonic tissues determines anterior-posterior polarity of the early mouse embryo. Cell 92:797-808.

Wang S, Yu X, Zhang T, Zhang X, Zhang Z, Chen Y. 2004. Chick Pcl2 regulates the left-right asymmetry by repressing Shh expression in Hensen's node. Development 131:4381-4391.

Warren KS, Fishman MC. 1998. "Physiological genomics": mutant screens in zebrafish. Am J Physiol 275:H1-7.

Wasiak S, Lohnes D. 1999. Retinoic acid affects left-right patterning. Dev Biol 215:332-342.

Wehrmaker A. 1969. Right-left asymmetry and *situs inversus* in *Triturus alpertris*. Wilhelm Roux's Archive Dev. Biol. 163:1-32.

Whitman M. 2001. Nodal signaling in early vertebrate embryos: themes and variations. Dev Cell 1:605-617.

Wiechmann AF, Wirsig-Wiechmann CR. 1993. Distribution of melatonin receptors in the brain of the frog Rana pipiens as revealed by in vitro autoradiography. Neuroscience 52:469-480.

Yamamoto M, Mine N, Mochida K, Sakai Y, Saijoh Y, Meno C, Hamada H. 2003. Nodal signaling induces the midline barrier by activating Nodal expression in the lateral plate. Development 130:1795-1804.

Yan YT, Gritsman K, Ding J, Burdine RD, Corrales JD, Price SM, Talbot WS, Schier AF, Shen MM. 1999. Conserved requirement for EGF-CFC genes in vertebrate left-right axis formation. Genes Dev 13:2527-2537.

Yan YT, Liu JJ, Luo Y, E C, Haltiwanger RS, Abate-Shen C, Shen MM. 2002. Dual roles of Cripto as a ligand and coreceptor in the nodal signaling pathway. Mol Cell Biol 22:4439-4449.

Yanez J, Anadon R. 1994. Afferent and efferent connections of the habenula in the larval sea lamprey (Petromyzon marinus L.): an experimental study. J Comp Neurol 345:148-160.

Yanez J, Anadon R. 1996. Afferent and efferent connections of the habenula in the rainbow trout (Oncorhynchus mykiss): an indocarbocyanine dye (DiI) study. J Comp Neurol 372:529-543.

Yashiro K, Shiratori H, Hamada H. 2007. Haemodynamics determined by a genetic programme govern asymmetric development of the aortic arch. Nature 450:285-288.

Yelon D, Horne SA, Stainier DY. 1999. Restricted expression of cardiac myosin genes reveals regulated aspects of heart tube assembly in zebrafish. Dev Biol 214:23-37.

Yeo C, Whitman M. 2001. Nodal signals to Smads through Cripto-dependent and Cripto-independent mechanisms. Mol Cell 7:949-957.

Yokouchi Y, Vogan KJ, Pearse RV, 2nd, Tabin CJ. 1999. Antagonistic signaling by Caronte, a novel Cerberus-related gene, establishes left-right asymmetric gene expression. Cell 98:573-583.

Yoshioka H, Meno C, Koshiba K, Sugihara M, Itoh H, Ishimaru Y, Inoue T, Ohuchi H, Semina EV, Murray JC, Hamada H, Noji S. 1998. Pitx2, a bicoid-type homeobox gene, is involved in a lefty-signaling pathway in determination of left-right asymmetry. Cell 94:299-305.

Yu X, St Amand TR, Wang S, Li G, Zhang Y, Hu YP, Nguyen L, Qiu MS, Chen YP. 2001. Differential expression and functional analysis of Pitx2 isoforms in regulation of heart looping in the chick. Development 128:1005-1013.

Zhang J, Talbot WS, Schier AF. 1998. Positional cloning identifies zebrafish one-eyed pinhead as a permissive EGF-related ligand required during gastrulation. Cell 92:241-251.

Zhang L, Zhou H, Su Y, Sun Z, Zhang H, Zhang L, Zhang Y, Ning Y, Chen YG, Meng A. 2004. Zebrafish Dpr2 inhibits mesoderm induction by promoting degradation of nodal receptors. Science 306:114-117.

Zhang XM, Ramalho-Santos M, McMahon AP. 2001. Smoothened mutants reveal redundant roles for Shh and Ihh signaling including regulation of L/R asymmetry by the mouse node. Cell 105:781-792.

Zhou X, Sasaki H, Lowe L, Hogan BL, Kuehn MR. 1993. Nodal is a novel TGF-beta-like gene expressed in the mouse node during gastrulation. Nature 361:543-547.

Chapter II

Nodal Signaling Promotes the Speed and Directional Movement of Cardiomyocytes in Zebrafish

Maria Inês Baptista and Alexander Schier

Developmental Dynamics 237:3624 – 3633, 2008

DEVELOPMENTAL DYNAMICS 237:3624–3633, 2008

SPECIAL ISSUE RESEARCH ARTICLE

Nodal Signaling Promotes the Speed and Directional Movement of Cardiomyocytes in Zebrafish

Maria Ines Medeiros de Campos-Baptista,[1,4] Nathalia Glickman Holtzman,[2,3] Deborah Yelon,[2] and Alexander F. Schier[1*]

Members of the Nodal family regulate left-right asymmetry during vertebrate organogenesis, but it is unclear how Nodal signaling controls asymmetric morphogenesis at the cellular level. We used high-resolution time-lapse imaging in zebrafish to compare the movements of cardiomyocytes in the presence or absence of Nodal signaling. Loss of Nodal signaling in late-zygotic mutants for the Nodal co-receptor *one-eyed pinhead* (L*Zoep*) abolished the leftward movement of cardiomyocytes. Global heart rotation was blocked but cardiomyocyte neighbor relationships were maintained as in wild type. Cardiomyocytes in L*Zoep* mutants moved more slowly and less directionally than their wild-type counterparts. The phenotypes observed in the absence of Nodal signaling strongly resemble abnormalities found in BMP signaling mutants. These results indicate that a Nodal-BMP signaling cascade drives left-right heart morphogenesis by regulating the speed and direction of cardiomyocyte movement. *Developmental Dynamics 237:3624–3633, 2008.* © 2008 Wiley-Liss, Inc.

Key words: Nodal; heart; zebrafish; morphogenesis; left-right

Accepted 15 September 2008

INTRODUCTION

Vertebrate organs such as heart, intestine, spleen, and liver have left-right asymmetric morphologies and positions within the body cavity. Left-sided expression of Nodal signals during embryogenesis is thought to initiate organ lateralization (reviewed in Levin, 2005; Tabin, 2005; Raya and Belmonte, 2006; Shiratori and Hamada, 2006). Nodal signals are expressed in the left lateral plate mesoderm (LPM) and activate the asymmetric expression of downstream genes such as *lefty2* (*lft2*) (reviewed in Hamada et al., 2002; Schier, 2003; Shen, 2007). In the absence of Nodal signaling, organ laterality becomes randomized or disrupted (Levin et al., 1995; Chen et al., 1997; Yan et al., 1999; Bamford et al., 2000; Concha et al., 2000; Liang et al., 2000; Brennan et al., 2002; Long et al., 2003; Duboc et al., 2005), but it is largely unclear how Nodal affects asymmetric organogenesis at the cellular level.

The heart is the first organ to exhibit asymmetry in vertebrates (reviewed in Trinh and Stainier, 2004; Ramsdell, 2005). In the zebrafish, bilateral cardiac precursors form in the anterior lateral plate mesoderm (LPM) and then undergo a series of

Additional Supporting Information may be found in the online version of this article.

[1]Department of Molecular and Cellular Biology, Center for Brain Science, Broad Institute, Harvard Stem Cell Institute, Harvard University, Cambridge, Massachusetts
[2]Developmental Genetics Program and Department of Cell Biology, Kimmel Center for Biology and Medicine, Skirball Institute of Biomolecular Medicine, New York University School of Medicine, New York, New York
[3]Department of Biology, Queens College, The City University of New York, Flushing, New York
[4]Gulbenkian PhD Programme in Biomedicine, Oeiras, Portugal

Grant sponsor: NIH; Grant number: R01 GM56211; Grant sponsor: Gulbenkian PhD Program; Grant number: FCT SFRH/BD/11801/2003.

***Correspondence to: Department of Molecular and Cellular Biology, Center for Brain Science, Broad Institute, Harvard Stem Cell Institute, Harvard University, 16 Divinity Avenue, Cambridge, MA 02138. E-mail: schier@mcb.harvard.edu**

DOI 10.1002/dvdy.21777
Published online 11 November 2008 in Wiley InterScience (www.interscience.wiley.com).

morphogenetic movements to assemble the heart tube. First, cardiac precursors migrate toward the embryonic midline and meet anteriorly and posteriorly. This process leads to the formation of a cardiac cone that is left-right symmetric (Holtzman et al., 2007). Second, in a process called cardiac jogging, cardiomyocytes are displaced both anteriorly and to the left (Chen et al., 1997; Rohr et al., 2008; Smith et al., 2008). Concomitantly, cells within the right side of the cardiac cone involute, and the entire cardiac cone undergoes a clockwise rotation (Rohr et al., 2008; Smith et al., 2008). These morphogenetic processes are the first manifestations of left-right asymmetry and lead to the positioning of right and left cardiac cone cells to ventral and dorsal parts of the heart tube, respectively. In parallel, central and peripheral cells of the cardiac cone give rise to the ventricle and atrium, respectively (reviewed in Trinh and Stainier, 2004). Finally, the linear heart tube loops rightwards, positioning the ventricle to the right side of the atrium (reviewed in Trinh and Stainier, 2004).

Several signaling pathways have been implicated as regulators of asymmetric heart morphogenesis, including components of the Nodal and BMP signaling pathways (Zhang and Bradley, 1996; Chen et al., 1997; Ramsdell and Yost, 1999; Schilling et al., 1999; Branford et al., 2000; Chang et al., 2000; Breckenridge et al., 2001; Hamada et al., 2002; Piedra and Ros, 2002; Schlange et al., 2002; Schier, 2003; Kishigami et al., 2004; Kishigami and Mishina, 2005; Chocron et al., 2007; Shen, 2007; Mine et al., 2008; Monteiro et al., 2008; Smith et al., 2008). The BMP signaling pathway is activated predominantly within the left side of the zebrafish heart (Chen et al., 1997; Chocron et al., 2007; Smith et al., 2008). When this asymmetry is disrupted by hyperactivation or blocking of BMP signaling, cardiomyocyte movement slows and meandering increases, and the heart tube fails to jog leftwards or rotate clockwise (Chen et al., 1997; Schilling et al., 1999; Monteiro et al., 2008; Smith et al., 2008). Moreover, ectopic sources of BMP can direct the direction of cardiac jogging and cardiomyocyte movement (Smith et al., 2008). These results have suggested that asymmetric BMP signaling underlies the asymmetric movement and rotation of the zebrafish heart.

Several loss-of-function studies have revealed the importance of Nodal signaling in the lateralization of the zebrafish heart. The Nodal gene *spaw* is expressed in the left LPM and activates the Nodal pathway within the left side of the heart, as evidenced by the left-side-specific activation of the Nodal downstream gene *lft2* (Long et al., 2003). Morpholino-mediated knockdown of *spaw* affects the leftward but not the anterior displacement of the heart (Long et al., 2003). Loss of Nodal signaling leads to involution in the posterior region instead of the right section of the cardiac cone (Rohr et al., 2008). These morphogenetic abnormalities disrupt cardiac jogging and lead to a linear heart tube positioned at the midline. Heart morphogenesis is similarly disrupted in late-zygotic mutants for the Nodal co-receptor *oep* (Yan et al., 1999). The late expression of *oep* in the left and right LPM can be abolished by injecting *oep* mRNA into maternal-zygotic *oep* mutants, restoring *oep* function in mesendoderm induction but not in left-right patterning (Gritsman et al., 1999; Yan et al., 1999). In these LZ*oep* mutants, the Nodal pathway is not activated in the LPM, and heart looping is randomized (Yan et al., 1999). Similarly, loss of FoxH1 (zebrafish *schmalspur*), a transcriptional mediator of Nodal signaling, disrupts cardiac jogging (Chen et al., 1997; Pogoda et al., 2000; Sirotkin et al., 2000).

These findings have suggested that the Nodal signal *spaw* activates the Nodal pathway via Oep and FoxH1 within the left side of the developing heart and promotes lateralization by driving asymmetric morphogenesis. Yet it is largely unclear how Nodal signaling affects heart morphogenesis at the single cell level. Interestingly, it has been found that asymmetric BMP expression is dependent on asymmetric Nodal signaling (Chen et al., 1997; Chocron et al., 2007). In light of recent cell-tracking studies (Rohr et al., 2008; Smith et al., 2008), we therefore hypothesized that loss of Nodal signaling might lead to similar cellular defects as observed in loss- or gain-of-function BMP mutants. Here we test this idea and use time-lapse in vivo imaging to analyze the movement of cardiomyocytes in wild type and LZ*oep* mutants. We find that disruption of Nodal signaling reduces the speed and directional movement of cardiomyocytes and disrupts the leftward morphogenesis and rotation of the cardiac cone. These results indicate that Nodal generates left-right asymmetry by regulating the speed and direction of cardiomyocyte movement. The striking similarity to BMP pathway mutants suggests that a TGFβ signaling cascade involving Nodal and BMP underlies the asymmetric behavior of zebrafish cardiomyocytes.

RESULTS

Distinct Expression Patterns of Nodal Signaling Genes During Heart Lateralization

Previous studies have shown that *spaw, lft2*, and *oep* are expressed in the LPM in the region of the developing heart (Zhang et al., 1998; Bisgrove et al., 1999, 2000; Thisse and Thisse, 1999; Long et al., 2003), but the exact overlap of expression patterns has not been studied in detail. To gain a higher resolution view of Nodal signaling during heart lateralization, we performed double in situ hybridization analyses of Nodal pathway genes, the heart marker *cmlc2* (Yelon et al., 1999) and the midline marker *shh* (Krauss et al., 1993) (Fig. 1). At the 21-somite stage, *cmlc2* marked the cardiac cone shortly after fusion of the left and right heart fields (Fig. 1A). *spaw* was expressed in the anterior LPM (Long et al., 2003), adjacent to but not overlapping the left domain of *cmlc2* expression (Fig. 1D). In contrast, *lft2* expression overlapped the left domain of *cmlc2* expression (Bisgrove et al., 1999, 2000; Long et al., 2003) (Fig. 1B and C) and juxtaposed the *spaw* expression domain (Fig. 1E). *oep* was expressed in the left and right LPM (Zhang et al., 1998), adjacent to and within the developing heart (Fig. 1E and G), thus defining the maximum territory competent to respond to Nodal signals (Gritsman et al., 1999). Together with previous studies (Zhang et al., 1998; Bisgrove et al., 1999, 2000;

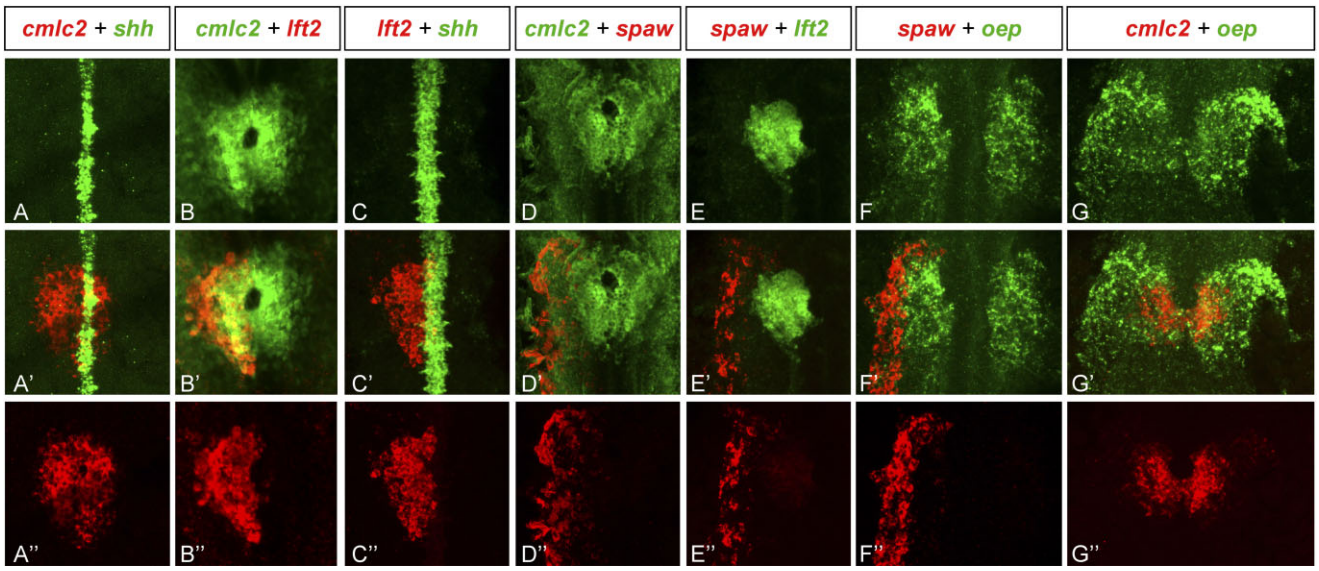

Fig. 1. Expression of Nodal pathway genes in the lateral plate mesoderm. Confocal images of double fluorescent in situ RNA hybridization of *spaw, lft2*, and *oep* with respect to the midline marker *shh* and the heart marker *cmlc2* at the 21-somite stage. Single channel expression (**A–G** and **A"–G"**) and overlay (**A'–G'**). All images are dorsal views of the embryo, anterior to the top and left to the left. Note broad expression of *oep* in left and right LPM (F and G) and more restricted expression of *spaw* in left non-cardiac LPM (F' and F") and *lft2* in left cardiac LPM (B' and B"). *spaw* is expressed adjacent to *lft2* (E').

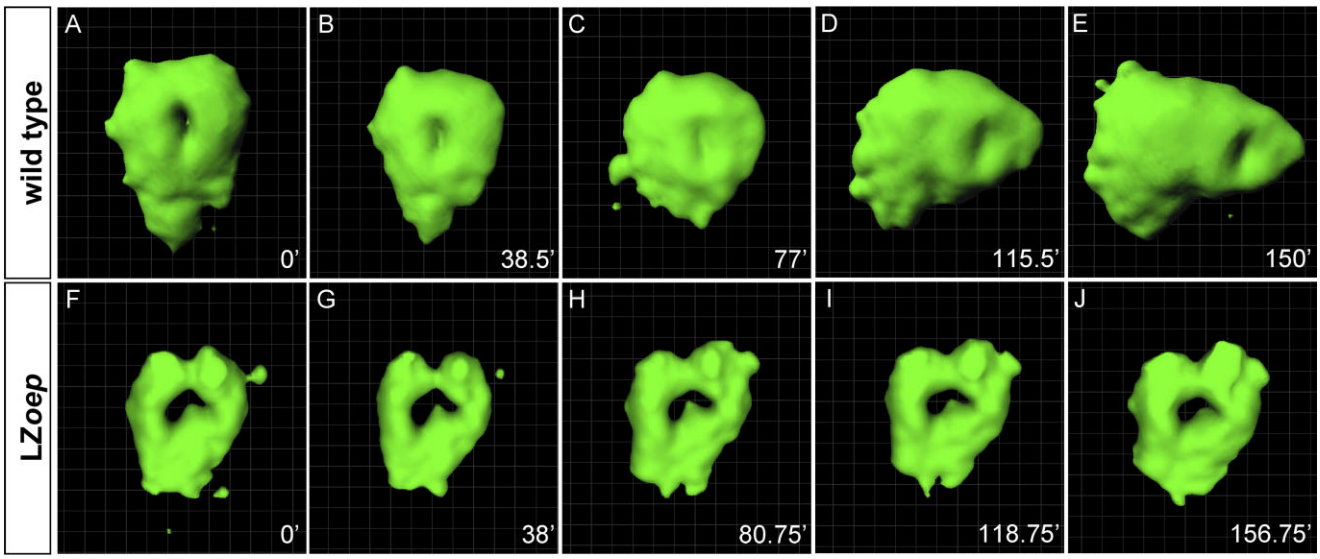

Fig. 2. Isosurface rendering of heart morphogenesis in wild type and LZ*oep* mutants. *cmlc2*-GFP cells label the cardiac cone and heart tube. Imaris software created an isosurface representing points of constant fluorescent intensity within the 3D volume. Cardiac cone is initially symmetric in wild type (A, B) and LZ*oep* mutant (F, G). Note the leftwards and anterior displacement of the heart in wild type (**C–E**) but not in LZ*oep* mutants (**H–J**). For detailed views from different angles, see Supplemental Movies 2 (wild type) and 6 (LZ*oep*). Pictures were cropped to keep the heart in the center and do not maintain the positions of the coordinate systems. For movements with respect to coordinate systems, see Supplemental Movies 2 (wild type) and 6 (LZ*oep*).

Thisse and Thisse, 1999; Long et al., 2003), these results indicate that *spaw* expression in the left non-cardiac LPM activates the Nodal signaling pathway in adjacent ipsilateral heart progenitors in an *oep*-dependent manner at the onset of asymmetric morphogenesis.

Position-Dependent Differences in Cardiomyocyte Movements During Heart Lateralization

To analyze the cellular basis of heart lateralization, we used high-resolution 4D confocal time-lapse imaging of cardiomyocyte movement using a similar approach as Smith et al. (2008). Transgenic *cmlc2:gfp* embryos express GFP in all cardiomyocytes throughout cardiac morphogenesis (Huang et al., 2003) (see Supp. Movie 1, which is available online). Cell tracking and isosurface rendering revealed that the first sign of

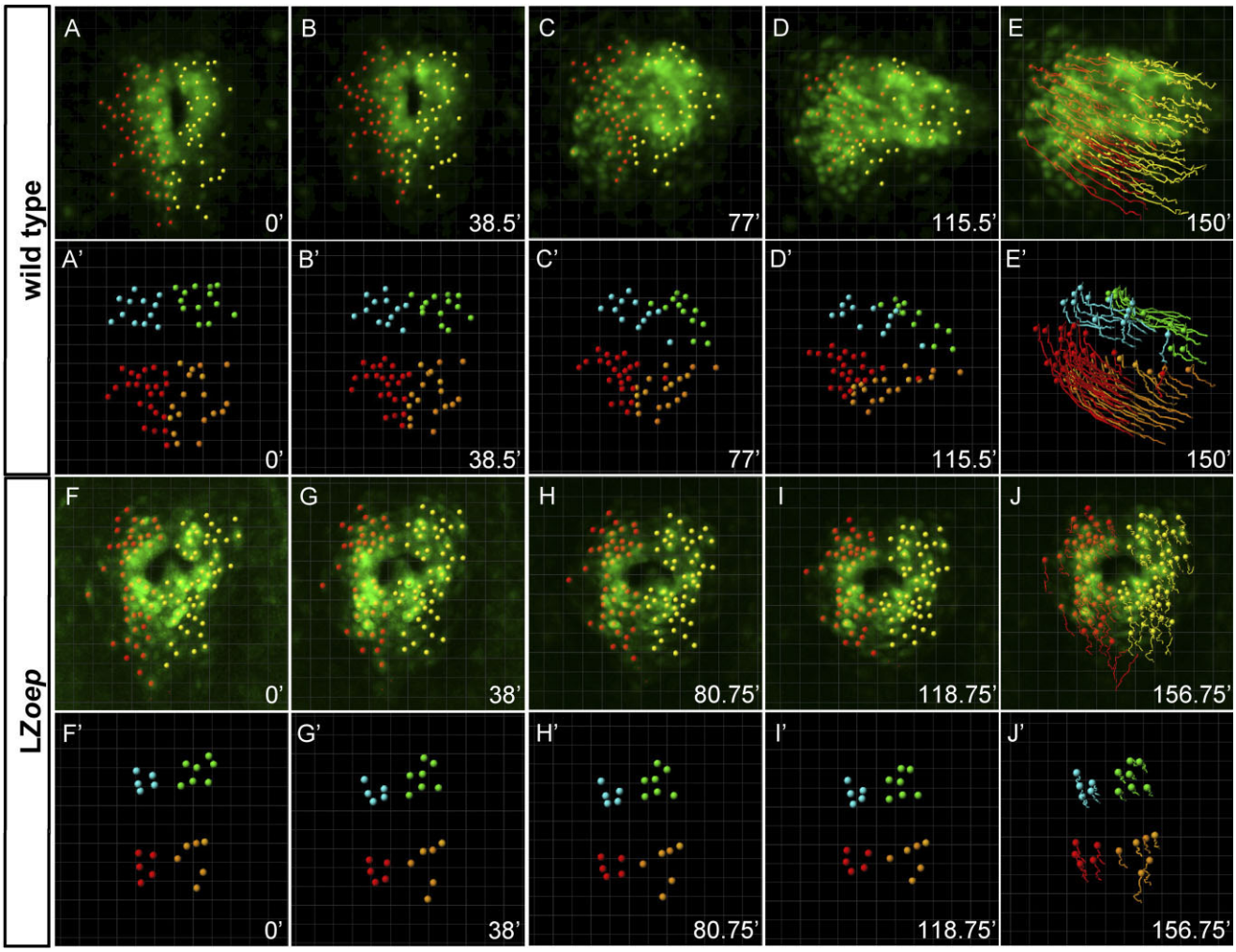

Fig. 3. Tracking of single cells in wild type and LZ*oep* mutants. Confocal 3D-images showing individual *cmlc2*-GFP cells that were manually tracked starting at the onset of cardiac cone formation. First (**A–E**) and third (**F–J**) rows: green *cmlc2*-GFP expression; red: cells within the left side of cardiac cone; yellow: cells within the right side of cardiac cone. For detailed views from different angles, see Supplemental Movies 1 (wild type) and 5 (LZ*oep*). Second (**A'–E'**) and fourth (**F'–J'**) rows: tracking of quadrants. Quadrants were defined by grouping left-anterior cells (blue), left-posterior cells (red), right anterior cells (green), and right-posterior cells (orange). For detailed views from different angles, see Supplemental Movies 3 (wild type) and 7 (LZ*oep*). Pictures were cropped to keep the heart in the center and do not maintain the position of the coordinate systems. For movements with respect to coordinate systems, see Supplemental Movies 3 (wild type) and 7 (LZ*oep*).

asymmetry was apparent shortly after cardiac fusion, when anterior and leftward displacement initiated and cardiomyocytes located on the right involuted (Fig. 2A–E; Supp. Movies 1 and 2) (Rohr et al., 2008; Smith et al., 2008). To gain quantitative insights into heart morphogenesis, we tracked individual cells using Imaris software and measured the direction, displacement, meandering, and speed of cells (Fig. 3; Supp. Movie 1; Supp. Fig. 1) (Smith et al., 2008). In contrast to a recent study (Smith et al., 2008), we analyzed heart morphogenesis per se, independent of the movement of the entire heart within the embryo. Using the position of the lumen as a stationary reference point, we tracked the movement of cells within the heart. This allowed us to measure cardiomyocyte movements with respect to each other rather than the potential drift of the embryo during imaging or the displacement of the entire heart within the embryo. As described below and in Supplemental Figure 2, our conclusions largely agree with the recent study by Smith et al. (2008), despite the different means of analysis.

To quantitate heart morphogenesis, we first compared four territories: left anterior (LA), right anterior (RA), left posterior (LP), and right posterior (RP) (Supp. Movie 3; Figs. 3–5). Analysis of each cell track provided measurements of the speed, displacement, and meandering of a cell (Smith et al., 2008). Speed was defined as distance moved/time interval, displacement rate as distance from first to last location/entire time interval, and meandering index as total distance traveled/displacement (Supp. Fig. 1) (Smith et al., 2008). Comparison of posterior and anterior cells revealed that posterior cells moved faster than anterior cells, had higher displacement rates, and a higher meandering index (Fig. 4A, C, E, G, and I). These results indicate that posterior cells move faster and more directionally than anterior cells (Smith et al., 2008). To determine the direction of

Developmental Dynamics

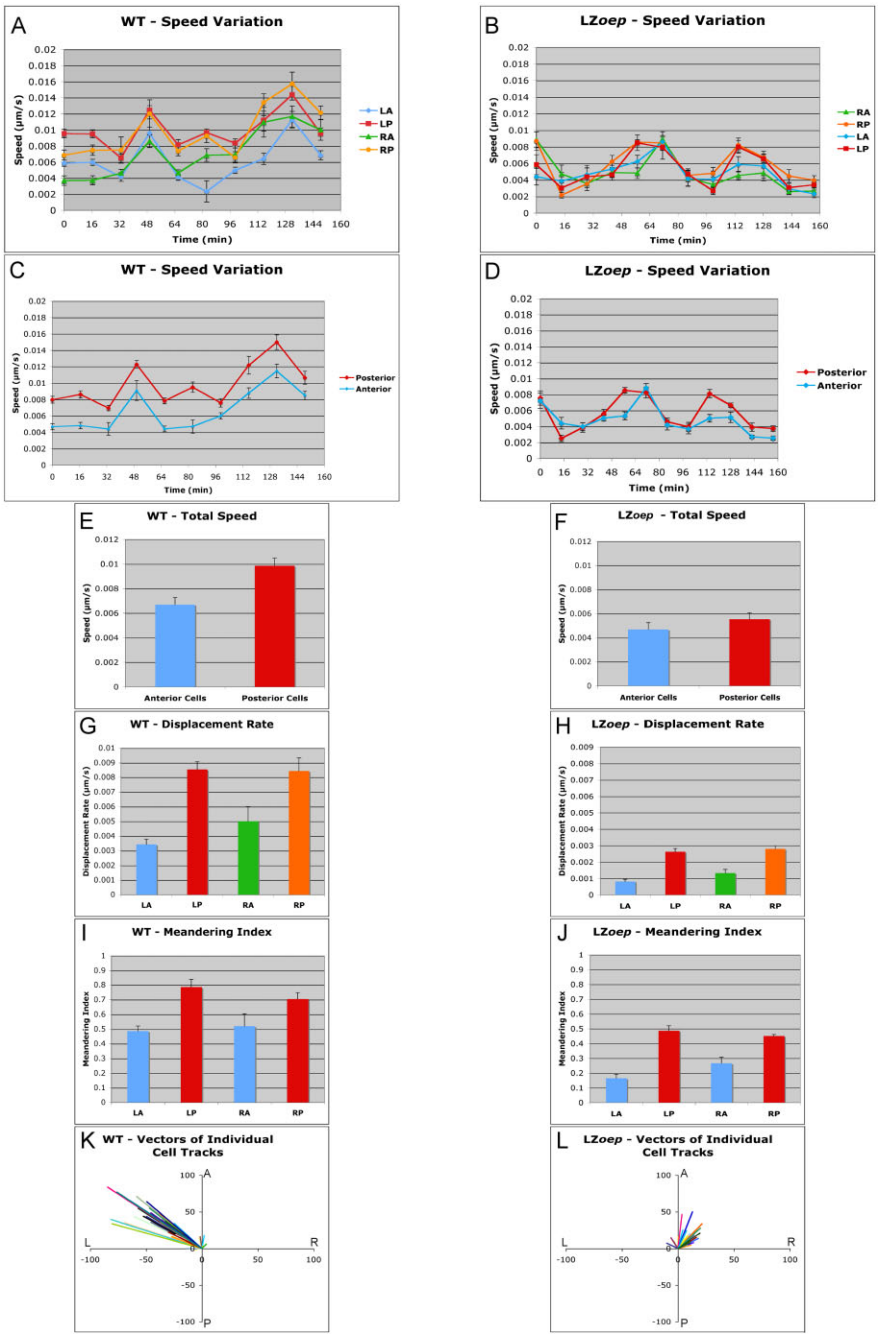

Fig. 4. Quantitative analysis of anterior and posterior cell movements in wild type and LZ*oep* mutants. *cmlc2*-GFP cells in left-anterior (LA), left-posterior (LP), right-anterior (RA), and right-posterior (RP) quadrants were tracked and different parameters were measured using Imaris Software. Speed variation indicates speed of a cell during a given time interval. Total speed, displacement rate, and meandering index were determined as described in Experimental Procedures and Supplemental Figure 1. Note the higher speed (**A, C, E**), displacement rate (**G**), and meandering index (**I**) of posterior cells as compared to anterior cells in wild type. These differences are reduced in LZ*oep* mutants. Cardiomyocytes in LZ*oep* mutants have lower speed (**B, D, F**), displacement rate (**H**), and meandering index (**J**) as compared to wild type. Differences between posterior and anterior cells are attenuated in LZ*oep* mutants. Vectors of individual cells illustrate the angle and length of x/y displacement of cells (A, anterior; P, posterior; L, left; R, right). Note the leftwards and anterior displacement of wild type cells (**K**). LZ*oep* mutant cells displace less and mostly anteriorly (L). Statistics: (E) $P < 0.05$; (F) $P > 0.05$; (G) LA vs. LP, $P < 0.05$; RA vs. RP, $P < 0.05$; LA vs. RA, $P > 0.05$; LP vs. RP, $P > 0.05$; (H) LA vs. LP, $P < 0.05$; RA vs. RP, $P < 0.05$; LA vs. RA, $P > 0.05$; LP vs. RP, $P > 0.05$; (I) LA vs. LP, $P < 0.05$; RA vs. RP, $P < 0.05$; LA vs. RA, $P > 0.05$; LP vs. RP, $P > 0.05$; (J) LA vs. LP, $P < 0.05$; RA vs. RP, $P < 0.05$; LA vs. RA, $P > 0.05$; LP vs. RP, $P > 0.05$.

movement, we performed vector analyses that included displacement length and angle with respect to the anterior-posterior and left-right axes. These measurements showed that the large majority of individual cardiomyocytes moved leftwards and anteriorly (Fig. 4K), consistent with the overall morphogenetic change of the cardiac cone (Rohr et al., 2008; Smith et al., 2008).

To determine if there are differences between cardiomyocytes located on the left or right side, we compared speed, displacement rate, and meandering index. Consistent with the findings by Smith et al. (2008), we did not find significant differences between left and right cells using these measures (Fig. 4A, G, I). However, extending previous studies (Rohr et al., 2008; Smith et al., 2008), we quantified the dorsal-ventral displacement of cells and found that cells on the right, but not the left, were displaced ventrally (Fig. 5A). This observation is consistent with the observed involution of cells located in the right heart cone (Rohr et al., 2008) and reveals that the first signs of asymmetric morphogenesis are the leftwards displacement of all cardiomyocytes and the ventral displacement of cardiomyocytes located in the right heart cone.

The large number of tracked cells also allowed us to study the movement of cells located in the inner and outer regions of the cardiac cone. Consistent

Fig. 5. Quantitative analysis of left, right, ventricular, and atrial cell movements in wild type and LZoep mutants. Left and right *cmlc2*-GFP cells were tracked and Z-axis (dorsal-ventral) displacement of cells was measured. Note the asymmetric, ventral displacement of cells on the right in wild type (**A**) but not in LZ*oep* mutants (**B**). Ventricular cells (located at the apex of the cardiac cone) and atrial cells (located at the base of the cardiac cone) were tracked using Imaris. Speed variation indicates speed of a cell during a given time interval. Total speed, displacement rate, and meandering index were determined as described in Experimental Procedures and Supplemental Figure 1. Note the higher speed (**C, E**), displacement rate (**G**), and meandering index (**I**) of atrial cells as compared to ventricular cells in wild-type. These differences are reduced in LZ*oep* mutants. LZ*oep* mutant cells have lower speed (**D, F**), displacement rate (**H**), and meandering index (**J**) compared to wild type. **K:** Degree of clockwise rotation of cardiac cone. Note the lack of rotation in LZ*oep* mutants. Statistics: (E–K) $P < 0.05$.

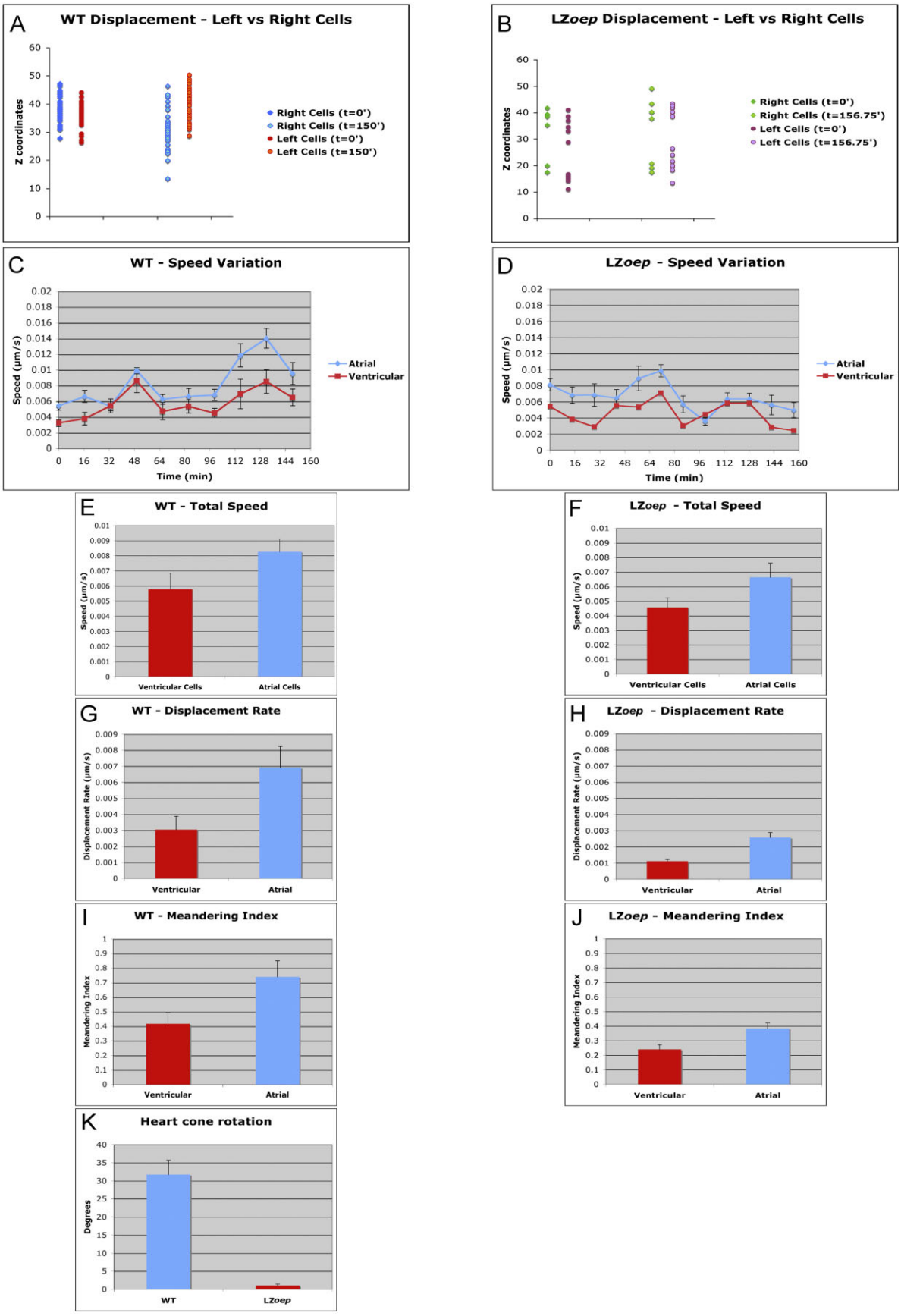
A
WT Displacement - Left vs Right Cells
Z coordinates
Right Cells (t=0')
Right Cells (t=150')
Left Cells (t=0')
Left Cells (t=150')
B
LZoep Displacement - Left vs Right Cells
Z coordinates
Right Cells (t=0')
Right Cells (t=156.75')
Left Cells (t=0')
Left Cells (t=156.75')
C
WT - Speed Variation
Speed (µm/s)
Time (min)
Atrial
Ventricular
D
LZoep - Speed Variation
Speed (µm/s)
Time (min)
Atrial
Ventricular
E
WT - Total Speed
Speed (µm/s)
Ventricular Cells
Atrial Cells
F
LZoep - Total Speed
Speed (µm/s)
Ventricular Cells
Atrial Cells
G
WT - Displacement Rate
Displacement Rate (µm/s)
Ventricular
Atrial
H
LZoep - Displacement Rate
Displacement Rate (µm/s)
Ventricular
Atrial
I
WT - Meandering Index
Meandering Index
Ventricular
Atrial
J
LZoep - Meandering Index
Meandering Index
Ventricular
Atrial
K
Heart cone rotation
Degrees
WT
LZoep

Fig. 5.

with gene expression patterns for atrial and ventricular markers (Yelon et al., 1999), we found that the atrial precursors were located in the outer region of the cone and had a higher speed, displacement rate, and meandering index than the ventricular cells, which were located in the inner region of the cone (Fig. 5C, E. G, and I).

To quantify the global changes in heart morphogenesis, we measured the initial and final position of cells placed in regions LA, LP, RA, and RP. This analysis confirmed the previously observed ~30° clockwise rotation of the cardiac cone. (Fig. 5K) (Smith et al., 2008). The clockwise rotation and the leftwards and anterior movement of individual cardiomyocytes reflected the overall morphogenesis of the heart. This result indicated that the coherent movement of individual cardiomyocytes underlies overall heart morphogenesis. Coherence could be generated if neighbor relationships between individual cardiomyocytes did not change extensively (Rohr et al., 2008; Smith et al., 2008). Tracking of groups of cells confirmed that neighbor relationships were maintained during heart lateralization (Supp. Movie 4). These results confirm and extend previous studies (Rohr et al., 2008; Smith et al., 2008) and indicate that differential but coherent cell displacement and direction underlie asymmetric heart morphogenesis in wild type.

Loss of Nodal Signaling Decreases the Speed and Increases the Meandering of Cardiomyocytes

To determine how and when lack of Nodal signaling affects heart morphogenesis, we analyzed LZ*oep* embryos (Supp. Movies 5–8). These mutants lack *spaw* and *lft2* expression in the left LPM, indicating the loss of Nodal signaling, but form normal mesendoderm and are viable (Gritsman et al., 1999; Yan et al., 1999). To analyze overall heart morphogenesis, we used isosurface rendering. Cardiomyocytes formed the cardiac cone in LZ*oep* mutants, but in striking contrast to wild type, the heart failed to tilt leftwards and displayed reduced anterior displacement (Fig. 2F–J; Supp. Movie 6). Consequently, the heart in LZ*oep* mutants remained positioned at the midline. As an additional measure of asymmetry, we analyzed cardiac rotation. Strikingly, clockwise rotation was abolished in LZ*oep* mutants (Fig. 5K). These results support the model that absence of Nodal signaling disrupts the earliest steps of cardiac lateralization.

To quantitatively compare wild type and LZ*oep* mutants, we used cell tracking analyses (Figs. 3–5; Supp. Movies 5 and 7). Strikingly, cardiomyocytes in LZ*oep* mutants moved more slowly and meandered more (Fig. 4B, D, F, and J). These defects resulted in a strongly reduced displacement rate (Fig. 4J). To determine the direction of movement, we performed vector analysis. Cardiomyocytes in LZ*oep* mutants did not move leftwards and displaced anteriorly much less than wild type (Fig. 4L). These results reveal that cardiomyocyte movement in LZ*oep* mutants is slower, less directional, and largely symmetric compared to wild type.

To determine if different regions in the LZ*oep* mutant heart have distinct characteristics as in wild type, we performed detailed tracking analyses. Strikingly, differences between anterior and posterior, between left and right, and between atrial and ventricular cells were strongly reduced or absent (Figs. 4 and 5). For example, right cells were not displaced ventrally (Fig. 5B) and posterior cells were not significantly faster than anterior cells (Fig. 4F). These results suggest that the loss of asymmetric behavior of cardiomyocytes underlies the loss of cardiac cone asymmetry in LZ*oep* mutants.

To determine if cardiomyocytes in LZ*oep* mutants lose their coherence, we analyzed neighbor relationships (Supp. Movie 8). Despite the abnormal direction and speed of cardiomycytes, cells continued to move as cohorts, as in wild type. These results indicate that Nodal signaling is not required for the integrity of the heart tube but regulates the speed and directionality of cardiomyocyte movement.

DISCUSSION

The cellular mechanisms underlying left-right asymmetric organogenesis are largely elusive. A deeper understanding rests on detailed analyses of cell movements, shapes, and rearrangements during this process in wild type (Horne-Badovinac et al., 2003; Yashiro et al., 2007; Davis et al., 2008; Kurpios et al., 2008; Rohr et al., 2008; Smith et al., 2008). For instance, cell shape analyses in the amniote dorsal mesentery have suggested a structural basis for the asymmetric tilting and rotation of the gut tube (Davis et al., 2008; Kurpios et al., 2008). Columnar epithelization and mesenchymal condensation on the left side lead the mesentery to take on a trapezoidal shape that leads to a leftward tilt of the gut. In the zebrafish heart, cell movement analyses have revealed that cardiomyocytes move anteriorly and leftwards as a cohort while the heart cone rotates clockwise (Chen et al., 1997; Rohr et al., 2008; Smith et al., 2008). Our studies confirm these results and reveal two additional quantitative differences. First, cells on the right are displaced more ventrally than their left-side neighbors. This displacement reflects the involution of cells in the right heart cone (Rohr et al., 2008). Second, atrial cells move faster and more directionally than ventricular cells and, therefore, have higher displacement rates. These results highlight the potential of single cell tracking to dissect the cellular processes underlying asymmetric morphogenesis during left-right development.

Components of the Nodal signaling pathway are expressed asymmetrically during left-right heart morphogenesis (Hamada et al., 2002; Schier, 2003; Shen, 2007). Our double in situ hybridization analysis confirms and extends previous studies and shows that *spaw* and *lft2* are expressed in adjacent regions of the left LPM, with only *lft2* being activated in heart progenitors (Zhang et al., 1998; Bisgrove et al., 1999, 2000; Thisse and Thisse, 1999; Long et al., 2003). The largely non-overlapping expression domains of *spaw* and *lft2* are unusual for *nodal* and *lefty* genes. For example, during mesendoderm induction, the Nodal signals *cyclops* and *squint* are co-expressed with *lefty1* and *lefty2* in the blastula margin (Schier and Talbot, 2005). It is conceivable that *lft2* can only be activated in the heart because other LPM cells lack components of

the Nodal signaling pathway (Gritsman et al., 1999). However, our finding that the Nodal co-receptor *oep* is expressed bilaterally in all LPM cells suggests that the restricted expression of *oep* is unlikely to restrict Nodal signaling to the heart. It is possible that other components of the Nodal signaling pathway are absent in non-cardiac cells. Blocking BMP signaling during mid-somitogenesis blocks induction of *lft2* (Chocron et al., 2007), indicating that other signaling pathways or transcription factors might also restrict *lft2* expression to the left heart field.

Nodal signaling is required for normal left-right morphogenesis (Hamada et al., 2002; Schier, 2003; Shen, 2007). Previous studies have shown that loss of Nodal signaling in zebrafish results in abnormal heart morphogenesis, resulting in randomized heart looping and loss of initial leftwards jogging (Chen et al., 1997; Yan et al., 1999; Long et al., 2003; Rohr et al., 2008). For example, cardiac cells in *spaw* morphants do not displace leftwards and cells on the right side of the heart do not involute (Long et al., 2003; Rohr et al., 2008). Our quantitative analysis of LZ*oep* mutants shows that loss of Nodal signaling affects the direction of movement of individual cardiomyocytes during early heart development. Anterior movement is reduced and leftwards migration is abolished. In addition, our results show that loss of Nodal signaling also affects the speed of cardiomyocyte movement. Cardiomyocytes move more slowly and meander more, resulting in strongly reduced displacement. The differences between anterior/posterior, left/right, and atrial/ventricular cells are reduced or absent. Taken together, these results suggest that Nodal signaling provides a directional cue and promotes the speed of heart cells.

It is unclear whether specific cell shape changes underlie the differential movement and rotation of anterior/posterior, left/right, and atrial/ventricular cardiomyocytes. Studies of cell movements during zebrafish gastrulation and germ cell migration have shown that changes in cell polarity and protrusions are associated with abnormal movement (Solnica-Krezel, 2005; Raz and Reichman-Fried, 2006; Rohde and Heisenberg, 2007). Cardiomyocytes display small extensions restricted to the basal surface and chamber-specific cell shapes (Rohr et al., 2008). Future studies will address whether these properties are regulated by Nodal signaling.

The cellular and morphogenetic phenotypes in LZ*oep* mutants become apparent at the same time, making it difficult to resolve cause-and-effect relationships. Slower and more meandering movements of individual cells might lead to a block of the overall asymmetric morphogenesis of the heart. Alternatively, overall abnormal morphogenesis and lack of directionality might restrict the speed of individual cells. Detailed analysis of additional mutants might be able to separate the processes we quantified here. For instance, mutants that do not slow down cardiomyocytes might still lead to left-right defects.

How does Nodal signaling drive asymmetric morphogenesis? The activation of the Nodal signaling pathway in the left heart cone suggests that Nodal regulates heart morphogenesis directly. This contrasts with the rotation of the gut, which is driven by shape changes in the associated dorsal mesentery, and the asymmetric maintenance of the sixth branchial arch artery, which is regulated by differential haemodynamics caused by asymmetric development of the heart outflow tract (Yashiro et al., 2007; Davis et al., 2008; Kurpios et al., 2008). It is unclear how activation of Nodal signaling within the left side of the cardiac cone changes cell behavior throughout the heart. We favor a model wherein Nodal signaling acts quite locally in *lft2*-expressing cells and secondary interactions within the heart lead to the complex morphogenetic behaviors. These interactions could involve relay signals (*lft2*-expressing cells signal to neighboring cells) or mechano-physical interactions (shape changes in *lft2*-expressing cells induce shape changes in neighboring cells). It is thus conceivable that a small group of cells (e.g., the *lft2*-expressing cells) act as organizers to drive asymmetric morphogenesis. Mosaic analysis could address this question.

Interestingly, morphogenesis in the absence of Nodal signaling is not completely blocked. Anterior movement still occurs and heart jogging and heart looping eventually take place in the absence of Nodal signaling, resulting in heterotaxic but viable animals (Yan et al., 1999). These observations suggest that there are Nodal-independent morphogenetic events that might be driven autonomously within the heart or indirectly by surrounding tissue. For example, it is conceivable that the elongation and straightening of the embryo (Kimmel et al., 1995) contributes to asymmetric morphogenesis as the heart interacts with surrounding tissues.

Recent studies have revealed that asymmetric BMP signaling regulates asymmetric heart morphogenesis in zebrafish (Chen et al., 1997; Schilling et al., 1999; Chocron et al., 2007; Monteiro et al., 2008; Smith et al., 2008). Loss of BMP signaling reduces the speed, displacement rate, and meandering index of heart cells and abolishes leftward displacement and rotation (Smith et al., 2008). These phenotypes are strikingly similar to the LZ*oep* phenotypes we describe here. Moreover, ectopic sources of BMP can attract cardiomyocytes (Smith et al., 2008). Nodal signaling is required for the asymmetric expression of BMP4 in the heart cone (Chen et al., 1997; Chocron et al., 2007). It is therefore conceivable that the effects of asymmetric Nodal signaling are mediated via asymmetric BMP signaling. Moreover, BMP signaling and Nodal signaling also act further upstream during left-right development (Zhang and Bradley, 1996; Chen et al., 1997; Ramsdell and Yost, 1999; Schilling et al., 1999; Branford et al., 2000; Chang et al., 2000; Breckenridge et al., 2001; Hamada et al., 2002; Piedra and Ros, 2002; Schlange et al., 2002; Schier, 2003; Kishigami et al., 2004; Kishigami and Mishina, 2005; Chocron et al., 2007; Shen, 2007; Mine et al., 2008; Monteiro et al., 2008). Hence, a cascade of asymmetrically activated TGFβ signaling pathways appears to drive asymmetric heart morphogenesis.

EXPERIMENTAL PROCEDURES

Fish Lines

Tg(cmlc2:gfp) and LZ*oep* lines were described previously (Yan et al., 1999; Huang et al., 2003).

In Situ Hybridization

Double fluorescent in situ hybridization probes were labeled with fluorescein (Roche) and digoxygenin (Roche). Detection was based on fluorescein or Cy3 tyramide deposition (Perkin Elmer; Schoenebeck et al., 2007). Embryos were mounted in benzylbenzoate/benzylalcohol for photography.

Imaging and Data Analysis

At the 15-somite stage, embryos were manually dechorionated and then mounted at the 18-somite stage in glass-bottom culture dishes using 0.8% low-melt agarose in E3 embryo medium. Imaging was performed on a Zeiss LSM 5 Pascal confocal microscope with LSM software. The microscope stage was heated to 30°C to keep embryos at 28.5°C during the time-lapse recordings. Stacks were acquired every 5.5 min for wild type and 4.75 min for LZ*oep* mutants. Z-stacks were rendered in 3D and analyzed with Imaris software (Bitplane). 3D singe cell trackings and measurements (x/y/z coordinates) were performed manually using Imaris. The base of the lumen was chosen as reference point for the x/y/z coordinate system to analyze heart morphogenesis per se and to avoid confounding effects caused by the potential drift of the embryo during imaging or the movement of the heart within the embryo. Each measurement was obtained from the cells depicted in Figure 3A' and F' and in Supplemental Movies 3 and 7. The time window for quantitative measurements was from the onset of cardiac cone formation until the full leftward displacement of the cardiac cone in wild type (t = 150.0 min). Since the same morphological landmark does not develop in LZ*oep* mutants and to directly compare LZ*oep* cardiomyocyte movement to wild type cardiomyocyte movement, the time interval for analysis of LZ*oep* mutants was 156.75 min from the formation of the cardiac cone. Cell positions were defined by x/y/z coordinates at each time point. Time intervals between each tracked time point were 16.5 min in wild type and 14.25 min in LZ*oep* mutants. The following parameters were measured (Smith et al., 2008): speed = track length/time interval; total speed = total track length/total time (i.e., sum of the average distance traveled by the cells within each time interval divided by the total track time); displacement rate = total displacement length/total time (i.e., position of each cell at the end of the track - position at t = 0 divided by the total track time); meandering index = total displacement length/total track length; displacement of left vs. right cells: the z-axis coordinates of each cell were analyzed at t = 0 and at the end of the track. Rotation angle was obtained by drawing an imaginary square connecting cells in each quadrant of the heart cone at the beginning and at the end of the time-lapse (Smith et al., 2008). Statistical analysis and graphics were obtained in Excel (Microsoft).

ACKNOWLEDGMENTS

We thank Steven Zimmerman for fish care and members of the Schier and Yelon labs for helpful discussions. Thanks to Sheu Shu-Hsien and the Lichtman lab for help with Imaris software. This work was supported in part by NIH grant R01 GM56211 to A.F.S. and by Gulbenkian PhD Program (FCT SFRH/BD/11801/2003) to M.I.M.C.-B.

REFERENCES

Bamford RN, Roessler E, Burdine RD, Saplakoglu U, dela Cruz J, Splitt M, Goodship JA, Towbin J, Bowers P, Ferrero GB, Marino B, Schier AF, Shen MM, Muenke M, Casey B. 2000. Loss-of-function mutations in the EGF-CFC gene CFC1 are associated with human left-right laterality defects. Nat Genet 26: 365–369.

Bisgrove BW, Essner JJ, Yost HJ. 1999. Regulation of midline development by antagonism of lefty and nodal signaling. Development 126:3253–3262.

Bisgrove BW, Essner JJ, Yost HJ. 2000. Multiple pathways in the midline regulate concordant brain, heart and gut left-right asymmetry. Development 127:3567–3579.

Branford WW, Essner JJ, Yost HJ. 2000. Regulation of gut and heart left-right asymmetry by context-dependent interactions between xenopus lefty and BMP4 signaling. Dev Biol 223:291–306.

Breckenridge RA, Mohun TJ, Amaya E. 2001. A role for BMP signalling in heart looping morphogenesis in Xenopus. Dev Biol 232:191–203.

Brennan J, Norris DP, Robertson EJ. 2002. Nodal activity in the node governs left-right asymmetry. Genes Dev 16:2339–2344.

Chang H, Zwijsen A, Vogel H, Huylebroeck D, Matzuk MM. 2000. Smad5 is essential for left-right asymmetry in mice. Dev Biol 219:71–78.

Chen JN, van Eeden FJ, Warren KS, Chin A, Nusslein-Volhard C, Haffter P, Fishman MC. 1997. Left-right pattern of cardiac BMP4 may drive asymmetry of the heart in zebrafish. Development 124: 4373–4382.

Chocron S, Verhoeven MC, Rentzsch F, Hammerschmidt M, Bakkers J. 2007. Zebrafish Bmp4 regulates left-right asymmetry at two distinct developmental time points. Dev Biol 305:577–588.

Concha ML, Burdine RD, Russell C, Schier AF, Wilson SW. 2000. A nodal signaling pathway regulates the laterality of neuroanatomical asymmetries in the zebrafish forebrain. Neuron 28:399–409.

Davis NM, Kurpios NA, Sun X, Gros J, Martin JF, Tabin CJ. 2008. The chirality of gut rotation derives from left-right asymmetric changes in the architecture of the dorsal mesentery. Dev Cell 15:134–145.

Duboc V, Rottinger E, Lapraz F, Besnardeau L, Lepage T. 2005. Left-right asymmetry in the sea urchin embryo is regulated by nodal signaling on the right side. Dev Cell 9:147–158.

Gritsman K, Zhang J, Cheng S, Heckscher E, Talbot WS, Schier AF. 1999. The EGF-CFC protein one-eyed pinhead is essential for nodal signaling. Cell 97:121–132.

Hamada H, Meno C, Watanabe D, Saijoh Y. 2002. Establishment of vertebrate left-right asymmetry. Nat Rev Genet 3:103–113.

Holtzman NG, Schoenebeck JJ, Tsai HJ, Yelon D. 2007. Endocardium is necessary for cardiomyocyte movement during heart tube assembly. Development 134: 2379–2386.

Horne-Badovinac S, Rebagliati M, Stainier DY. 2003. A cellular framework for gut-looping morphogenesis in zebrafish. Science 302:662–665.

Huang CJ, Tu CT, Hsiao CD, Hsieh FJ, Tsai HJ. 2003. Germ-line transmission of a myocardium-specific GFP transgene reveals critical regulatory elements in the cardiac myosin light chain 2 promoter of zebrafish. Dev Dyn 228:30–40.

Kimmel CB, Ballard WW, Kimmel SR, Ullmann B, Schilling TF. 1995. Stages of embryonic development of the zebrafish. Dev Dyn 203:253–310.

Kishigami S, Mishina Y. 2005. BMP signaling and early embryonic patterning. Cytokine Growth Factor Rev 16:265–278.

Kishigami S, Yoshikawa S, Castranio T, Okazaki K, Furuta Y, Mishina Y. 2004. BMP signaling through ACVRI is required for left-right patterning in the early mouse embryo. Dev Biol 276:185–193.

Krauss S, Concordet JP, Ingham PW. 1993. A functionally conserved homolog of the Drosophila segment polarity gene hh is expressed in tissues with polarizing activity in zebrafish embryos. Cell 75: 1431–1444.

Kurpios NA, Ibanes M, Davis NM, Lui W, Katz T, Martin JF, Belmonte JC, Tabin CJ. 2008. The direction of gut looping is established by changes in the extracellular matrix and in cell:cell adhesion. Proc Natl Acad Sci USA 105:8499–8506.

Levin M. 2005. Left-right asymmetry in embryonic development: a comprehensive review. Mech Dev 122:3–25.

Levin M, Johnson RL, Stern CD, Kuehn M, Tabin C. 1995. A molecular pathway determining left-right asymmetry in chick embryogenesis. Cell 82:803–814.

Liang JO, Etheridge A, Hantsoo L, Rubinstein AL, Nowak SJ, Izpisua Belmonte JC, Halpern ME. 2000. Asymmetric nodal signaling in the zebrafish diencephalon positions the pineal organ. Development 127:5101–5112.

Long S, Ahmad N, Rebagliati M. 2003. The zebrafish nodal-related gene southpaw is required for visceral and diencephalic left-right asymmetry. Development 130: 2303–2316.

Mine N, Anderson RM, Klingensmith J. 2008. BMP antagonism is required in both the node and lateral plate mesoderm for mammalian left-right axis establishment. Development 135:2425–2434.

Monteiro R, van Dinther M, Bakkers J, Wilkinson R, Patient R, ten Dijke P, Mummery C. 2008. Two novel type II receptors mediate BMP signalling and are required to establish left-right asymmetry in zebrafish. Dev Biol 315:55–71.

Piedra ME, Ros MA. 2002. BMP signaling positively regulates Nodal expression during left right specification in the chick embryo. Development 129:3431–3440.

Pogoda HM, Solnica-Krezel L, Driever W, Meyer D. 2000. The zebrafish forkhead transcription factor FoxH1/Fast1 is a modulator of nodal signaling required for organizer formation. Curr Biol 10:1041–1049.

Ramsdell AF. 2005. Left-right asymmetry and congenital cardiac defects: getting to the heart of the matter in vertebrate left-right axis determination. Dev Biol 288: 1–20.

Ramsdell AF, Yost HJ. 1999. Cardiac looping and the vertebrate left-right axis: antagonism of left-sided Vg1 activity by a right-sided ALK2-dependent BMP pathway. Development 126:5195–5205.

Raya A, Belmonte JC. 2006. Left-right asymmetry in the vertebrate embryo: from early information to higher-level integration. Nat Rev Genet 7:283–293.

Raz E, Reichman-Fried M. 2006. Attraction rules: germ cell migration in zebrafish. Curr Opin Genet Dev 16:355–359.

Rohde LA, Heisenberg CP. 2007. Zebrafish gastrulation: cell movements, signals, and mechanisms. Int Rev Cytol 261:159–192.

Rohr S, Otten C, Abdelilah-Seyfried S. 2008. Asymmetric involution of the myocardial field drives heart tube formation in zebrafish. Circ Res 102:e12–19.

Schier AF. 2003. Nodal signaling in vertebrate development. Annu Rev Cell Dev Biol 19:589–621.

Schier AF, Talbot WS. 2005. Molecular genetics of axis formation in zebrafish. Annu Rev Genet 39:561–613.

Schilling TF, Concordet JP, Ingham PW. 1999. Regulation of left-right asymmetries in the zebrafish by Shh and BMP4. Dev Biol 210:277–287.

Schlange T, Arnold HH, Brand T. 2002. BMP2 is a positive regulator of Nodal signaling during left-right axis formation in the chicken embryo. Development 129:3421–3429.

Schoenebeck JJ, Keegan BR, Yelon D. 2007. Vessel and blood specification override cardiac potential in anterior mesoderm. Dev Cell 13:254–267.

Shen MM. 2007. Nodal signaling: developmental roles and regulation. Development 134:1023–1034.

Shiratori H, Hamada H. 2006. The left-right axis in the mouse: from origin to morphology. Development 133:2095–2104.

Sirotkin HI, Gates MA, Kelly PD, Schier AF, Talbot WS. 2000. Fast1 is required for the development of dorsal axial structures in zebrafish. Curr Biol 10:1051–-1054.

Smith KA, Chocron S, von der Hardt S, de Pater E, Soufan A, Bussmann J, Schulte-Merker S, Hammerschmidt M, Bakkers J. 2008. Rotation and asymmetric development of the zebrafish heart requires directed migration of cardiac progenitor cells. Dev Cell 14:287–297.

Solnica-Krezel L. 2005. Conserved patterns of cell movements during vertebrate gastrulation. Curr Biol 15:R213–228.

Tabin C. 2005. Do we know anything about how left-right asymmetry is first established in the vertebrate embryo? J Mol Histol 36:317–323.

Thisse C, Thisse B. 1999. Antivin, a novel and divergent member of the TGFbeta superfamily, negatively regulates mesoderm induction. Development 126:229–240.

Trinh LA, Stainier DY. 2004. Cardiac development. Methods Cell Biol 76:455–473.

Yan YT, Gritsman K, Ding J, Burdine RD, Corrales JD, Price SM, Talbot WS, Schier AF, Shen MM. 1999. Conserved requirement for EGF-CFC genes in vertebrate left-right axis formation. Genes Dev 13:2527–2537.

Yashiro K, Shiratori H, Hamada H. 2007. Haemodynamics determined by a genetic programme govern asymmetric development of the aortic arch. Nature 450: 285–288.

Yelon D, Horne SA, Stainier DY. 1999. Restricted expression of cardiac myosin genes reveals regulated aspects of heart tube assembly in zebrafish. Dev Biol 214: 23–37.

Zhang H, Bradley A. 1996. Mice deficient for BMP2 are nonviable and have defects in amnion/chorion and cardiac development. Development 122:2977–2986.

Zhang J, Talbot WS, Schier AF. 1998. Positional cloning identifies zebrafish one-eyed pinhead as a permissive EGF-related ligand required during gastrulation. Cell 92:241–251.

Chapter III

Bilateral and right-sided expression of Nodal confirm role in promoting speed and directional movement of the cardiomyocytes and need of cardiac rotation for proper heart cone formation

Maria Inês Baptista and Alexander Schier

NOTE:

The results presented in this chapter for the wild type and the LZ*oep* mutants were included in the following article:

de Campos-Baptista MI, Holtzman NG, Yelon D, Schier AF. (2008) Nodal signaling promotes the speed and directional movement of cardiomyocytes in zebrafish.

Developmental Dynamics, Dec;237(12):3624-33.

Bilateral and right-sided expression of Nodal confirm role in promoting speed and directional movement of the cardiomyocytes and need of cardiac rotation for proper heart cone formation

Maria Inês Baptista and Alexander Schier

Department of Molecular and Cellular Biology, Center for Brain Science, Broad Institute, Harvard Stem Cell Institute, Harvard University, Cambridge, Massachusetts, USA; Instituto Gulbenkian de Ciência, 2780-156 Oeiras, Portugal.

ABSTRACT

Nodal is a member of the TGFβ family that regulates left-right asymmetry during vertebrate organogenesis. In the context of heart development, Nodal is expressed asymmetrically in the left lateral plate mesoderm (LPM). We have recently shown that the Nodal signaling cascade drives left-right heart morphogenesis by regulating the speed and direction of cardiomyocytes movement. These conclusions were obtained by the analysis of late-zygotic mutants for the Nodal co-receptor *one-eyed pinhead* (LZ*oep)*, which lack Nodal signaling. Here we used high-resolution time-lapse imaging in zebrafish to compare the movements of cardiomyocytes upon bilateral Nodal expression (*no tail* morphants) and when Nodal is asymmetrically expressed in the right LPM (*polaris* morphants). Bilateral Nodal signaling (*ntl* MO) abolished the leftward movement of cardiomyocytes and global heart rotation was blocked, resembling the LZ*oep* phenotype. However, cells moved faster and traveled anteriorly. Cells from both the left and the right side involuted. Contrary to LZ*oep*, neighbor relationships were not maintained. Right expression of Nodal signaling (*pol* MO) lead to rightward movement of cardiomyocytes and global heart counter-clockwise rotation was observed. Cells moved with similar speed as their wild-type counterparts. Contrary to the wild type, both left and right cells involuted. Cell neighbor relationships were maintained. These results strengthen the model that Nodal signaling promotes speed and

directional movement of the cardiomyocytes and show that proper asymmetric cardiac morphogenesis requires speed, directionality and cardiac rotation.

INTRODUCTION

The Nodal signaling pathway has been implicated in the establishment of left-right asymmetry both of the position and morphology of the internal organs of all vertebrates studied so far. The majority of the Nodal genes present a conserved expression pattern in the left side of the lateral plate mesoderm (LPM) and the brain region. They activate downstream targets that are equally asymmetrically expressed, such as *lefty2* and *pitx2*.

The heart is the first organ to exhibit asymmetry in vertebrates and left-right asymmetry persists as the bilateral heart fields coalesce to form the primary heart tube. Heart morphogenesis initiates with the migration of the cardiac precursors in the anterior LPM. They meet at the midline, fuse and form the cardiac cone, which then jogs to the left due to an anterior and leftward displacement of the cardiomyocytes. Cells on the right involute under the left cells and the cardiac cone undergoes a clockwise rotation, giving rise to the ventral and dorsal portions of the heart tube. The heart tube loops to the right, positioning the ventricle to the right of the atrium (reviewed by Stainier, 2001).

One of the first morphological signs of asymmetry during the zebrafish heart organogenesis is directed rotation and displacement of the cardiac cone. Errors in left-right axis determination lead most of the times to defects associated with complex congenital heart malformations, revealing how extremely susceptible to disturbances in embryonic left-right patterning the developing heart is (Ramsdell, 2005). It is of great importance to understand how global left-right axial patterning overlaps with morphogenetic processes of heart development.

We have recently shown that, at the cellular level, Nodal affects asymmetric organogenesis by promoting the speed and directional movement of the cardiomyocytes in the zebrafish (de Campos-Baptista et al., 2008). In late zygotic *oep* embryos (LZ*oep*), which lack Nodal signaling, heart laterality is randomized and disrupted. Speed and directional movement of cardiac cells, leftward

morphogenesis and rotation of the heart cone are reduced. Heart defects may also arise from bilateral or rightward expression of Nodal. However, it is not known how Nodal affects organogenesis at the cellular level when it is erroneously expressed in the right side or bilaterally.

No tail (*ntl*) is the zebrafish homologue of the mouse *brachyury* gene and encodes a T-box transcription factor. In *ntl* mutants the notochord precursors are present but fail to differentiate, resulting in a lack of notochord (Halpern et al., 1993). These embryos display bilateral expression of genes involved in the Nodal-signaling pathway, such as *lefty2* in the heart field. Although the embryonic midline has been implicated in left-right development in vertebrates, the mechanisms by which it regulates asymmetric gene expression and organ morphogenesis are unknown. Bilateral expression of the Nodal signaling pathway results in disrupted left-right morphogenesis. Heart looping in *ntl* mutants shifts from being prominently right-sided to being both right and left-sided (Bisgrove et al., 2000). Although several studies reported on how heart looping is affected by bilateral expression of Nodal, it is not yet clear how the earliest morphogenetic signs of cardiac asymmetry (rotation and displacement of the cardiac cone) are affected. The same stands for when Nodal is expressed asymmetrically in the right LPM, as observed in *polaris* mutants.

Polaris (*pol*) encodes an intraflagellar protein and is involved in ciliary assembly (Murcia et al., 2000). Motile cilia play a pivotal role in initiating a left-sided signaling cascade, such as the Nodal pathway, and establishing the left-right axis during mouse and zebrafish embryogenesis (Harvey, 1998). *Pol* knockdown results in misexpression of normally left-side-specific genes, including *southpaw* (*spaw*) and *lefty2* (*lft2*), and causes randomization of the heart looping. In 30% of the cases, these genes are expressed in the right LPM (Bisgrove et al., 2005).

In this work we use high-resolution time-lapse imaging to better understand the cellular changes occurring when Nodal is expressed bilaterally or in the right LPM. We analyze the movement of cardiomyocytes in *ntl* morphants and *pol* morphants, respectively. We find that, like in the LZ*oep* embryos, in *ntl* morphants the heart fails to rotate although it extends anteriorly. In *pol* morphants the cardiomyocytes exhibit similar meandering, displacement and speed to their wild

type counterparts and there is heart cone rotation, although to a lesser extent. These results confirm and extend our previous observations of Nodal generating left-right asymmetry by regulating the speed and direction of cardiomyocyte movement.

RESULTS

We have previously described the cellular basis of heart lateralization in wild type zebrafish embryos, when Nodal is expressed asymmetrically in the left LPM. Here we want to address how this process is affected when Nodal is expressed bilaterally or solely in the right side LPM.

To analyze the cellular basis of heart lateralization, we used high-resolution 4D confocal time-lapse imaging of cardiomyocyte movement using a similar approach as Smith et al. (2008). Transgenic *cmlc2*:GFP embryos express GFP in all cardiomyocytes throughout cardiac morphogenesis (Huang et al., 2003). To gain quantitative insights into heart morphogenesis, we tracked individual cells using Imaris software and measured the direction, displacement, meandering, and speed of cells. As described in our previous work, measurements were performed independently of the movement of the entire heart within the embryo.

Bilateral Nodal signaling disrupts asymmetric heart morphogenesis

To determine how bilateral Nodal signaling affects heart morphogenesis, we analyzed *no tail* morphant embryos (*ntl* MO). No tail encodes a T-box transcription factor, homologous to the mouse T (*brachury*) gene, and zebrafish embryos injected with *ntl* morpholino fail to form a notochord. Due to some mechanism yet not fully understood, disruption of the notochord leads to bilateral expression of the Nodal gene *spaw* and its inhibitor *lefty2* (Fig. 1A and 1B) (Halpern et al., 1993; Danos and Yost, 1996; Odenthal et al., 1996; Chen et al., 1997; Bisgrove et al., 2000; Amack and Yost, 2004).

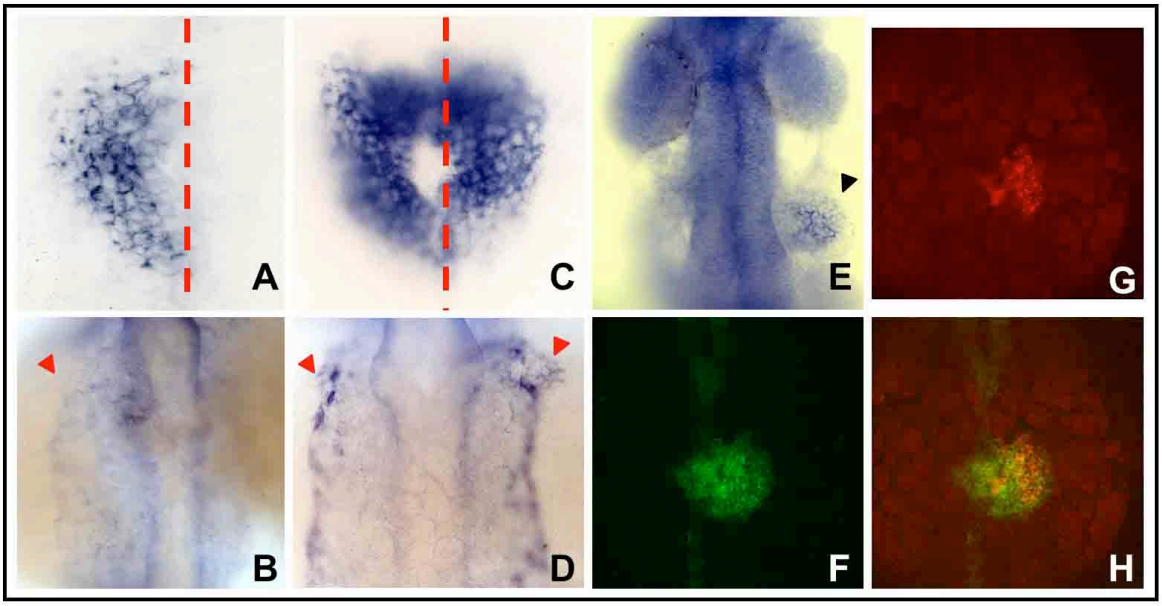

Figure 1 - Expression of genes in the Nodal signaling pathway in wild-type, *ntl* MO and *pol* MO. *In situ* hybridization: In wild type, *lft2* and *spaw* are expressed in the left LPM (**A** and **B**, respectively). Arrowhead in (**B**) indicates *spaw* expression. *lft2* and *spaw* are bilaterally expressed in *ntl* MO (**C** and **D**, respectively). Red dashed line marks the midline. Red arrowheads indicate bilateral expression of *spaw* (**D**). *Lft2* is expressed in the right LPM of *pol* MO (**E**, balck arrowhead)**.** Confocal images of double fluorescent *in situ* hybridization: expression of *cmlc2* (heart marker) and *shh* (midline marker) in green (**F**). *lft2* (in red) is expressed in the right side of the heart (**G** and **H**, single channel and overlay, respectively).

In *ntl* morphants cardiomyocytes displace anteriorly and cardiac rotation is reduced

To analyze overall heart morphogenesis, we used isosurface rendering. As observed in the wild type (Fig. 2A-E), cardiomyocytes formed the cardiac cone and progressed to form the heart tube in *ntl* MO. However, cardiac cells displaced anteriorly and failed to move leftward (Fig. 2K-O; Suppl.Movie 2). Consequently, the heart in *ntl* MO remains positioned at the midline and extends toward anterior.

Since leftward heart morphogenesis is accompanied by a ~ 30° clockwise rotation in the wild type (Fig. 5A'''), we analyzed the degree of cardiac rotation in *ntl* MO as an additional measure of asymmetry.

Cardiac rotation was abolished in *ntl* MO (Fig. 5A'''). The absence of cardiac rotation in *ntl* MO partially resembles the phenotype in LZ*oep* mutant embryos that lack

Nodal signaling (Fig. 2F-J and Fig. 5A'''). Both *ntl* MO and LZ*oep* mutants have the heart placed at the midline and lack the leftward rotation. However, *ntl* MO cardiomyocytes migrate while in LZ*oep* mutant cardiac cells are mostly immotile during the same time period.

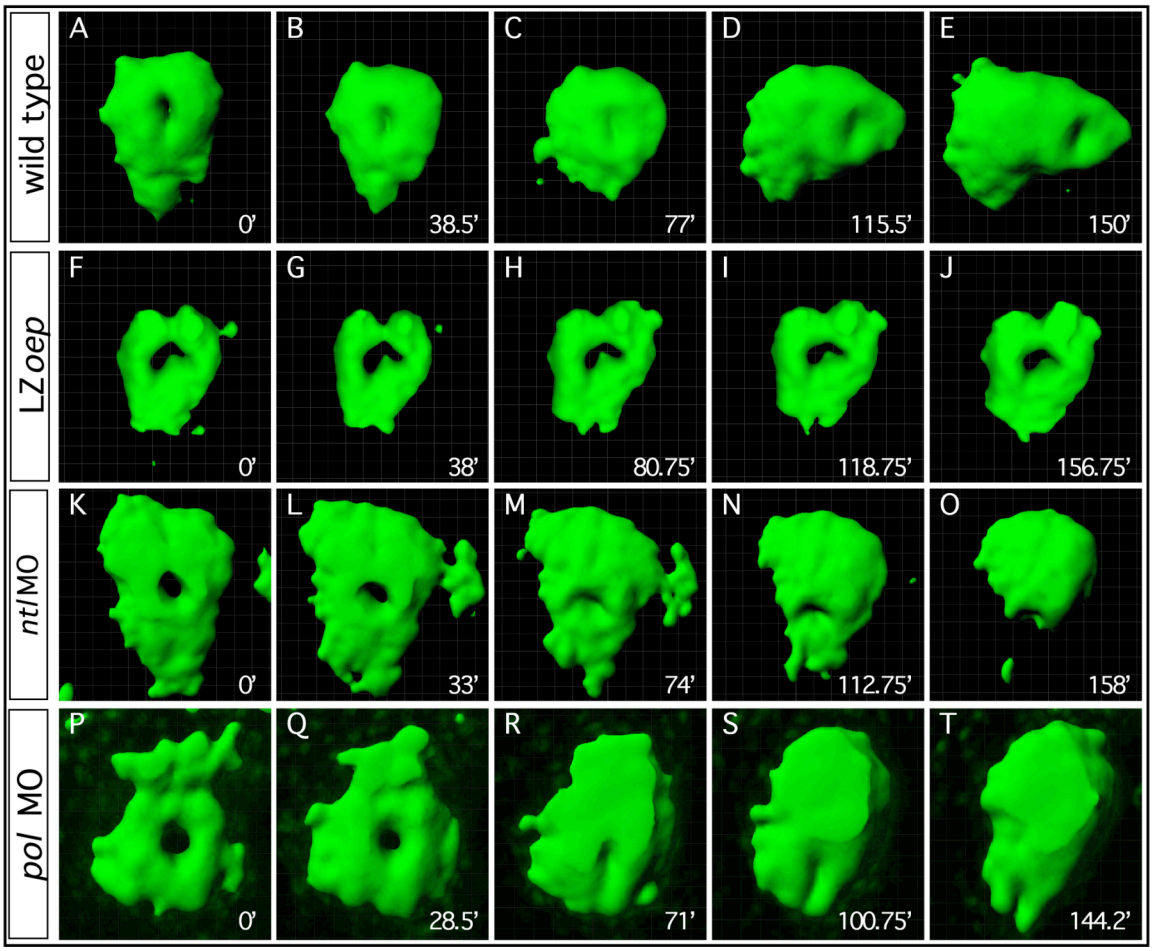

Figure 2 - Isosurface rendering of heart morphogenesis in wild type, LZ*oep* mutants, *ntl* and *pol* morphants. *cmlc2*-GFP cells label the cardiac cone and heart tube. Imaris software created an isosurface representing points of constant fluorescent intensity within the 3D volume. Cardiac cone in initially symmetric in wild type (**A**), LZ*oep* mutant (**F**), *ntl* (**K**) and *pol* (**P**) morphants. Note the leftwards and anterior displacement of the heart in wild type (**B-E**) but not in LZ*oep* mutants (**G-J**). In *ntl* MO the heart displaces anteriorly (**L-O**) and in *pol* MO the heart displays rightward and anterior displacement (**Q-T**). For detailed views from different angles see Suppl. Movies 2 (wild type) and 6 (LZ*oep*) from Chapter II. For detailed views from different angles see Suppl. Movies 2 (*ntl MO*) and 6 (*pol* MO) from Chapter III. Pictures were cropped to keep the heart in the center and do not maintain the positions of the coordinate systems.

Position-dependent differences in cardiomyocyte movements during heart lateralization in *ntl* morphants

We performed cell-tracking analysis on the *ntl* MO embryos in order to quantitatively compare it with the wild type data previously reported (Fig. 3K-O, Fig. 3K'-O' and Suppl. Movie 3). We first divided the heart field in four territories to be compared: left anterior (LA), right anterior (RA), left posterior (LP) and right posterior (RP). Analysis of each cell track yielded measurements of speed, displacement and meandering of a cell (Smith et al., 2008). Speed was defined as distance traveled/time interval, displacement rate as distance from first to last location/entire time interval, and meandering index as displacement/total distance traveled (Smith et al., 2008). Comparison of the posterior and anterior cells revealed that posterior cells moved faster than anterior cells (Fig. 4C, 4C', 4C''), similarly to the wild type (Fig. 4A, 4A', 4A''). However, cells in *ntl* MO moved slightly more slowly than the wild type counterparts (Fig. 4A'' and 4C''). A tendency for posterior or anterior cells to have higher displacement rate or meandering index was not observed (Fig. 5C and 5C'), contrary to the wild type (Fig. 5A and 5A'). These results indicate that overall posterior cells move faster than anterior cells but that both exhibit variable displacement and meandering.

To determine if there are differences between the *ntl* MO cardiomyocytes located in the left and in the right LPM we compared speed, displacement rate and meandering index. We did not find significant differences between left and right cells using these measurements (Fig. 4C, Fig. 5C and 5C'), similarly to what has been described for the wild type (Fig. 4A, Fig. 5A and 5A'). However, quantification of the dorsal-ventral displacement of cells revealed that both cells on the right and on the left side were ventrally displaced (Fig. 6C and Suppl. Movie 2). This differs from what has been described for the wild type, where only the cells located in the right heart cone involuted (Fig. 6A and Suppl. Movie 2 from Chapter II).

In *ntl* morphants cardiomyocytes displace with variable direction

To determine the direction of the movement, we performed vector analysis, including displacement length and angle formed with respect to the anterior-posterior and left-right axes (Fig. 5). The large majority of the cardiomyocytes in *ntl* MO moved rightward and displaced anteriorly within the time period considered (158') (Fig. 5C''), whereas the wild type cells moved prominently leftward (Fig. 5A'').

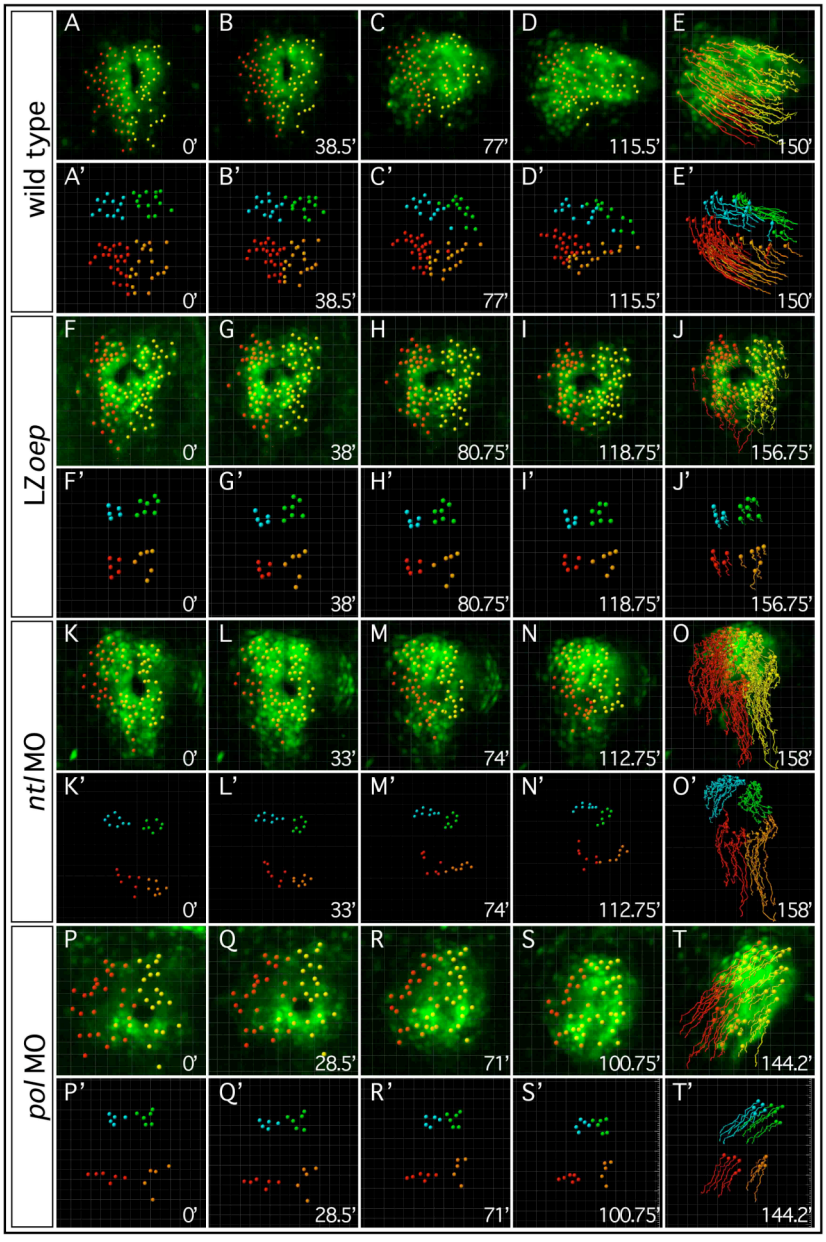

Figure 3 – Tracking of single cells in wild type, LZ*oep* mutants, *ntl* and *pol* morphants. Confocal 3D-images showing individual *cmlc2*-GFP manually tracked starting at the onset of cardiac cone formation. First (**A-E**), third (**F-J**), fifth (**K-O**) and seventh (**P-T**) rows: green *cmlc2*-GFP expression; red: cells within the left side of cardiac cone; yellow: cells within the right side of the cardiac cone. For detailed views from different angles, see Supplemental Movies 1 (wild type) and 5 (LZ*oep*), from Chapter II, and Supplemental Movies 1 (*no tail*) and 5 (*polaris*), from Chapter III. Second (**A'-E'**), fourth (**F'-J'**), sixth (**K'-O'**) and eighth (**P'-T'**) rows: tracking of quadrants. Quadrants defined by grouping left-anterior cells (blue), left-posterior cells (red), right-anterior cells (green) and right-posterior cells (orange). For detailed views from different angles, see Supplemental Movies 3 (wild type) and 7 (LZ*oep*), from Chapter II, and Supplemental Movies 3 (*no tail*) and 7(*polaris*), from Chapter III. Pictures were cropped to keep the heart in the center and do not maintain the position of the coordinate systems. For movements with respect to coordinate systems, see

Supplemental Movies 3 (wild type) and 7 (LZ*oep*), from Chapter II, and Supplemental Movies 3 (*no tail*) and 7 (*polaris*), from Chapter III.

Analyses of the *ntl* MO movies shows that cells in the *ntl* MO did not move in a straight line but had alternating movement direction instead (Suppl. Movie 1 and Suppl. Movie 2). Due to this observation we applied the same measurements to the total extent of the movie (510' long). This revealed that the *ntl* MO cardiomyocytes displaced prominently anteriorly (Fig. 5C'''), suggesting a lack of consistent directional cues during heart lateralization. These results show that cardiomyocyte speed in *ntl* MO is similar to the one observed in the wild type but subjected to variable directional cues.

Atrial and ventricular cells movement is not altered in *ntl* MO

We also addressed the movement of cells located in the inner and outer regions of the cardiac cone. According to gene expression patterns of ventricular and atrial markers, we observed that the *ntl* MO atrial precursors, located in the outer region of the cone, showed higher speed, displacement rate and meandering index than the ventricular cells, located in the inner region of the cone (Fig. 7C, 7C', 7C''and 7C'''). This mimics what was observed in the wild type (Fig. 7A, 7A', 7A'' and 7A''') and suggests that bilateral expression of Nodal does not alter the dynamics between inner and outer cells of the cardiac cone.

Cell neighbor relationships are disrupted in *ntl* morphants

Previous studies have reported that coherent movement of individual cardiomyocytes underlies overall heart morphogenesis. Coherence can be generated if neighbor relationships between individual cardiomyocytes do not change extensively. We analyzed neighbor relationships in *ntl* MO. While in wild type cell neighbor relationships are maintained (Fig. 8 A1-A5, start to end), in *ntl* morphants changes in cellular neighbor relationships were registered in ~ 60% of the cases (5/8) (Fig. 8 D1-D5, start to end and Suppl. Movie 4).

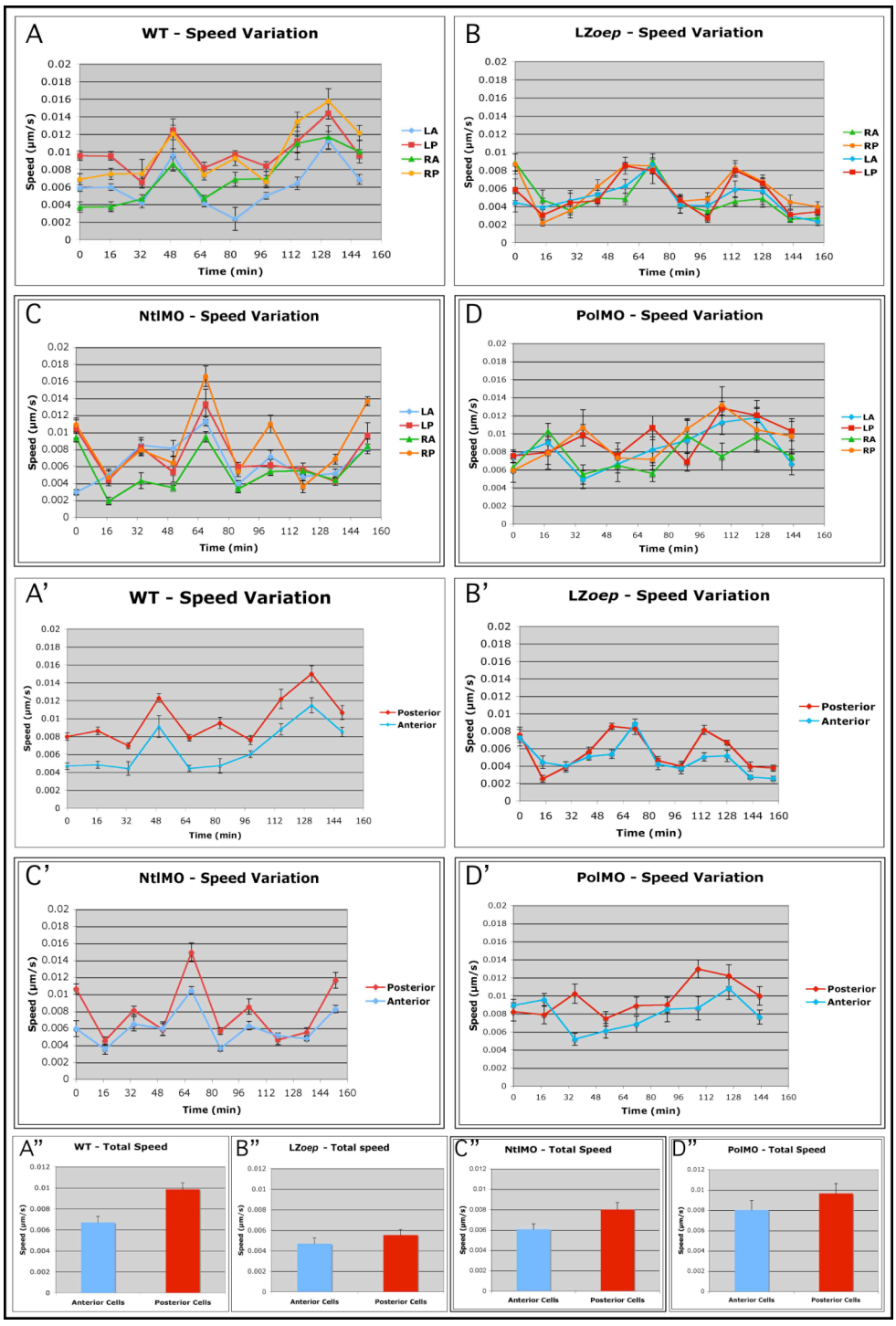

Figure 4 – Quantitative analysis of anterior and posterior cell movements in wild type, LZ*oep*, *ntl* and *pol* morphants. *Cmlc2*-GFP cells in left-anterior (LA), left-posterior (LP), right-anterior (RA), and right-posterior (RP) quadrants were tracked and different parameters were measured using Imaris software. Speed variation indicates speed of a cell during a given time interval. Total speed was determined as described in Experimental Procedures. Note the higher speed of posterior cells in *ntl* (**C, C', C''**) and *pol* (**D, D', D''**) morphants, similar to the wild type (**A, A', A''**). Cardiomyocytes in LZoep mutants have lower speed (**B, B', B''**). Statistics: (A'') $P < 0.05$; (B'') $P > 0.05$; (C'') $P < 0.05$; (D'') $P < 0.05$.

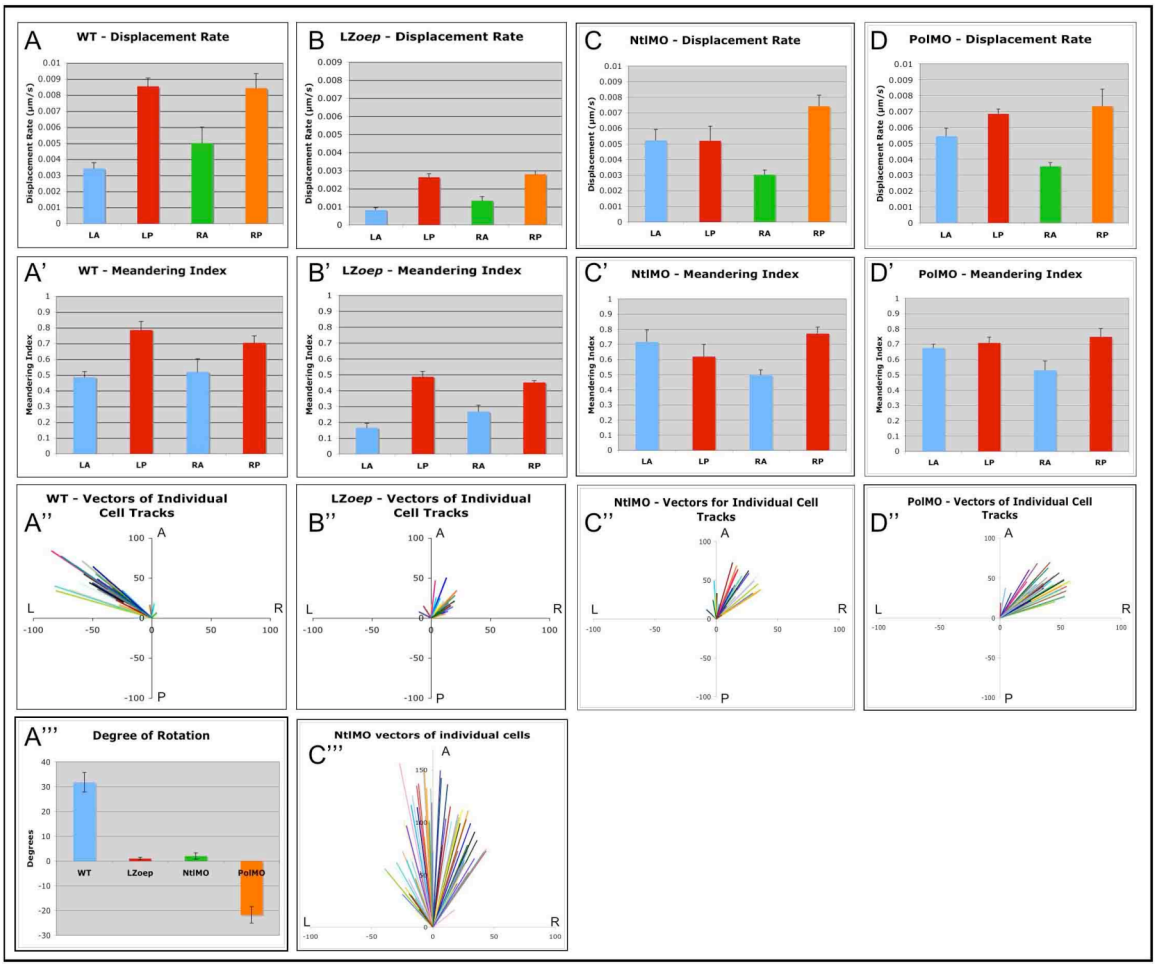

Figure 5 – Quantitative analysis of anterior and posterior cell movements in wild type, LZ*oep* mutants, *ntl* and *pol* morphants. *Cmlc2*-GFP cells in left-anterior (LA), left-posterior (LP), right-anterior (RA), and right-posterior (RP) quadrants were tracked and different parameters were measured using Imaris software. Displacement rate and meandering index were determined as described in Experimental Procedures. *ntl* (**C, C'**) and *pol* (**D, D'**) morphants have displacement rate and meandering index similar to wild type (**A, A'**). LZ*oep* mutants have lower displacement rate (**B**) and meandering index (**B'**). Vectors of individual cells illustrate the angle and length of x/y displacement of cells. (A, anterior; P, posterior; L, left; R, right). Note the rightward and anterior displacement of *polaris* cells (**D''**), contrary to the leftward movement of the wild type cells (**A''**). *ntl* cells vary their direction of movement, from the initial 158' (**C''**) to the end of the movie, 510' (**C'''**). LZ*oep* cells displace mostly anteriorly (**B''**). **A''':** Degree of clockwise rotation of cardiac cone. Note the counterclockwise rotation of the *polaris* morphants. in a slight minor degree than the clockwise rotation of the wild type. *ntl* morphants almost lack rotation, similar to LZ*oep.* Statistics: (A, B, C and D) LA vs LP, $P < 0.05$; RA vs RP, $P < 0.05$; LA vs RA, $P > 0.05$; LP vs RP, $P > 0.05$; (B); (A', B', C' and D') LA vs LP, $P < 0.05$; RA vs RP, $P < 0.05$; LA vs RA, $P > 0.05$; LP vs RP, $P > 0.05$.

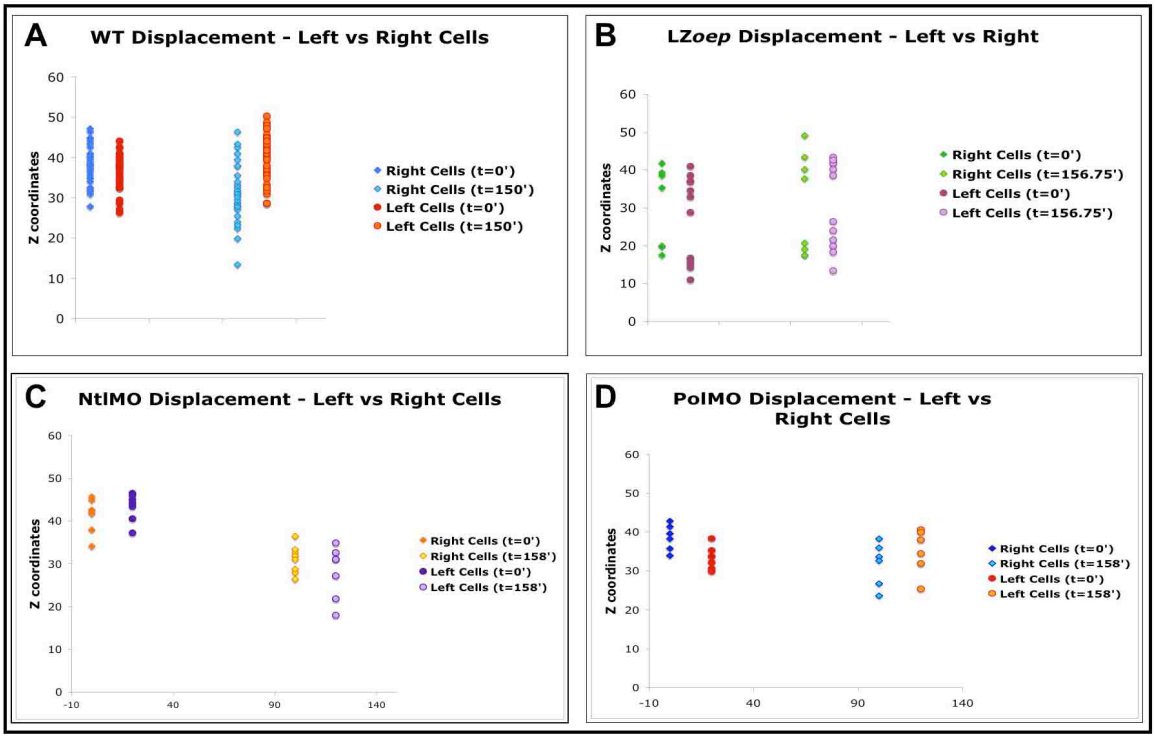

Figure 6 – Quantitative analysis of left and right cell movements in wild type, LZ*oep* mutants, *ntl* and *pol* morphants. Left and right *cmlc2*-GFP cells were tracked and Z-axis (dorsal-ventral) displacement of cells was measured. Note both left and right cells displace ventrally in *ntl* morphant. In *pol* morphants left and right cells displace ventrally, although left cell displace more. This is not the total mirror image of the wild type. In LZ*oep* mutants cells do not displace ventrally.

This suggests that coherence can be maintained even if neighbor relationships are altered. It also supports the idea that *ntl* MO cells are subjected to different directional cues. Although bilateral Nodal signaling induces changes in cell neighbor relationships, the integrity of the heart tube is maintained. As previously suggested, it confirms that unilateral Nodal signaling is not required for integrity maintenance.

Cardiomyocytes move rightward when exposed to Nodal signaling in the right LPM

To determine how right-sided expression of Nodal signaling affects heart morphogenesis, we analyzed *polaris* morphants (*pol* MO). Polaris is involved in ciliary assembly. Correlation between defects in monocilia structure or movement,

alterations in Nodal flow and aberrant left-right development has been shown in several mouse mutants. *pol* MO show randomized heart and gut laterality and Nodal related genes, such as *spaw* and *lefty2*, are expressed in the right side of the LPM in ~30% of the cases. We analyzed the embryos were Nodal signaling was expressed in the right side (Fig. 1C, 1D, 1E and 1F).

In *pol* morphants the cardiac cone rotates counterclockwise

To analyze overall heart morphogenesis, we used isosurface rendering. The first sign of asymmetry was shortly after cardiac fusion, when cells moved anteriorly. Contrary to what was found in wild type, cardiac cells displaced rightward instead of leftward (Fig. 2P-2T and Suppl. Movie 6). In order to quantify the degree of rotation, we measured the angle formed by the cells and the anterior-posterior and left-right axis during cardiac rotation. In *pol* MO cardiac rotation is of ~20° in a counterclockwise direction and the cardiomyocytes move prominently to the right (Fig. 5A'''). This seems to suggest a mirror image phenotype to that observed in the wild type, where the rotation is of ~30° clockwise. To further explore this hypothesis, we quantified the z-axis position of the right and the left cells. Although the left cells move underneath, this is also noticeable in the right cells (Fig. 2P-2T and Suppl. Movie 6).

Position-dependent differences in cardiomyocytes movements during heart lateralization in *pol* morphants

To quantify heart morphogenesis in *pol* MO, we used cell-tracking analyses (Fig. 3P-3T and 3P'-3T'). Comparison of posterior and anterior cells revealed that posterior cells moved faster than anterior cells, had higher displacement rates and a higher meandering index (Fig. 4D, 4D' and 4D'', Fig. 5D and 5D'). These results indicate that, even though in a different direction, posterior cardiomyocytes move faster and more directionally than anterior cardiomyocytes, as observed in the wild type.

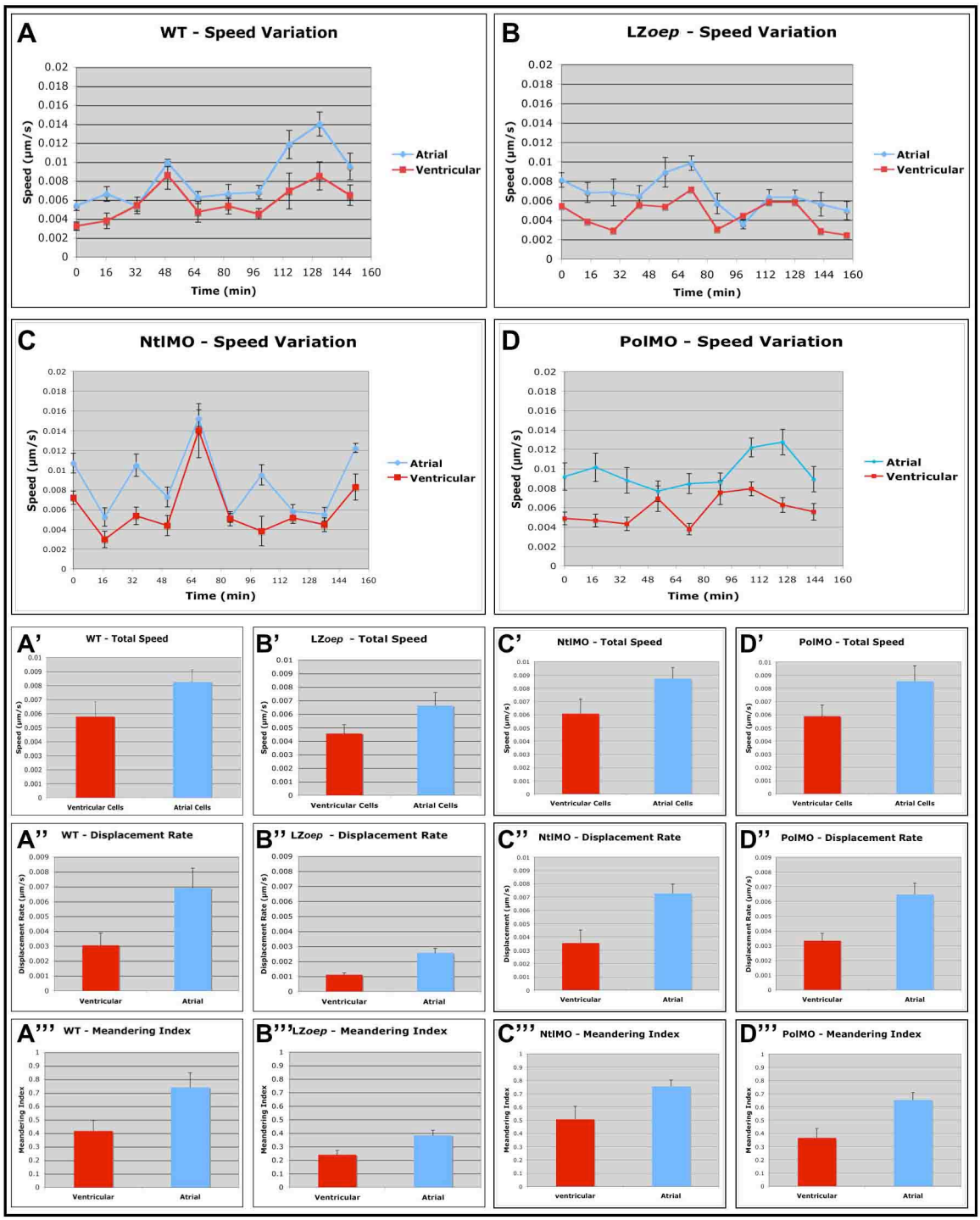

Figure 7 – Quantitative analysis of ventricular and atrial cell movements in wild type, LZ*oep* mutants, *ntl* and *pol* morphants. Ventricular cells (located at the apex of the cardiac cone) and atrial cells (located at the base of the cardiac cone) were tracked using Imaris. Speed variation indicates speed of a cell during a given time interval. Total speed, displacement rate, and meandering index were determined as described in Experimental Procedures. Speed, displacement rate and

meandering index in *ntl* morphants (**C and C', C'', C'''**, respectively) and in *pol* morphants (**D and D', D'', D'''**, respectively) was higher in atrial cells, as observed in the wild type (**A, A', A'', A'''**). These differences are reduced in LZ*oep* (**B, B', B'', B'''**). Statistics: (A'-D'; A''-D''; A'''-D''') $P < 0.05$.

To determine if there are differences between the *pol* MO cardiomyocytes located in the left or in the right side of the midline we compared speed, displacement rate and meandering index. We did not find significant differences between left and right cells using these measurements, similarly to what has been described for the wild type (Fig. 4D, Fig. 5D and 5D'). However, as mentioned previously, quantification of the dorsal-ventral displacement of cells revealed that the cells in the left side were ventrally displaced, as well as the cells on the right (Fig. 6D and Suppl. Movie 6).

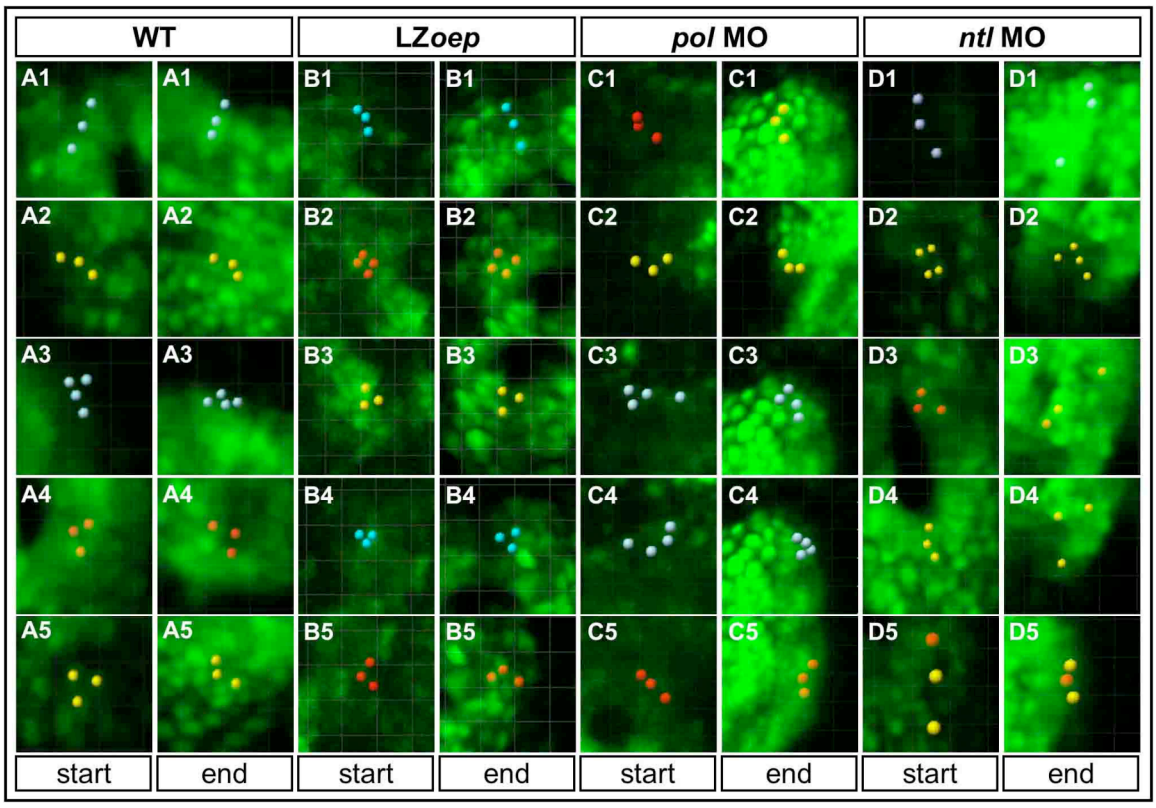

Figure 8 – Cell neighbor relationships in wild type, LZ*oep* mutant, *ntl* and *pol* morphants. Groups of *cmlc2*-GFP cells were tracked from the beginning to the end of the time interval considered. Cell neighbor relationships were maintained in wild type (**A1-A5** start to **A1-A5** end), LZ*oep* mutant (**B1-B5** start to **B1-B5** end), and *pol* morphant (**C1-C5** start to **C1-C5** end). Note cell neighbor relationships are not maintained in *ntl* morphant (**D1-D5** start to **D1-D5** end).

Atrial and ventricular cells movement is not altered in *pol* morphants

We also addressed the movement of the *pol* MO cardiomyocytes located in the inner and outer regions of the cardiac cone, ventricular and atrial cells, respectively, according to described gene expression patterns. We found that atrial precursors had higher speed, displacement rate and meandering index than the ventricular cells (Fig. 7D, 7D', 7D'' and 7D'''). This agrees with what was described for the wild type.

Cell neighbor relationships are maintained in *pol* morphants

To determine if the cardiomyocytes in *pol* MO lose their coherence we analyzed neighbor relationships by tracking groups of cells. Neighbor relationships were maintained during heart lateralization (Fig 8 C1-C5, start to end and Suppl. Movie 8).

Note: Results for LZ*oep* mutants were included for better comparison and understanding of the overall results.

DISCUSSION

Although the past few years have seen rapid progress in our understanding of left-right organogenesis in vertebrates, it is still unclear how this is achieved at the cellular level. In order to better understand how asymmetric morphogenesis is cellularly orchestrated it is necessary to perform detailed analysis on the cell movements, shapes and cell rearrangements occurring during this process. For instance, heart chamber morphology in the zebrafish develops via changes in cell shape, leading to characteristic chamber curvatures. Elongation and orientation of outer-curvature cells, coupled with the maintenance of cuboidal shapes by inner-curvature cells accounts for the shape of the expanded ventricle (Auman et al., 2007). Recent studies, including our own, have used the zebrafish heart as a model system to address asymmetric morphogenesis at the cellular level and have shown that cardiomyocytes move anteriorly and leftward in a cohesive fashion while the heart cone rotates clockwise. Single cell tracking analyses permitted quantifying cell

speed, displacement and meandering, revealing that differences exist between anterior and posterior cells, atrial and ventricular precursors but not between left and right cells. Moreover, cells on the right heart field displace more ventrally than their left-side counterparts. This displacement reflects the involution of cells in the right heart cone (Rohr et al., 2008). Atrial cells present different kinetics than ventricular cells, moving faster, more directionally and with higher displacement rates. These results emphasize the potential of single cells tracking to clarify the cellular processes leading to asymmetric morphogenesis during left-right development.

Nodal and members of the downstream signaling cascade are expressed asymmetrically during left-right cardiac morphogenesis (Hamada et al., 2002; Schier, 2003; Shen, 2007). *spaw* and *lft2* are adjacently expressed in the left LPM and only *lft2* is activated in the heart progenitors. Our *in situ* hybridization results confirm that when the midline structures are not properly formed, as in *ntl* mutants, the Nodal signaling pathway is activated in both sides of the LPM and *lft2* is bilaterally expressed. It is conceivable that the notochord functions as a barrier to prevent Nodal signaling activation in the right LPM. Nodal signaling activation in the right LPM would be possible since the Nodal co-receptor *oep* is expressed bilaterally in all LPM cells (de Campos-Baptista et al., 2008). For example, knockout mice lacking *lefty-1* expression in the prospective floor plate (midline) present bilateral expression of *nodal*, *lft2* and *pitx2* (downstream target of Nodal normally expressed on the left side). In fact, all mouse mutants at present lacking *lefty-1* expression have midline-barrier defects. However, it is not known to date how can *Lefty1* function as a midline barrier.

The Nodal signaling cascade is necessary for proper left-right morphogenesis (Hamada et al., 2002; Schier, 2003; Shen, 2007) and several studies have shown that loss of Nodal signaling in zebrafish leads to abnormal cardiac morphogenesis, namely randomized heart looping and loss of initial leftwards jogging (Chen et al., 1997; Yan et al., 1999; Long et al., 2003; Rohr et al., 2008). We have recently proposed that Nodal signaling participates in embryonic heart development in the zebrafish by promoting cell speed and providing directional movement to the

cardiomyocytes. Our present quantitative analysis of *Ntl* and *Pol* morphants shows that disruption of normal Nodal signaling affects the direction of movement of individual cardiomyocytes during embryonic heart development.

In *Ntl* MO, cardiac cells move anteriorly but fail to migrate leftwards. Instead, they tend to move in a straight line towards the head. In *Pol* MO, cardiomyocytes migrate anteriorly and migrate rightwards instead of leftwards, as observed in the wild type. Extending our previous work, these results support the model that Nodal signaling provides directional cues to the cardiomyocytes. When expressed in the right LPM, Nodal signaling instructs the cells to move rightwards (*Pol* MO). When Nodal signaling is bilaterally expressed, individual cardiomyocytes receive directional cues from both left and right LPMs and the end result is an anterior dislocation (*Ntl* MO). In addition, our results show that bilateral or right-sided expression of Nodal signaling maintains the speed at which the cardiomyocytes move, resembling their wild type counterparts. Conceptually, *Ntl* MO (bilateral Nodal signaling) and *LZoep* mutants (lack Nodal signaling) represent the same developmental context. Either by being absent or by canceling itself due to its bilateral expression, Nodal signaling cannot provide a left or right directional bias to the developing heart. However, Nodal signaling is still able to promote cell speed. Both *Ntl* MO and LZ*oep* mutant embryos have the heart placed at the midline and lacking the leftward rotation, but cells migrate in *Ntl* MO. Taken together, these results strongly support the role of Nodal signaling to promote cardiac cells speed and directional movement of cardiomyocytes in zebrafish, as presented in our previous work.

Previous studies have described the ventral involution of the cardiac cells of the right side of the heart cone. Interestingly, our analyses of *Ntl* MO and *Pol* MO has revealed that this displacement occurs in both the right and the left cardiomyocytes located in the most posterior region of heart cone. In *Pol* MO the cells are instructed by Nodal signaling to move rightwards. However, not only the left cells displace ventrally, as predicted, but also the right cells. In *Pol* MO, the initial rotation is anticlockwise and to a lesser extent than the wild type counterparts (~20° instead of ~30°). These observations suggest that a reduction on the degree of cardiac rotation

affects normal unilateral involution of the heart cells. Similarly, in *Ntl* MO the clockwise rotation observed in the wild type is absent. Cells are instructed by Nodal signaling to move, although lacking directional cues. Ventral involution of cardiac cells occurs in the right and the left sides of the heart cone. All together, these observations suggest two important aspects of asymmetric cardiac development. First, unilateral Nodal signaling promotes the initial heart cone rotation. Second, for proper left-right morphogenesis of the zebrafish heart, cells have to receive positive and cohesive input on speed, direction and rotation. Failure in any of this factors leads to abnormal asymmetric morphogenesis. In *Pol* MO, although Nodal was unilaterally expressed in the right side of the LPM and promoted an anticlockwise rotation of the heart cone, the rotation was not as pronounced as observed in the wild type. It is possible that the levels of Nodal signaling induced in the right LPM by the morpholino injection were lower than what they would normally be. Variable levels of Nodal signaling can occur when the pathway is disrupted. It has been reported that in *ntl* zebrafish mutants, *lft2* expression often appears to be expressed at higher levels than in their wild type siblings (Bisgrove et al., 2000).

Despite the slightly reduced angle of cardiac rotation, we believe *Pol* MO to be a suitable system to analyze heart morphogenesis when Nodal is expressed in the right LPM. Several genes have been implicated in the regulation of asymmetric heart morphogenesis in zebrafish, including not only components of the Nodal signaling pathway but also of the BMP signaling pathway, predominantly activated within the left side of the heart. Nodal signaling is required for asymmetric expression of BMP4 in the heart cone (Chen et al., 1997; Chocron et al., 2007). Recent work has shown that implantation of BMP soaked beads in the right-side LPM can direct the displacement and rotation of the heart cone. No quantification was possible though due to high variability in cardiomyocytes movement in such an artificial system. In *Pol* MO expressing Nodal in the right LPM cardiomyocytes move in a coherent way and quantification of heart cone rotation and the displacement of the cardiac cells is possible.

Coherent movement of individual cardiomyocytes underlies overall heart morphogenesis and coherence can be generated if neighbor relationships between

individual cardiomyocytes do not change extensively. The fact that our analyses of neighbor relationships in *ntl* MO cardiomyocytes revealed that these change suggests that coherence can be maintained even if neighbor relationships are altered. It is also in accordance with *ntl* MO being instructed with bilateral directionality. Although bilateral Nodal signaling induces changes in cell neighbor relationships, the integrity of the heart tube is maintained. This confirms that unilateral Nodal signaling is not required for integrity maintenance.

In our previous analyses of *LZoep* mutants it was not possible to resolve the cause-and-effect relationships between cellular and morphogenetic events during heart development since these appeared at the same time. Lack of directionality, slower and more meandering movements of cardiomyocytes could be the cause blocking overall asymmetric cardiac morphogenesis. Alternatively, cells could move at a slow speed due to overall abnormal morphogenesis and lack of directionality. The present analysis of *Ntl* MO and *Pol* MO sheds some light upon this problem. Directionality and speed of movement are uncoupled events. Heart cone rotation is dependent on directional cues but independent on cells being able to displace. In *Ntl* MO there is no directionality bias nor rotation but there is speed.

How does Nodal signaling drive asymmetric morphogenesis? Because *lefty2* is expressed in the left side of the heart in the wild type, bilaterally expressed in *Ntl* MO and expressed in the right side of the heart in *Pol* MO we propose a model wherein Nodal acts locally in *lft2*-expressing cells. The complex morphogenetic behaviors that follow are due to secondary interactions within the heart. It is possible that the *lft2*-expressing cells function as organizers to drive asymmetric morphogenesis. Cell transplants could address this question, by generating mosaic cardiac tissue.

EXPERIMENTAL PROCEDURE

Fish Lines

Tg(cmlc2:gfp) was described previously (Yan et al., 1999; Huang et al., 2003).

In Situ Hybridization

For *in situ* hybridizations, embryos were fixed in 4% paraformaldehyde, rinsed in PBS, dehydrated into absolute methanol and stored at -20°C. Riboprobes were synthesized from linearized DNA templates using T7 polymerase and digoxigenin labeling mix. In situ hybridizations were carried out as previously described (Stachel *et al*., 1993; Hauptmann and Gerster, 1994). Double fluorescent in situ hybridization probes were labeled with fluorescein (Roche) and digoxygenin (Roche). Detection was based on fluorescein or Cy3 tyramide deposition (Perkin Elmer; Schoenebeck et al., 2007). Probes used include: *shh*, *lefty2* and *cmlc2*. Embryos were mounted in benzylbenzoate/ benzylalcohol for photography.

Morpholinos

Morpholino to block translation of *No tail* MO was synthesized and injected as previously described (Nasevicius and Ekker, 2000). *Polaris* splice blocking-morpholino was synthesized and injected as described before (Bisgrove *et al*., 2005).

Imaging and Data Analysis

At the 15-somite stage, embryos were manually dechorionated and mounted at the 18-somite stage in glass-bottom culture dishes using 0.8% low-melt agarose in E3 embryo medium. Imaging was performed on a Zeiss LSM 5 Pascal confocal microscope with LSM software. The microscope stage was heated to 30°C to keep embryos at 28.5°C during the time-lapse recordings. Stacks were acquired every 5 min for *Ntl* MO and 4.75 min for *Pol* MO. Z-stacks were rendered in 3D and analyzed with Imaris software (Bitplane). 3D single cell tracking and measurements (x/y/z coordinates) were performed manually using Imaris. The base of the lumen was chosen as reference point for the x/y/z coordinate system to analyze heart

morphogenesis *per se* and to avoid confounding effects caused by the potential drift of the embryo during imaging or the movement of the heart within the embryo. Each measurement was obtained from the cells depicted in Figure 3K' and 3P' and in Supplemental Movies 3 and 7. The time window for quantitative measurements was from the onset of cardiac cone formation until the full leftward displacement of the cardiac cone (t =158.0 min for *Ntl* MO; t=144.2 min for *Pol* MO). Cells position was defined by x/y/z coordinates at each time point. Time intervals between each tracked time point were 15.0 min in wild type and 14.25 min in *Pol* MO mutants. The following parameters were measured (Smith et al., 2008): speed _ track length/time interval; total speed _ total track length/total time (i.e., sum of the average distance traveled by the cells within each time interval divided by the total track time); displacement rate _ total displacement length/total time (i.e., position of each cell at the end of the track - position at t=0 divided by the total track time); meandering index _ total displacement length/total track length; displacement of left vs. right cells: the z-axis coordinates of each cell were analyzed at t=0 and at the end of the track. Rotation angle was obtained by drawing an imaginary square connecting cells in each quadrant of the heart cone at the beginning and at the end of the time-lapse (Smith et al., 2008). Statistical analysis and graphics were obtained in Excel (Microsoft).

ACKNOWLEDGEMENTS

We thank members of the Schier and the Yelon lab for helpful discussions and Steven Zimmerman for fish care. Thanks to Sheu-Shu-Hsien and the Lichtman lab for help with Imaris software. This work was supported by NIH grant R01 GM56211 to A.F.S. and by Gulbenkian PhD Program (FCT SFRH/BD/11801/2003) to M.I.M.C.-B.

REFERENCES

Amack JD, Yost HJ. 2004. The T box transcription factor no tail in ciliated cells controls zebrafish left-right asymmetry. Curr Biol 14:685-690.

Auman HJ, Coleman H, Riley HE, Olale F, Tsai HJ, Yelon D. 2007. Functional modulation of cardiac form through regionally confined cell shape changes. PLoS Biol 5:e53.

Bisgrove BW, Essner JJ, Yost HJ. 2000. Multiple pathways in the midline regulate concordant brain, heart and gut left-right asymmetry. Development 127:3567-3579.

Bisgrove BW, Snarr BS, Emrazian A, Yost HJ. 2005. Polaris and Polycystin-2 in dorsal forerunner cells and Kupffer's vesicle are required for specification of the zebrafish left-right axis. Dev Biol 287:274-288.

Chen JN, van Eeden FJ, Warren KS, Chin A, Nusslein-Volhard C, Haffter P, Fishman MC. 1997. Left-right pattern of cardiac BMP4 may drive asymmetry of the heart in zebrafish. Development 124:4373-4382.

Chocron S, Verhoeven MC, Rentzsch F, Hammerschmidt M, Bakkers J. 2007. Zebrafish Bmp4 regulates left-right asymmetry at two distinct developmental time points. Dev Biol 305:577-588.

Danos MC, Yost HJ. 1996. Role of notochord in specification of cardiac left-right orientation in zebrafish and Xenopus. Dev Biol 177:96-103.

de Campos-Baptista MI, Holtzman NG, Yelon D, Schier AF. 2008. Nodal signaling promotes the speed and directional movement of cardiomyocytes in zebrafish. Dev Dyn 237:3624-3633.

Halpern ME, Ho RK, Walker C, Kimmel CB. 1993. Induction of muscle pioneers and floor plate is distinguished by the zebrafish no tail mutation. Cell 75:99-111.

Hamada H, Meno C, Watanabe D, Saijoh Y. 2002. Establishment of vertebrate left-right asymmetry. Nat Rev Genet 3:103-113.

Harvey RP. 1998. Cardiac looping--an uneasy deal with laterality. Semin Cell Dev Biol 9:101-108.

Huang CJ, Tu CT, Hsiao CD, Hsieh FJ, Tsai HJ. 2003. Germ-line transmission of a myocardium-specific GFP transgene reveals critical regulatory elements in the cardiac myosin light chain 2 promoter of zebrafish. Dev Dyn 228:30-40.

Long S, Ahmad N, Rebagliati M. 2003. The zebrafish nodal-related gene southpaw is required for visceral and diencephalic left-right asymmetry. Development 130:2303-2316.

Murcia NS, Richards WG, Yoder BK, Mucenski ML, Dunlap JR, Woychik RP. 2000. The Oak Ridge Polycystic Kidney (orpk) disease gene is required for left-right axis determination. Development 127:2347-2355.

Odenthal J, Haffter P, Vogelsang E, Brand M, van Eeden FJ, Furutani-Seiki M, Granato M, Hammerschmidt M, Heisenberg CP, Jiang YJ, Kane DA, Kelsh RN, Mullins MC, Warga RM, Allende ML, Weinberg ES, Nusslein-Volhard C. 1996. Mutations affecting the formation of the notochord in the zebrafish, Danio rerio. Development 123:103-115.

Ramsdell AF. 2005. Left-right asymmetry and congenital cardiac defects: getting to the heart of the matter in vertebrate left-right axis determination. Dev Biol 288:1-20.

Rohr S, Otten C, Abdelilah-Seyfried S. 2008. Asymmetric involution of the myocardial field drives heart tube formation in zebrafish. Circ Res 102:e12-19.

Schier AF. 2003. Nodal signaling in vertebrate development. Annu Rev Cell Dev Biol 19:589-621.

Shen MM. 2007. Nodal signaling: developmental roles and regulation. Development 134:1023-1034.

Smith DJ, Blake JR, Gaffney EA. 2008. Fluid mechanics of nodal flow due to embryonic primary cilia. J R Soc Interface 5:567-573.

Stainier DY. 2001. Zebrafish genetics and vertebrate heart formation. Nat Rev Genet 2:39-48.

Yan YT, Gritsman K, Ding J, Burdine RD, Corrales JD, Price SM, Talbot WS, Schier AF, Shen MM. 1999. Conserved requirement for EGF-CFC genes in vertebrate left-right axis formation. Genes Dev 13:2527-2537.

Chapter IV

Leftward displacement of the prospective endocardium is the first visible sign of asymmetry during left-right morphogenesis of the zebrafish heart

Maria Inês Baptista and Alexander Schier

Leftward displacement of the prospective endocardium is the first visible sign of asymmetry during left-right morphogenesis of the zebrafish heart

Maria Inês Baptista and Alexander Schier

Department of Molecular and Cellular Biology, Center for Brain Science, Broad Institute, Harvard Stem Cell Institute, Harvard University, Cambridge, Massachusetts, USA; Instituto Gulbenkian de Ciência, 2780-156 Oeiras, Portugal.

ABSTRACT

The heart is the first organ to exhibit left right asymmetry in vertebrates. Although many studies have addressed how asymmetric morphology develops, it is still unclear what is/are the first visible sign/s of asymmetry and how these are coupled, if at all. During cardiac development in zebrafish several events take place when asymmetry initiates. The cardiac cone shifts to the left and the prospective endocardium (the lumen) is displaced to the left side of the midline. There is leftward rotation, leftward extension of the most left-anterior cells and cardiomyocytes on the right side involute under the cardiac structure. Here we address which of these processes happens first and how asymmetric morphology proceeds. Our results suggest that leftward displacement of the prospective endocardium is the first visible sign of asymmetry. Lumen displacement precedes rotation and left extension of the heart cone. Rotation and extension may occur separately or at the same time, in no particular order. No involution was observed prior to lumen displacement, rotation and/or leftward cell extension.

INTRODUCTION

In zebrafish, as in most vertebrates, the first organ to develop left right asymmetry is the heart (Stainier, 2001). Cardiac progenitor cells, located on each side of the embryonic midline, in the lateral plate mesoderm (LPM), migrate toward the midline and fuse to form the cardiac cone (Stainier, 2001; Glickman and Yelon,

2002). The cardiac cone is a central flat disc, aligned with the midline, centered on a lumen (prospective endocardium). A model has been proposed where the cone undergoes telescopic extension into a linear heart tube. The heart tube is displaced and extends to the left LPM, to later generate a two-chambered heart, with blood circulation by 24 hours post-fertilization (Yelon et al., 1999; Trinh and Stainier, 2004). Heart tube extension is preceded by a tilting process, referred to as heart jogging, during which the venous pole is positioned toward the left side of the embryo (Stainier, 2001).

The transition from heart cone to heart tube involves a series of morphogenetic processes and tissue dynamics that are yet not fully understood. Recent studies have shown that the asymmetric patterning occurring during heart morphogenesis involves the rotation of the heart cone, converting the initial left-right polarity of the cone into dorsal-ventral polarity (Smith et al., 2008). Immunohistochemical staining on sections of zebrafish embryos has revealed that the formation of the heart tube is driven by an asymmetric myocardial involution of the cells on the right side. Leftward involution of the cells in the right side generates the ventral floor of the heart tube (Rohr et al., 2008). We have recently confirmed the aforementioned observations (de Campos-Baptista et al., 2008) and report here further observations complementing these findings.

Additionally to heart cone rotation and myocardial involution, at the onset of initial asymmetric morphology we have observed a displacement of the lumen toward the left side of the embryonic midline and a leftward extension of the left-anterior cardiac tissue. Heart cone rotation, involution of cells on the right, leftward lumen displacement and tissue extension are processes observed during the initial acquisition of asymmetry of the zebrafish heart. To date, there is no information on how these correlate to each other. What is the first visible sign of asymmetry? Could there be more than one? Do these processes occur in a specific order? Are they coupled? By using double fluorescent in situ hybridization and 3D reconstructions we addressed these questions.

Our work suggests that leftward lumen displacement is the first visible sign of asymmetry, followed by heart cone rotation and leftward extension. Rotation and extension can occur simultaneously, separately. Except for lumen displacement to be the first visible sign of asymmetry, rotation and extension do not occur in any specific order. Involution was not observed as an initial visible sign of asymmetry, suggesting this process to be the end result of lumen displacement, heart cone rotation and leftward extension.

RESULTS

Several studies have addressed the process of asymmetry acquisition in the zebrafish heart. However, it is not yet clear what the first visible sign of asymmetry is, morphologically.

In order to address this question, we undertook a series of double fluorescent *in situ* hybridizations on zebrafish embryos fixed every 10 minutes, starting at 20 somites. Two probes were used: *sonic hedgehog* (*shh*), as a landmark for the embryonic midline and *cardiac myosin light chain* (*cmlc2*), as a marker for the cardiomyocytes, the heart cells. We assessed lumen displacement, heart cone rotation, leftward extension and leftward involution.

Recent observations, including our own, have established asymmetry to begin between 20 and 21 somite stage. Each somite takes 30 minutes to form, at 28.5°C. Thus, 3 time-points were taken between each somite formation, allowing a more detailed observation of the morphogenetic changes occurring within this time period.

Lumen displacement was assessed by its position relative to the midline. Heart cone rotation was classified as positive when lumen symmetry was disrupted comparing to the midline and/or posterior end cells were displaced regarding the midline. Leftward extension of the cardiac cells was assessed by higher thickness of the left side of the cardiac cone relative to the right side. Involution was addressed by 3D reconstruction of confocal images and spatial rotation.

Leftward lumen displacement is the fist visible sign of asymmetry in the zebrafish heart

Twenty-seven embryos were analyzed (Table 1). Leftward lumen displacement was the only morphological event to take place before others were observed (9/27) (Fig. 1B and 1B'). Other morphological landmarks of asymmetry were only registered after lumen displacement already took place (Fig. 1C-1E; Fig. 1C'-1E'). These results suggest leftward lumen displacement to be the first visible sign of asymmetry during left-right morphogenesis of the zebrafish heart. Heart cone rotation and leftward extension of the cardiac cells were observed with a frequency of 26% (7/27) and 33% (9/27), respectively. These processes are not coupled since rotation without extension occurred in 18.5% (5/27) of the cases (Fig. 1C and 1C') and extension without rotation was observed in 26% (7/27) of the cases (Fig.1D and 1D'). Heart cone rotation and leftward extension were observed simultaneously in 2 embryos (7.4%) (Fig. 1E and 1E').

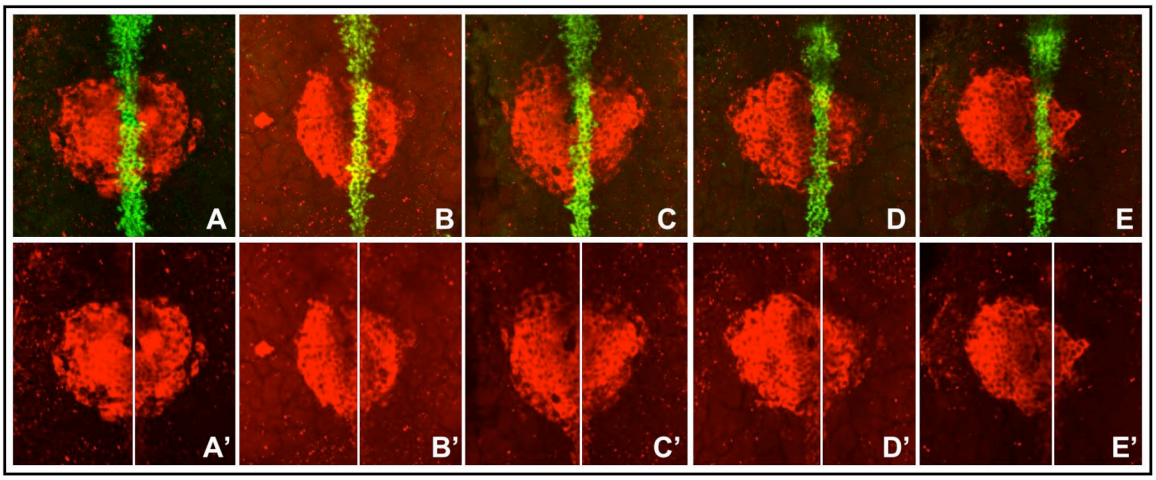

Fig\ure 1 - Asymmetry landmarks in the zebrafish heart. Confocal images of double fluorescent *in situ* RNA hybridization of the midline marker *shh* (green) and the heart marker *cmlc2* (red), between the 20 and 21-somite stage. Single channel expression (**A'-E**) and overlay (**A-E**). White line demarcates the midline. The heart is aligned with the midline before asymmetry initiates (**A, A'**). Leftward lumen displacement (**B, B'**) is visible before heart cone rotation (**C, C'**) and extension of the cells in the left side (**D, D'**). Heart cone rotation and extension of the cells in the left side can occur simultaneously (**E, E'**). Leftward lumen displacement is always visible after asymmetry initiated (**B-E** and **B'-E'**).

Table1 – Asymmetry landmarks in the zebrafish heart from 20 to 21 somites

EMBRYO	Left Lumen	Rotation	Left Extension	Involution
1	yes	no	yes	no
2	yes	yes	no	no
3	yes	yes	no	no
4	no	no	no	no
5	no	no	no	no
6	yes	no	no	no
7	yes	no	no	no
8	yes	no	yes	no
9	yes	no	no	no
10	yes	no	no	no
11	yes	no	no	no
12	yes	no	no	no
13	yes	yes	no	no
14	no	no	no	no
15	yes	yes	no	no
16	yes	yes	yes	no
17	yes	no	no	no
18	yes	no	no	no
19	yes	no	no	no
20	yes	yes	yes	no
21	yes	no	yes	no
22	yes	no	yes	no
23	yes	no	yes	no
24	yes	yes	no	no
25	no	no	no	no
26	yes	no	yes	no
27	yes	no	yes	no

Involution of cardiomyocytes in the right side of the heart cone is a late event of asymmetric morphogenesis

Involution of the right cells toward the left side of the cardiac cone was never observed within the time frame analyzed (data not shown), even after lumen displacement, heart cone rotation and leftward extension of the cardiomyocytes took place. This result suggests that involution of the heart cells from the right side toward the left side is a process happening later during asymmetric heart morphogenesis and a consequence of early processes such as leftward lumen displacement, heart cone rotation and leftward extension of cardiac cells.

Our results suggest that lumen displacement is the first visible sign of asymmetry and that this process is followed by heart cone rotation and/or leftward extension of the cardiac cells. These three processes happen early during cardiac asymmetric morphogenesis while involution of the right cells is only observed after asymmetry has been initiated.

DISCUSSION

The formation of complex organs requires the concerted development of groups of cells, including coordinated regulation of their shapes and movements. Many vertebrate organs, such as the heart and the gut, derive from mono-layered epithelia that undergo a series of morphogenetic events, determinant for proper organ shape and function.

In vertebrates, the majority of the internal organs is shaped and placed asymmetrically within the body cavity. Several processes are at the base of asymmetric morphogenesis. Gut looping in zebrafish results from asymmetric migration of the neighboring lateral plate mesoderm and mutations disrupting the epithelial structure perturb migration and inhibit looping (Horne-Badovinac et al., 2003). Likewise, asymmetric involution of the right heart field myocardium occurs at the onset of cardiac asymmetry acquisition, generating the ventral floor of the heart tube (Rohr et al., 2008).

Although asymmetric involution has been reported to initiate the transition from heart cone into heart tube, other events take place while the right heart field

involutes. Recent studies, including our own, have reported that the cardiomyocytes move anteriorly and leftwards as a whole, at the same time the heart cone rotates clockwise (de Campos-Baptista et al., 2008; Smith et al., 2008). We have also observed a leftward displacement of the prospective endocardium relative to the midline and extension of the left heart cells during the same period (unpublished data). It is still largely elusive how cardiac asymmetric morphogenesis is initiated in zebrafish and how the initial morphogenetic processes take place relative to each other. Understanding this phenomenon in the heart will shed light on such an important and fundamental aspect of embryonic development and organogenesis in general.

Our studies address this problem and reveal that leftward lumen displacement is the first visible sign of asymmetry during early heart formation. Our double fluorescent *in situ* hybridization analysis extends previous studies and shows that lumen displacement initiates asymmetric morphology of the cardiac structure. Heart cone rotation and extension of the cardiac cells in the left side contribute for the general asymmetry of the cardiac structure but are observed only after lumen displacement took place, independent of each other. The fact that these two processes are not coupled and occur in no special order suggests that asymmetric morphology is only controlled at the level of initiation.

It is intriguing to observe that the asymmetric morphology of the zebrafish heart appears to always initiate with the prospective endocardium being displaced to the left side of the embryonic midline but is followed by two possible different processes, not particularly organized in time. One could envision that once a process is triggered (in this case lumen displacement) a cascade of morphological mechanisms ensues, in order to properly form an organ. For instance, the looping of the zebrafish heart results from the asymmetric migration of the neighboring lateral plate mesoderm. Mutations that disrupt the epithelial structure of the LPM perturb this asymmetric migration and inhibit gut looping (Horne-Badovinac et al., 2003). In the gut, looping follows LPM migration. In the heart, no specific process seems to follow leftward lumen displacement. What then is the physiological relevance of the leftward lumen displacement in the context of heart formation? In LZ*oep* mutant

embryos the direction of movement of individual cardiomyocytes is significantly reduced, compared to the wild type phenotype. The anterior movement and leftward displacement of the heart cells is greatly diminished and the cardiac structure mostly remains symmetrically aligned with the embryonic midline. The lumen is not displaced to the left relative to the midline (de Campos-Baptista et al., 2008). However, cardiac morphogenesis is not completely abolished. Despite its delay, the anterior movement of the cardiomyocytes still occurs and heart jogging and looping eventually take place, resulting in heterotaxia (Yan et al., 1999). These observations seem to suggest that, although being the first visible sign of heart asymmetry, the leftward displacement of the prospective endocardium is not required for the progression and proper formation of the heart. Instead, lumen displacement appears to dictate the direction toward which the heart tube must jog and elongate. One interesting experiment would be to address lumen displacement in *polaris* mutants and verify if a rightward displacement of the lumen occurs before the heart jogs to the right side of the embryo. Taking from our observations of LZ*oep* mutant embryos, lacking Nodal signaling, leftward displacement of the prospective endocardium seems to be dependent on an active Nodal signaling pathway. It is not clear though, if Nodal regulates this process directly or indirectly. The myocardial progenitor fields are located between the underlying yolk syncytial layer and the overlying pharyngeal endoderm. These neighboring tissues are essential for the directed migration of progenitor cells and for zebrafish heart cone formation (Alexander and Stainier, 1999; Reiter et al., 1999; Sakaguchi et al., 2006). Studies on a possible regulation of lumen displacement by these tissues, as on the involvement of Nodal signaling, will be required in order to dissect and clarify these issues. It is appealing to consider that heart cone rotation and leftward expansion of the left-most anterior cells might also be dependent on the same processes.

3D analysis and spatial rotation of confocal images of double fluorescent *in situ* hybridizations revealed that involution of the right myocardium does not occur at the onset of asymmetric cardiac morphogenesis. Involution happens later, after lumen displacement, heart cone rotation and extension of the left side cells took place. This result suggests that the involution happening during heart asymmetry

acquisition is a consequence of the earlier processes and not a generator of asymmetry. The fact that in LZ*oep* mutants a heart tube still forms (Yan et al., 1999) indicates that cell involution occurs. Contrary to lumen displacement, this process does not seem to depend on *Nodal* signaling. However, the site of invagination appears to be dictated by the direction toward which the initial lumen displacement takes place. In wild type, the lumen displaces to the left side of the embryonic midline and a counter-lateral involution of cells occurs (de Campos-Baptista et al., 2008). Although the lumen position has not yet been addressed in *polaris* and *no tail* mutants, the site of invagination appears to be always positioned in the opposite side relative to where the heart extends (Chapter III). Assuming that the direction of lumen displacement establishes the direction toward which the heart tube jogs and extends, these observations strongly suggest that the site of involution depends on the direction of lumen displacement. Studies on the lumen position of *no tail* and *polaris* mutants will be crucial to clarify this question.

Overall, our results show that asymmetric morphogenesis of the zebrafish heart consists of a set of processes, the first of which is leftward lumen displacement. This process appears to depend on an active Nodal signaling pathway. Asymmetric morphology is only controlled at the level of initiation and as a consequence of the earlier processes taking place during initial heart formation, involution of the right myocardium occurs. Cardiomyocyte invagination seems to be independent of Nodal signaling. However, the site of invagination appears to be determined by the direction toward which the lumen is displaced.

Our studies extend previous work and provide a deeper understanding of how early asymmetry is generated at the morphological level, but it generates pressing questions at the molecular level. Knowing what genes govern such events and how these correlate to known left-right pathways (such as the Nodal signaling) will be crucial for the complete understanding of asymmetric development.

EXPERIMENTAL PROCEDURE

In Situ Hybridization

For in situ hybridizations, embryos were fixed in 4% paraformaldehyde, rinsed in PBS, dehydrated into absolute methanol and stored at -20°C. Riboprobes were synthesized from linearized DNA templates using T7 polymerase and digoxigenin and DNP labeling mix. Double fluorescent in situ hybridization probes were labeled with fluorescein (Roche) and digoxygenin (Roche). Detection was based on fluorescein or Cy3 tyramide deposition (Perkin Elmer; Schoenebeck et al., 2007). Probes used include: *shh*, and *cmlc2*. Embryos were mounted in benzylbenzoate/ benzylalcohol for photography.

Imaging and Data Analysis

Embryos were mounted and imaging was performed on a Zeiss LSM 5 Pascal confocal microscope with LSM software. Z-stacks were rendered in 3D and analyzed with Imaris software (Bitplane).

AKNOWLEDGEMENTS

We thank all the members of the Schier lab for helpful discussion and input and Steven Zimmerman for fish care.

REFERENCES

Alexander J, Stainier DY. 1999. A molecular pathway leading to endoderm formation in zebrafish. Curr Biol 9:1147-1157.

de Campos-Baptista MI, Holtzman NG, Yelon D, Schier AF. 2008. Nodal signaling promotes the speed and directional movement of cardiomyocytes in zebrafish. Dev Dyn 237:3624-3633.

Glickman NS, Yelon D. 2002. Cardiac development in zebrafish: coordination of form and function. Semin Cell Dev Biol 13:507-513.

Horne-Badovinac S, Rebagliati M, Stainier DY. 2003. A cellular framework for gut-looping morphogenesis in zebrafish. Science 302:662-665.

Reiter JF, Alexander J, Rodaway A, Yelon D, Patient R, Holder N, Stainier DY. 1999. Gata5 is required for the development of the heart and endoderm in zebrafish. Genes Dev 13:2983-2995.

Rohr S, Otten C, Abdelilah-Seyfried S. 2008. Asymmetric involution of the myocardial field drives heart tube formation in zebrafish. Circ Res 102:e12-19.

Sakaguchi T, Kikuchi Y, Kuroiwa A, Takeda H, Stainier DY. 2006. The yolk syncytial layer regulates myocardial migration by influencing extracellular matrix assembly in zebrafish. Development 133:4063-4072.

Smith KA, Chocron S, von der Hardt S, de Pater E, Soufan A, Bussmann J, Schulte-Merker S, Hammerschmidt M, Bakkers J. 2008. Rotation and asymmetric development of the zebrafish heart requires directed migration of cardiac progenitor cells. Dev Cell 14:287-297.

Stainier DY. 2001. Zebrafish genetics and vertebrate heart formation. Nat Rev Genet 2:39-48.

Trinh LA, Stainier DY. 2004. Cardiac development. Methods Cell Biol 76:455-473.

Yan YT, Gritsman K, Ding J, Burdine RD, Corrales JD, Price SM, Talbot WS, Schier AF, Shen MM. 1999. Conserved requirement for EGF-CFC genes in vertebrate left-right axis formation. Genes Dev 13:2527-2537.

Yelon D, Horne SA, Stainier DY. 1999. Restricted expression of cardiac myosin genes reveals regulated aspects of heart tube assembly in zebrafish. Dev Biol 214:23-37.

Chapter V

- Discussion -

Symmetry is a prominent feature of developmental morphology during embryogenesis and a wide variety of symmetries exist to the animal body-plan: spherical (e.g. volvox), chiral (e.g. snails, ciliates), radial (e.g. sea anemone), bilateral (e.g. planaria) and pseudo-bilateral (e.g. man). Vertebrates have a generally bilaterally symmetrical body-plan but, as explored and presented in this thesis, symmetry is broken by the consistently asymmetric placement of various internal organs, such as the heart, liver, spleen and gut, or the asymmetric development of paired organs (such as brain hemispheres and lungs). During development symmetries are continuously broken. For instance, the radial symmetry of the early blastoderm of the chick embryo is broken into a bilateral symmetry when the Köhler's sickle appears and then the primitive streak. This is further broken into a definitive pseudo-symmetry by the rightward looping of the heart tube.

Many fascinating biological questions arise with the establishment of left-right asymmetry. Why does asymmetry exist at all? What are the structural and physiological implications of asymmetry in the context of heart, gut and brain development? Why are all individuals not only asymmetric but asymmetric to the same direction (i.e. given that individuals with full inversion, or *situs inversus*, are phenotipically functional and indistinguishable from their counterparts, why is there a consistent handedness and not a 50/50% ratio within the population)? Evolutionarily speaking, when did *handed* asymmetry appear? Were there true bilaterally symmetrical organisms prior to the emergence of oriented asymmetry? Is *handed* chirality connected in lower forms (such as chirality in some plants and snail shell coiling)? When, during development, does asymmetry begin in vertebrate embryos? How conserved are the molecular mechanisms establishing correct asymmetry in animals with different modes of gastrulation? How do these mechanisms translate into asymmetric morphogenesis? And isn't it interesting that the left-right axis can be consistently oriented with respect to the anterior-posterior and dorso-ventral axes in the absence of any macroscopic feature or chemistry or physics distinguishing left from right?

These and many other questions require a detailed understanding at the molecular, genetic, cellular and biochemical levels of the formation of biased asymmetry in

embryos in order to be answered. Although many layers and points of entry exist to approach the many aspects of asymmetry development, we have decided to address how the cells respond to asymmetric gene expression and asymmetric morphogenesis is directed.

Our studies reveal that the cardiomyocytes ought to have speed and a directed movement toward the left side of the embryo in order to properly place and extend the heart tube. Our results also show that *Nodal* signaling is responsible for promoting the speed of the cardiac cells and for providing directional cues to the movement. However, speed and direction of movement appear to be uncoupled components of heart tube formation, taking from the experiments with embryos exhibiting bilateral expression of the Nodal signaling pathway. Having *Nodal* expressed in opposite sides of the lateral plate mesoderm appears to cancel any possible bias *Nodal* could provide relative to direction of movement. Nonetheless, the cardiomyocytes are still able to move, without exhibiting a leftward or rightward tendency. Thus, primarily *Nodal* is instructing the cells with positive movement, promoting their migration. But how can *Nodal* be doing so? What is the physical motor responding to Nodal signaling that is promoting cardiomyocytes movement?

One can envision that during embryogenesis many morphogenetic events are taking place and that the tissues adjacent to the cardiac cells could be driving the migration of the cardiac fields. The myocardial progenitor fields are located in the anterior lateral plate mesoderm, between the underlying yolk syncytial layer (YSL) and the overlaying pharyngeal endoderm. Could *Nodal* be instructing the yolk syncytial layer to function as a substrate for cardiomyocytes to migrate and form the heart tube, for example? Several genes have been shown to express in the yolk syncytial layer and promote the migration of cardiomyocytes. For instance, *Mtx1* encodes a transcription factor expressed in the extra-embryonic YSL and leads to *cardia bifida* when downregulated (meaning that the myocardial cells fail to migrate). *Mtx1* regulates the embryonic expression of *fibronectin*, disrupting the polarity of the myocardial precursors and extra-cellular matrix assembly (Sakaguchi et al., 2006). Likewise, *Spns2*, a multipass trans-membrane protein also expressed in the extra-

embryonic YSL, leads to *cardia bifida* when mutated (Sakaguchi et al., 2006; Kawahara et al., 2009). Snp2 in the YSL functions as a Sphingosine-1-phosphate (S1P) transporter. S1P is a secreted lipid mediator that acts in vascular development and by being transported by Snp2 is secreted and regulates the migration of myocardial precursors. Although these genes function at the initiation of migration of the cardiomyocytes toward the midline and fusion does not occur at the level of the midline, one possibility is that these genes could be regulated by *Nodal* after the cardiac fields have fused, when the heart tube begins to form. Conditional downregulation of these genes would be necessary to block their activity specifically when the heart tube initiates to form, after the bilateral cardiac fields have fused.

It is interesting to verify that the cardiomyocytes on either side of some *cardia bifida* mutants still progress to form a morphologically normal, beating, two-chambered heart. In mouse, *Foxp4* mutants exhibit *cardia bifida* and develop two highly differentiated, four-chambered, beating hearts on either side, showing that advanced cardiac morphogenesis does not require heart tube fusion (Li et al., 2004). These results suggest that the regulation of cardiomyocytes movement during heart tube formation by *Nodal* might not be via the yolk syncytial layer.

On the same note, *Nodal* does not appear to promote the migration of cardiomyocytes during heart tube formation by regulating the pharyngeal endoderm, the tissue overlaying the bilateral fields of cardiac cells. *Foxp4* is a member of the Fox gene family and is expressed in the early foregut endoderm (Lu et al., 2002). Pharynx endoderm is one of the components of the foregut and *Foxp4* mutant embryos develop several defects in foregut formation. Still, they are capable of forming a morphologically normal heart on either side of the midline showing that normal pharynx endoderm formation is not required.

Previous analyses in zebrafish have demonstrated that the endodermal layer is essential for myocardial migration, as all mutants that lack pharyngeal endoderm show cardia bifida (Alexander and Stainier, 1999; Reiter et al., 1999; Kikuchi et al., 2000). However, like in the mouse *Foxp4* mutants, some zebrafish mutants developing *cardia bifida* induced by deficiencies in pharyngeal endoderm can still generate two normal hearts on either left and right lateral plate mesoderm. This is

the case of *Gata5* mutant fish (Reiter et al., 1999). How could then *Nodal* be promoting the speed of the heart cells? What could be driving the movement of the cardiac cone? Some insight came from studies of the zebrafish gut.

The gut is an epithelial tube composed of a few cell types and surrounded by an innervated muscle layer. In terms of evolution, the gut, as an endodermal organ, precedes any mesodermal organs, as is the heart. The mesoderm, or middle layer, appeared approximately 40 million years after the emergence of the ectoderm and endoderm and was most probably a derivative of the endoderm. Thus, the mesoderm and the endoderm often originate from the same or adjacent regions of the embryo. It is tempting to assume that both tissues can undergo a series of similar morphogenetic events in order to give rise to the respective organs. In zebrafish, the first leftward bend in the developing intestine arises through a morphogenetic process known as gut looping. The *heart and soul* (*has*) mutation causes severe defects in asymmetric organ morphogenesis, in which gut looping fails to occur. *Has* encodes an atypical protein kinase C, aPKCλ, and this protein localizes to the apical junction complex in epithelial cells, establishing epithelial polarity (Ohno, 2001). The lateral plate mesoderm forms a highly polarized epithelium, with strong expression of aPKCs, localized apically, and the left and the right sides have a distinct asymmetry in their morphology and position. The left LPM is dorsal to the endoderm whereas the right LPM is ventro-lateral to the endoderm (Figure 5.1). During gut looping the LPM undergoes asymmetric migration: both sides of the LPM migrate medially, but the left side moves dorsal to the endoderm, whereas the right side undergoes a ventro-lateral migration directly adjacent to the endodermal rod (Figure 5.1 F to H). In *has* mutant embryos the gut does not loop because the epithelial structure of the LPM is severely disrupted, indicating that the asymmetric migration of the LPM is the motive force driving gut looping (Horne-Badovinac et al., 2003).

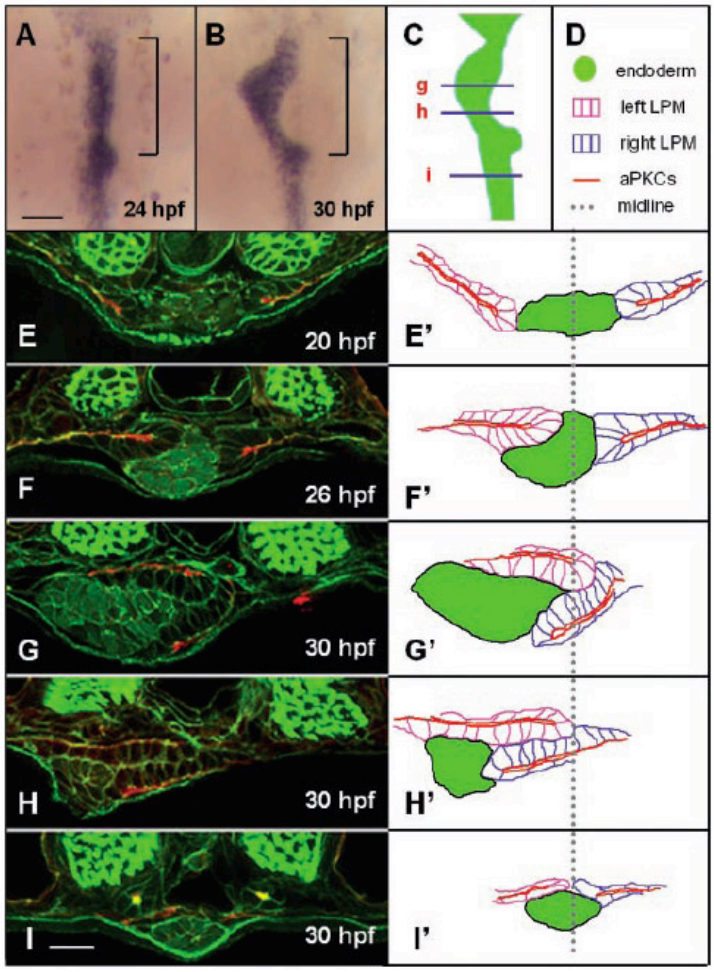

Figure 5.1 – Asymmetric migration of the LPM during gut looping. (A) and **(B)** whole-mount *in situ* hybridization with the endodermal marker *foxA3* reveals digestive tract morphology before (A) and immediately after (B) looping morphogenesis. Scale bar, 50µm. The looping region (brackets) lie between the caudal border of the pharyngeal endoderm and the pancreatic islet. Dorsal views, anterior to the top. **(C)** Diagram of the looped gut at 30hpf. Blue lines indicate position of sections in (G) to (I). **(D)** Key for the diagrams in (E') to (I'). **(E to I)** Transverse sections through the endoderm and LPM. aPKCs (red) show weak expression in the endoderm but are highly expressed and apically localized in the LPM epithelium. Most cells are outlined with cortical actin (green) and endodermal cells have weak cytoplasmic GFP. Dorsal to the top; scale bar, 20µm. **(E)** At 20hpf the endodermal rod lines in the midline and both sides of the LPM are at the same dorso-ventral level as the endodermal rod. **(F)** At 26hpf, both sides of the LPM have migrated medially. The left LPM is dorsal to the endoderm and the right LPM is beginning to migrate ventro-laterally. Although the LPM is markedly asymmetric at this stage, the developing intestine is still in the midline. Asymmetry seen within the endoderm is due to leftward budding of the liver. **(G)** and **(H)** At 30hpf the migration is complete. The developing intestine has shifted to the left and the position of the left versus the right LPM is highly asymmetric. **(I)** Posterior to the looping region, the LPM cells appear squamous and both sides of the LPM are dorsal to the endoderm. **(E' to I')** Diagrams of the relative positions of the LPM and endoderm in confocal images. Adapted from Horne-Badovinac et al., 2003.

As the bilateral cardiac fields are located in the lateral plate mesoderm, it is appealing to hypothesize that *Nodal* signal could be directing the non-cardiac LPM to be the driving force leading to the asymmetric migration of the cardiomyocytes. If so, down-regulation of southpaw expression, the *Nodal* gene expressed in the left LPM of the intestine, would prevent the gut from looping. In *spaw* morpholino

injected embryos gut looping is randomized, though (Horne-Badovinac et al., 2003), showing that when Nodal signaling is missing the direction of gut looping loses its bias to loop toward the left but the LPM still migrates. Should there be conservation between the mechanisms driving gut LPM migration and non-cardiac LPM migration, these observations suggest that it is not by regulating asymmetric migration of the non-cardiac LPM that *Nodal* dictates the migration of cardiomyocytes. One other option is that these mechanisms are not totally conserved, which might actually be the case. In zebrafish *has* mutants the cardiac cone does not tilt and fails to elongate into a tube. Migration does not progress normaly, suggesting that PKCλ-regulated epithelial polarity may be essential for these aspects of morphogenesis (Yelon et al., 1999). In other words, the cardiomyocytes do not migrate, suggesting that the integrity of the LPM is necessary for proper heart tube placement and extension.

Following the previous considerations, it is not possible to argue in favor or against a role for Nodal where *Nodal* signaling pathway might be instructing the movement of the cardiomyocytes by regulating the adjacent neighboring tissues, such as the pharyngeal endoderm and the yolk syncytial layer, or the non-cardiac lateral plate mesoderm. In fact, because the Nodal signaling pathway is active in the heart itself supports the idea of Nodal directly regulating cardiomyocytes migration. However, these considerations are highly speculative and would need strong experimental support in order to be confirmed. Many other possibilities could be raised in order to explain how Nodal confers speed and direction to the cardiomyocytes, both at the molecular and cellular level. Therefore, it seems necessary to identify what genes are downstream of Nodal signaling. It is crucial to understand how *Nodal* is providing the cardiomyocytes with the adequate speed and direction to properly form and place the heart tube. Microarrays performed on RNA from both wild type and LZ*oep* hearts would yield information on what genes are being regulated by *Nodal* in the zebrafish heart (by being up-regulated or down-regulated in the mutant). One could take advantage of the *cmlc2::GFP* transgenic fish and specifically select the green cells of the heart for RNA extraction. Moreover, it would be of great

interest to understand what genes are being regulated by *Nodal* specifically on the left side of the heart, as this is the side where the Nodal signaling pathway is activated. For that it would be useful to have a tool such as *lefty2::GFP* transgenic line, where only the left side of the heart (where *lefty2* is being expressed) would be green. The gene expression profile of these cells, when compared to that of LZ*oep* heart cells, will present differences that correspond to the genes being regulated by the Nodal signaling pathway on the left side. Also, comparison between the gene expression profile of the whole wild type heart and the gene expression profile of only the left region of the wild type heart will reveal if there are any genes being regulated on the right half of the heart, upon *Nodal* signal.

This leads to a more general question relative to the movement exhibited by the cardiomyocytes in the right half of the heart. Do these cardiomyocytes move as a consequence of the dislocation of the cells of the left side of the heart (responding to Nodal signal) or do they have to activate their own genetic program in order to move, as a response to *Nodal* signal on the left side? Again, comparison between the gene expression profile of the cells on the right side of wild type heart and right cells of LZ*oep* heart would be telling. Also, transplantation experiments would help answer this question. By transplanting a group of LZ*oep* cells into a population of cells expressing Nodal, for instance the cells on the left side of a wild type embryo, one can assess if the mutant cells, unable to receive *Nodal* signaling, move or if they end up being segregated from the overall cell population. Likewise, the autonomy of *Nodal* expressing cells can be addressed by transplanting *Nodal*-expressing wild type into the heart field of LZ*oep* mutants.

As cells move, they experience both external forces and internal forces, the latter being generated by the cytoskeleton. The cytoskeleton is a polymer network composed of actin, microtubules and intermediate filaments and, with respect to motility the actin cytoskeleton is regarded as the essential engine driving cell migration (Hofman et al., 1999; Betz et al., 2006). During cell migration it is generally accepted that the leading edge is the main motor, pulling the cell forward. This region of the cell tends to be highly active and is rich in mesh-like actin networks (Kaverina et al., 2002). The continuous creation of new actin networks at

the leading edge is considered to be essential for pulling the cell forward. This network formation is carried out with the help of numerous accessory proteins (Pollard et al., 2000): activating proteins (e.g. WASp) enabling nucleator proteins (e.g. arp2/3/complex) to initiate polymerization and assembly of new actin filaments; actin depolymerization promoting proteins (e.g. cofilin) also aid network growth; actin-binding proteins (e.g. profilin, thymosineβ-4) maintaining a steady actin monomer pool for polymerization; crosslinking and bundling proteins (e.g. filamin, α-actin, fascin) helping form connected actin networks; capping proteins (e.g. CapZ) controlling filament length by attaching to actin filament ends and stopping further polymerization; severing and fragmenting proteins (e.g. gelsolin, severin) cutting actin filaments and networks. All these proteins work together to coordinate actin network formation and bring about leading edge motility. A cell begins to move in response to an external signal in its surrounding environment. This can be a physical, chemical, diffusible or non-diffusible signal that is detected by receptor proteins located on the cell membrane. The signal is then transmitted by the receptors via signaling cascades to the interior of the cell. A cell is believed to sense the signal direction by spatially recognizing external gradients (receptor proteins become more concentrated on the side of the cell where the signal is present) (Parent and Devreotes, 1999). According to this general principle, it is extremely tempting to consider such signal to be *Nodal* and that the cardiomyocytes could be responding to this signal by organizing the actin cytoskeleton and forming a leading edge on the left side of the heart cone, just prior to the heart cone begins to form. However, the results from *foxh1* mutant mice contradict this possibility. As mentioned earlier, *foxh1* is a nuclear target of the TGF-β-Smad signaling pathway (Attisano et al., 2001), meaning it is downstream of Nodal signaling. Mice mutant for *foxh1* exhibit impaired heart formation, similar to the phenotype of *Nodal* mutants (von Both et al., 2004). This suggests that *Nodal* is sensed by the cells in a transcription-dependent manner and thus it is unlikely that *Nodal* acts as a chemoattractant.

It would be interesting to analyze the expression pattern of all the proteins involved in leading edge formation in the context of heart development and heart tube formation. It could be that an active and dynamic leading edge of actin filaments is visualized specifically on the left side of the embryonic heart cone. Furthermore, is would be interesting to address how are actin filaments and its accessory proteins affected in the heart field when the Nodal signaling pathway is absent or impaired. Regulation of the actin leading edge of the cardiomyocytes at the tip of the left heart cone could be another possibility for *Nodal* to promote the speed of cardiomyocytes.

Our work also tried to address how asymmetry acquisition occurs in terms of morphological/visual processes and how these are integrated during this process. Although our data is still preliminary and more experiments need to be performed, it is interesting to find that all embryos analyzed exhibited one common physical landmark at the onset of asymmetry initiation: in all of them, the leftward lumen displacement was the first visible sign of asymmetry. Of interest as well is to observe that after the lumen was displaced there is no particular order followed by the processes ensuing, as if only the initial event is important to be regulated. The lumen has been suggested to contain the endocardial precursors (Stainier et al., 1993; Glickman and Yelon, 2002). This tissue will give rise to the lining of the heart tube and mutations affecting the migration and correct placement of the endocardial precursors lead to cardiac defects. The heart does not form valves, for instance (Bussmann et al., 2007). However, the myocardial differentiation does not appear to be affected. Thus, it is necessary to have proper integration of the two lineages, myocardial and endocardial, in order to properly pattern the heart. It is plausible that the leftward lumen displacement is the first event to occur during asymmetry acquisition to ensure that both populations are well integrated. Once this has happened, both lineages will be able to progress as a whole and maybe that is why it is not so important to regulate the processes ensuing leftward lumen displacement. It is quite likely that lumen displacement is regulated by *Nodal* signaling and studies analyzing lumen position and heart tube formation will be necessary to clarify this hypothesis.

Directed cell migration is a central process in the development of multi-cellular organisms, required for the orchestrated movement of cells involved in tissue formation during embryonic development. Internal organ formation and placement requires asymmetric morphogenesis so that organs such as the heart, gut, intestine, liver, etc. can be adequately packed within the body cavity and function properly. Local processes involving differential control of cell proliferation and/or cell death, as well as instructive changes in cell fate and behavior are likely to be involved in directing asymmetric development of specific organs.

The Nodal signaling pathway has long been implicated in the establishment of left-right asymmetry. However, clear links between the activity of particular genes, like *Nodal*, and specific morphogenetic or proliferative functions in organ primordia are still poorly known.

With our work we aimed to add some knowledge to the field by trying to understand how cardiac cells interpret asymmetric *Nodal* expression and how this translates at the morphological level. Although new insights were revealed and we now understand the cardiomyocytes acquire speed and directional movement upon *Nodal* signaling, these answers lead to many other questions, opening several doors to other avenues of research regarding left-right asymmetry acquisition in the zebrafish heart.

Exploring those avenues and extending the knowledge on how asymmetric gene expression translates at the cellular and morphological level will be of great importance for a deeper understanding of organogenesis in particular, and embryogenesis in general.

REFERENCES

Alexander J, Stainier DY. 1999. A molecular pathway leading to endoderm formation in zebrafish. Curr Biol 9:1147-1157.

Attisano L, Silvestri C, Izzi L, Labbe E. 2001. The transcriptional role of Smads and FAST (FoxH1) in TGFbeta and activin signalling. Mol Cell Endocrinol 180:3-11.

Betz T, Lim D, Kas JA. 2006. Neuronal growth: a bistable stochastic process. Phys Rev Lett 96:098103.

Bussmann J, Bakkers J, Schulte-Merker S. 2007. Early endocardial morphogenesis requires Scl/Tal1. PLoS Genet 3:e140.

Glickman NS, Yelon D. 2002. Cardiac development in zebrafish: coordination of form and function. Semin Cell Dev Biol 13:507-513.

Hofman P, d'Andrea L, Guzman E, Selva E, Le Negrate G, Far DF, Lemichez E, Boquet P, Rossi B. 1999. Neutrophil F-actin and myosin but not microtubules functionally regulate transepithelial migration induced by interleukin 8 across a cultured intestinal epithelial monolayer. Eur Cytokine Netw 10:227-236.

Horne-Badovinac S, Rebagliati M, Stainier DY. 2003. A cellular framework for gut-looping morphogenesis in zebrafish. Science 302:662-665.

Kaverina I, Krylyshkina O, Small JV. 2002. Regulation of substrate adhesion dynamics during cell motility. Int J Biochem Cell Biol 34:746-761.

Kawahara A, Nishi T, Hisano Y, Fukui H, Yamaguchi A, Mochizuki N. 2009. The sphingolipid transporter spns2 functions in migration of zebrafish myocardial precursors. Science 323:524-527.

Kikuchi Y, Trinh LA, Reiter JF, Alexander J, Yelon D, Stainier DY. 2000. The zebrafish bonnie and clyde gene encodes a Mix family homeodomain protein that regulates the generation of endodermal precursors. Genes Dev 14:1279-1289.

Li S, Zhou D, Lu MM, Morrisey EE. 2004. Advanced cardiac morphogenesis does not require heart tube fusion. Science 305:1619-1622.

Lu MM, Li S, Yang H, Morrisey EE. 2002. Foxp4: a novel member of the Foxp subfamily of winged-helix genes co-expressed with Foxp1 and Foxp2 in pulmonary and gut tissues. Mech Dev 119 Suppl 1:S197-202.

Ohno S. 2001. Intercellular junctions and cellular polarity: the PAR-aPKC complex, a conserved core cassette playing fundamental roles in cell polarity. Curr Opin Cell Biol 13:641-648.

Parent CA, Devreotes PN. 1999. A cell's sense of direction. Science 284:765-770.

Pollard TD, Blanchoin L, Mullins RD. 2000. Molecular mechanisms controlling actin filament dynamics in nonmuscle cells. Annu Rev Biophys Biomol Struct 29:545-576.

Reiter JF, Alexander J, Rodaway A, Yelon D, Patient R, Holder N, Stainier DY. 1999. Gata5 is required for the development of the heart and endoderm in zebrafish. Genes Dev 13:2983-2995.

Sakaguchi T, Kikuchi Y, Kuroiwa A, Takeda H, Stainier DY. 2006. The yolk syncytial layer regulates myocardial migration by influencing extracellular matrix assembly in zebrafish. Development 133:4063-4072.

Stainier DY, Lee RK, Fishman MC. 1993. Cardiovascular development in the zebrafish. I. Myocardial fate map and heart tube formation. Development 119:31-40.

von Both I, Silvestri C, Erdemir T, Lickert H, Walls JR, Henkelman RM, Rossant J, Harvey RP, Attisano L, Wrana JL. 2004. Foxh1 is essential for development of the anterior heart field. Dev Cell 7:331-345.

Yelon D, Horne SA, Stainier DY. 1999. Restricted expression of cardiac myosin genes reveals regulated aspects of heart tube assembly in zebrafish. Dev Biol 214:23-37.